GAC-MAC
WINNIPEG
2013

AT THE
CENTRE OF
THE CONTINENT

AU
CENTRE DU
CONTINENT

FIELD TRIP GUIDEBOOK

Field Trip Guidebook FT-C5 / Open File OF2013-1

Ordovician-Silurian boundary interval in the Williston Basin outcrop belt of Manitoba: a record of global and regional environmental and biotic change

R.J. Elias, G.A. Young, L.A. Stewart, M.W. Demski, M.J. Porter, T.D. Lukie, G.S. Nowlan and E.P. Dobrzanski

Held in conjunction with
GAC®-MAC • AGC®-AMC
Joint Annual Meeting • Congrès annuel conjoint
May 22–24, 2013

GAC® | AGC®

MAC | AMC

This field trip was sponsored by the Paleontology Division of the Geological Association of Canada

Paleontology Division
Geological Association of Canada

Open File OF2013-1

Field Trip Guidebook FT-C5

Ordovician-Silurian boundary interval in the Williston Basin outcrop belt of Manitoba: a record of global and regional environmental and biotic change

by R.J. Elias, G.A. Young, L.A. Stewart, M.W. Demski, M.J. Porter, T.D. Lukie, G.S. Nowlan and E.P. Dobrzanski

Geological Association of Canada–Mineralogical Association of Canada Joint Annual Meeting, Winnipeg

May, 2013

Innovation, Energy and Mines

Hon. Dave Chomiak
Minister

Grant Doak
Deputy Minister

Mineral Resources Division

John Fox
Assistant Deputy Minister

Manitoba Geological Survey

C.H. Böhm
A/Director

When using information from this publication in other publications or presentations, due acknowledgment should be given to the Manitoba Geological Survey. The following reference format is recommended:

Elias, R.J., Young, G.A., Stewart, L.A., Demski, M.W., Porter, M.J., Lukie, T.D., Nowlan, G.S. and Dobrzanski, E.P. 2013: Ordovician-Silurian boundary interval in the Williston Basin outcrop belt of Manitoba: a record of global and regional environmental and biotic change; Geological Association of Canada–Mineralogical Association of Canada Joint Annual Meeting, Field Trip Guidebook FT-C5; Manitoba Innovation, Energy and Mines, Manitoba Geological Survey, Open File OF2013-1, 49 p.

NTS grid: 62I, 62P, 63G, 63J, 63K

Keywords: Stony Mountain Formation; Stonewall Formation; Fisher Branch Formation; biodiversification; mass extinction; biotic recovery; Hirnantian

External author addresses:

R.J. Elias, L.A. Stewart, M.W. Demski, M.J. Porter

Department of Geological Sciences, University of Manitoba, Winnipeg, MB R3T 2N2

(204) 474-8862, eliasrj@cc.umanitoba.ca

G.A. Young, E.P. Dobrzanski

The Manitoba Museum, 190 Rupert Avenue, Winnipeg, MB R3B 0N2

T.D. Lukie

Sarawak Shell Berhad, Locked Bag no. 1, Miri, Sarawak, Malaysia 98009

G.S. Nowlan

Geological Survey of Canada, 3303 33rd Street NW, Calgary, AB T2L 2A7

Published by:

Manitoba Innovation, Energy and Mines
Manitoba Geological Survey
360–1395 Ellice Avenue
Winnipeg, Manitoba
R3G 3P2 Canada
Telephone: (800) 223-5215 (General Enquiry)
(204) 945-4154 (Publication Sales)
Fax: (204) 945-8427
E-mail: minesinfo@gov.mb.ca
Website: manitoba.ca/minerals

This publication is available to download free of charge at manitoba.ca/minerals

Cover illustration: Roadcut exposing the red and gray *t*-marker bed (0.7 m thick) in the Stonewall Formation, looking north along Provincial Trunk Highway 6 in the Grand Rapids Uplands of Manitoba (Stop 8, photographed in 2008).

Abstract

The Williston Basin provides a record of events leading up to and following the end of the Ordovician Period, in an equatorial, epicontinental setting. The Stony Mountain Formation and the lower and middle parts of the Stonewall Formation represent cyclic sedimentation during transitional icehouse conditions, prior to the latest Ordovician Hirnantian Age. Deposition of the Stony Mountain Formation, with the Williams Member as its uppermost unit, was possibly followed by subaerial exposure. The lower and middle dolostone intervals of the Stonewall Formation are separated by the lower Stonewall marker bed, which may have been related to subaerial exposure in the marginal area of the basin, but not in the more basinal area.

Strata in the upper Stonewall Formation, above the base of the *t*-marker bed, are considered to be Hirnantian in age. The surface between the middle dolostone interval and the *t*-marker bed may have been subaerially exposed during the major, early Hirnantian glacio-eustatic regression. The *t*-marker bed and the overlying upper dolostone interval of the Stonewall Formation were possibly deposited during an interglacial transgressive phase. The Ordovician-Silurian boundary is placed at the disconformable contact between the Stonewall and Fisher Branch formations. Deposition of the Fisher Branch Formation began in earliest Silurian, Rhuddanian time, during a major transgression following the return to pre-Hirnantian climatic conditions.

Patterns of biogeography and biodiversity in the Stony Mountain Formation reflect an environmental gradient from deeper water in the southern area of the Williston Basin outcrop belt to shallower in the north, and a temporal change to shallower, more restricted conditions. Biotas in the Stony Mountain Formation and lower to middle Stonewall Formation represent the culmination of the Great Ordovician Biodiversification Event (GOBE). As the sea cooled before icehouse conditions in the Hirnantian, the marginal area of the basin served as a refugium for some Stony Mountain taxa, and exotic taxa arrived in the basin. The first pulse of the Late Ordovician mass extinction is recorded a short distance below the *t*-marker in the Stonewall Formation. The turnover from Late Ordovician to *Ozarkodina* conodont faunas and the appearance of a distinctive coral fauna in the upper Stonewall Formation are considered to have occurred during Hirnantian time. The Rhuddanian-age biota in the Fisher Branch Formation provides the first record of the Early Silurian biotic recovery in the Williston Basin.

SAFETY INFORMATION

General Information

The Geological Association of Canada (GAC) recognizes that its field trips may involve hazards to the leaders and participants. It is the policy of the GAC to provide for the safety of participants during field trips, and to take every precaution, reasonable in the circumstances, to ensure that field trips are run with due regard for the safety of leaders and participants. Field trip safety is a shared responsibility. The GAC has a responsibility to take all reasonable care to provide for the safety of the participants on its field trips. Participants have a responsibility to give careful attention to safety-related matters and to conduct themselves with due regard to the safety of themselves and others while on the field trips.

Field trip participants should be aware that any geological fieldwork, including field trips, can present significant safety hazards. Foreseeable hazards of a general nature include inclement weather, slips and falls on uneven terrain, falling or rolling rock, insect bites or stings, animal encounters and flying rock from hammering. **The provision and use of appropriate personal protective equipment (e.g., rain gear, sunscreen, insect repellent, safety glasses, work gloves and sturdy boots) is the responsibility of each participant.** Each field trip vehicle will be equipped with a moderate sized first-aid kit, and the lead vehicle will carry a larger, more comprehensive kit of the type used by the Manitoba Geological Survey for remote field parties.

Participants should be prepared for the possibility of inclement weather. In Manitoba, the weather in May is highly unpredictable. The average daily temperature in Winnipeg is 12°C, with record extremes of 37°C and -11°C. North-central Manitoba (Thompson) has an average daily temperature of 7°C, with record extremes of 33°C and -18°C (*Source:* Environment Canada). Consequently, participants should be prepared for a wide range of temperature and weather conditions, and should plan to dress in layers. A full rain suit and warm sweater are essential. Gloves and a warm hat could prove invaluable if it is cold and wet, and a sunhat and sunscreen might be just as essential in the heat and sun.

Above all, field trip participants are responsible for acting in a manner that is safe for themselves and their co-participants. This responsibility includes using personal protective equipment (PPE) when necessary or when recommended by the field trip leader, or upon personal identification of a hazard requiring PPE use. It also includes informing the field trip leaders of any matters of which they have knowledge that may affect their health and safety or that of co-participants. Field Trip participants should pay close attention to instructions from the trip leaders and GAC representatives at all field trip stops. Specific dangers and precautions will be reiterated at individual localities.

Specific Hazards

Some of the stops on this field trip may require short hikes, in some cases over rough, rocky, uneven or wet terrain. Participants should be in good physical condition and accustomed to exercise. Sturdy footwear that provides ankle support is strongly recommended. Some participants may find a hiking stick a useful aid in walking safely. Steep outcrop surfaces require special care, especially after rain. Access to bush outcrops may require traverses across muddy or boggy areas; in some cases it may be necessary to cross small streams or ditches. Field trip leaders are responsible for identifying such stops and making participants aware well in advance if waterproof footwear is required. Field trip leaders will also ensure that participants do not go into areas for which their footwear is inadequate for safety. In all cases, field trip participants must stay with the group.

Other field trip stops are located adjacent to roads, some of which may be prone to fast-moving traffic. At these stops, participants should pay careful attention to oncoming traffic, which may be distracted by the field trip group. Participants should exit vehicles on the shoulder-side of the road, stay off roads when examining or photographing outcrops, and exercise extreme caution in crossing roads.

Road cuts or rock quarries also present specific hazards, and participants MUST behave appropriately for the safety of all. Participants must be aware of the danger from falling debris and should stay well back from overhanging cliffs or steep faces. Participants must stay clear of abrupt drop-offs at all times, stay with the field trip group, and follow instructions from leaders.

Participants are asked to refrain from hammering rock. It represents a significant hazard to the individual and other participants, and is in most cases unnecessary. Many stops on this field trip include outcrop with unusual features that should be preserved for future visitors. If a genuine reason exists for collecting a sample, please inform the field trip leader, and then make sure it is done safely and with concern for others, ideally after the main group has departed the outcrop.

Subsequent sections of this guidebook contain the stop descriptions and outcrop information for the field trip. In addition to the general precautions and hazards noted above, the introductions for specific localities make note of any specific safety concerns. Field trip participants must read these cautions carefully and take appropriate precautions for their own safety and the safety of others.

TABLE OF CONTENTS

Page

Introduction

During latest Ordovician to earliest Silurian time, deposition and biotas were influenced globally by environmental changes that led to glaciation and deglaciation in south-polar Gondwana. At the centre of equatorial Laurentia, the Williston Basin preserves a record of global and regional changes in an epicontinental sea. Strata exposed in the Williston Basin outcrop belt of Manitoba provide a superb opportunity to examine this extraordinary interval in Earth history. On this field trip, classic localities north of Winnipeg in southern Manitoba will be compared with sites in two areas of west-central Manitoba — the Grand Rapids Uplands north of Grand Rapids, and Cormorant Hill northeast of The Pas. New research, integrating lithostratigraphy, biostratigraphy, and carbon-isotope chemostratigraphy, suggests that deposits of latest Ordovician, Hirnantian age are present and that the Ordovician-Silurian boundary is at a higher position than previously thought.

This field trip will focus on the Stony Mountain, Stonewall, and Fisher Branch formations. These predominantly carbonate strata provide a record of environments and events leading up to and following the major Hirnantian glacial episode. The succession of fossils represents the culmination of the Great Ordovician Biodiversification Event, the Late Ordovician mass extinction, and the Early Silurian recovery. The Williston Basin outcrop belt in Manitoba provides a dip section, from relatively basinal deposits in the south to more marginal facies in the north (Figure 1). On Day 1, we will visit the type sections of the three formations in the southern part of the outcrop belt (Stops 1–3). Exposures of correlative strata in the northern part of the outcrop belt will be examined in the Grand Rapids Uplands on Day 2 (Stops 4–8) and at Cormorant Hill on Day 3 (Stops 9–11).

Field trip itinerary

Day 1

- MANDATORY SAFETY ORIENTATION SESSION (in front of main entrance to Winnipeg Convention Centre): **7:45 a.m.**
  - **depart 8:00 a.m.**

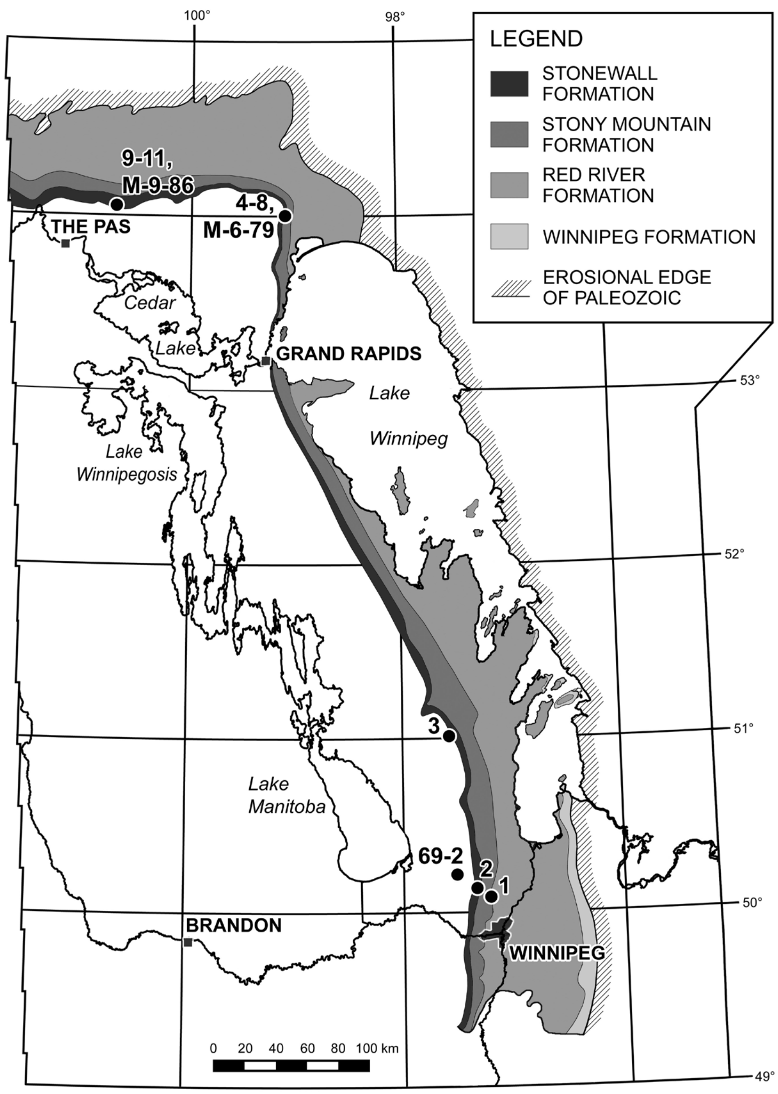

__Figure 1:__ Geological map of Ordovician formations in the Williston Basin outcrop belt of Manitoba (based on Corkery et al., 1994; McCabe and Bezys, 1998). Lowermost Silurian Fisher Branch Formation occurs on the southwest side of the Stonewall Formation. Map shows the locations of Stops 1–3 and core-hole 69-2 in southern Manitoba, Stops 4–8 and core-hole M-6-79 in the Grand Rapids Uplands, and Stops 9–11 and core-hole M-9-86 at Cormorant Hill.

- **STOP 1** (Stony Mountain quarries, west pit): **arrive 8:40 a.m.**
  - SNACK/DRINK: provided.
  - **depart 10:10 a.m.**
- **STOP 2** (Stonewall Quarry Park): **arrive 10:20 a.m.**
  - BAG LUNCH/DRINK: provided.
  - **depart 11:50 a.m.**
- REST STOP (Fisher Branch): **arrive 1:10 p.m.**
  - SNACK/DRINK: available for purchase.
  - **depart 1:25 p.m.**
- **STOP 3** (outcrops near Fisher Branch): **arrive 1:35 p.m.**
  - **depart 2:45 p.m.**
- REST STOP (Ashern): **arrive 3:25 p.m.**
  - SNACK/DRINK: available for purchase.
  - **depart 3:40 p.m.**
- DINNER (Grand Rapids): **arrive 6:10 p.m.**
  - MEAL AND EVENING SNACK/DRINK: available for purchase.
  - **depart 7:25 p.m.**
- LODGING (Grand Rapids): **arrive 7:40 p.m.**

Day 2
- DEPARTURE FOR BREAKFAST (prior to lodging check-out).
  - **depart 7:40 a.m.**
- BREAKFAST (Grand Rapids): **arrive 7:45 a.m.**
  - MEAL AND DAYTIME SNACKS/DRINKS: available for purchase.
  - **depart 8:45 a.m.**
- REST STOP AND LODGING CHECK-OUT (Grand Rapids): **arrive 8:50 a.m.**
  - **depart 9:10 a.m.**
- **STOP 4** (exposure beside Highway 6, 101.0 km north of Grand Rapids): **arrive 10:15 a.m.**
  - **depart 10:55 a.m.**
- **STOP 5** (exposure beside Highway 6, 98.4 km north of Grand Rapids): **arrive 11:00 a.m.**
  - **depart 11:40 a.m.**
- **STOP 6** (exposure near Highway 6, 97.6 km north of Grand Rapids): **arrive 11:45 a.m.**
  - return to vehicle: **12:25 p.m.**
  - BAG LUNCH/DRINK: provided.
- **STOP 7** (roadcut on Highway 6, 97.6 km north of Grand Rapids): after lunch.
  - **depart 1:55 p.m.**
- **STOP 8** (roadcut on Highway 6, 91.9 km north of Grand Rapids): **arrive 2:00 p.m.**
  - **depart 3:00 p.m.**
- REST STOP (junction of Highway 6 and Highway 39): **arrive 3:50 p.m.**
  - SNACK/DRINK: available for purchase.
  - **depart 4:05 p.m.**
- LODGING (The Pas): **arrive 6:25 p.m.**
  - DINNER AND EVENING SNACK/DRINK: available for purchase.

Day 3
- BREAKFAST AND DAYTIME SNACKS/DRINKS: available for purchase.
- LODGING CHECK-OUT (The Pas).
  - **depart 8:30 a.m.**
- **STOP 9** (quarry beside Road 287, south side of Cormorant Hill): **arrive 9:20 a.m.**
  - **depart 10:10 a.m.**
- **STOP 10** (roadcut on Road 287, north side of Cormorant Hill): **arrive 10:15 a.m.**
  - **depart 11:15 a.m.**
- **STOP 11** (quarry beside Road 287, top of Cormorant Hill): **arrive 11:20 a.m.**
  - **depart 11:40 a.m.**
- LUNCH (The Pas): **arrive 12:35 p.m.**
  - MEAL: available for purchase.
  - **depart 1:15 p.m.**
- REST STOP (Highway 6, south of junction with Highway 60): **arrive 3:35 p.m.**
  - SNACK/DRINK: available for purchase.
  - **depart 3:50 p.m.**
- REST STOP (Ashern): **arrive 6:00 p.m.**
  - SNACK/DRINK: available for purchase.
  - **depart 6:15 p.m.**
- END OF FIELD TRIP (Winnipeg Convention Centre): **8:20 p.m.**

The Ordovician to Early Silurian world

Overview

The Ordovician to Early Silurian (Llandovery) was an extraordinary time in Earth history (Sheehan, 2001; Servais et al., 2009, 2010; see time scale in Figure 2). The Paleozoic maximum of continental dispersal and igneous activity occurred in the Ordovician, when sea-floor spreading was rapid. The largest continent, Gondwana, was partly over the South Pole, and the second largest continent, Laurentia, was in an equatorial position (Figure 3). The Earth was in a greenhouse state, with the atmospheric partial pressure of CO_2 reaching a Phanerozoic peak that was perhaps 16 times higher than at present. Sea level rose greatly in the Ordovician, and at its maximum created the largest area of tropical shelves in the entire Phanerozoic Eon. There were frequent meteoritic impacts in the Middle Ordovician, following the largest documented asteroid breakup since the Precambrian (Schmitz et al., 2008).

The climate of the Late Ordovician to Early Silurian was bizarre (Finnegan et al., 2011). Despite the high atmospheric

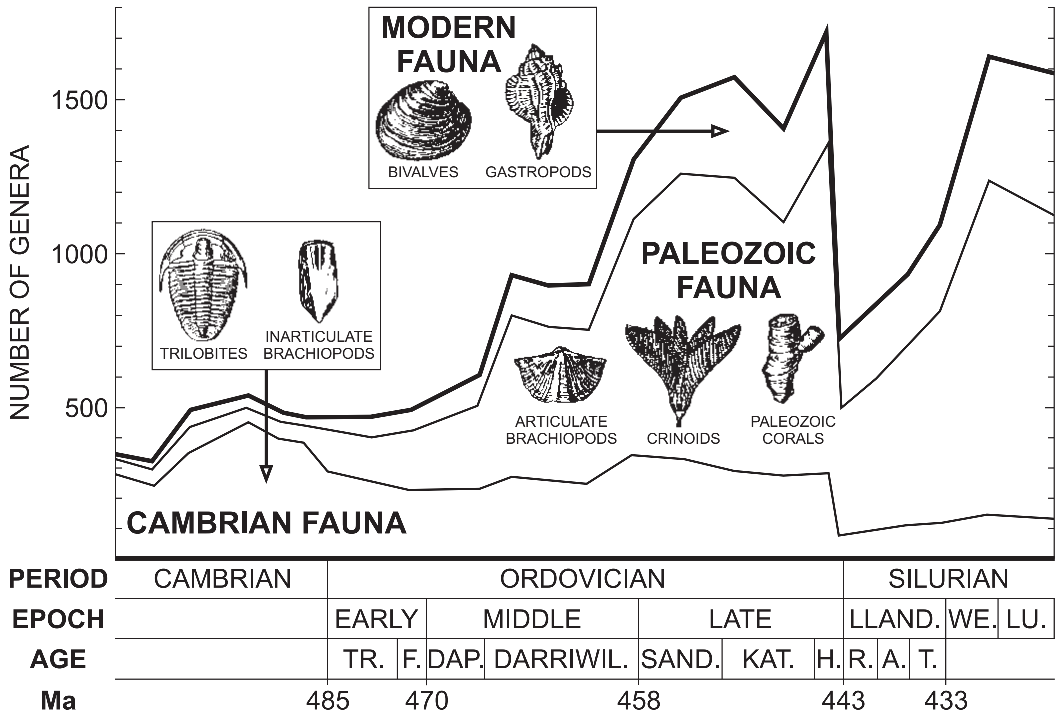

Figure 2: *Global genus-level diversity of marine animals from the mid Cambrian to near the end of the Silurian, showing contributions of the three Phanerozoic evolutionary faunas (based on Sepkoski, 1995, Figure 1; time scale updated using Schmitz et al., 2008, Figure 1, and International Commission on Stratigraphy, 2012; illustrations of principal faunal groups derived from Sepkoski, 1984, Figure 2). Abbreviations: Silurian epochs (chronological order), LLAND. = Llandovery, WE. = Wenlock, LU. = Ludlow; Ordovician and Silurian ages (chronological order), TR. = Tremadocian, F. = Floian, DAP. = Dapingian, DARRIWIL. = Darriwilian, SAND. = Sandbian, KAT. = Katian, H. = Hirnantian, R. = Rhuddanian, A. = Aeronian, T. = Telychian.*

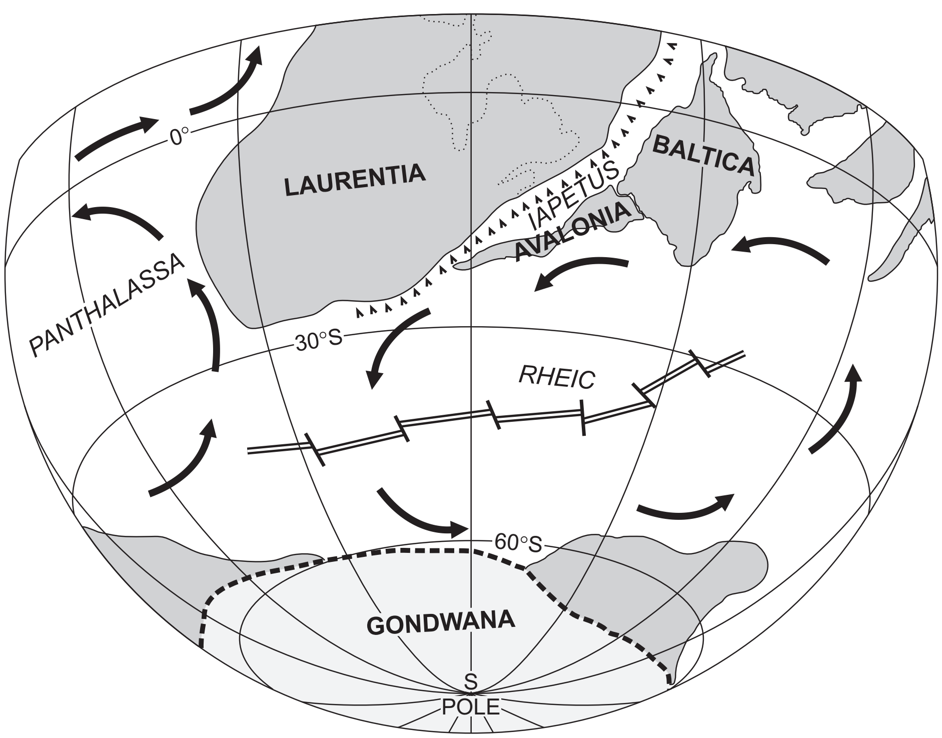

Figure 3: *Global view from the South Pole to latitude 10°N in the latest Ordovician Hirnantian Age, showing paleocontinents (shaded; dotted outline of modern coastline, including Hudson Bay and Gulf of St. Lawrence, for orientation in Laurentia), ice sheet on Gondwana (lighter shading with dashed outline), oceans, oceanic ridge (double lines), subduction zone (triangles), and possible oceanic currents (arrows) (based on Achab and Paris, 2007, Figure 1).*

partial pressure of CO_2, ice sheets developed on the south-polar area of Gondwana from Katian to Rhuddanian time (Figures 3, 4a, b). These sheets were not substantial in the early Katian, but moderate glaciations and deglaciations occurred in the mid to late Katian. Nevertheless, tropical ocean temperatures, apparently ranging from 32° to 37°C, were higher than those at present (Figure 4c). In the Hirnantian, however, there was a glacial maximum with an ice volume at least as great as that of the last glacial maximum in the Pleistocene. At the time of the Hirnantian maximum, there was a brief cooling pulse of about 5°C in the tropical ocean. Elevated temperatures seem to have returned with partial deglaciation in the late Hirnantian, even though moderate-sized ice sheets continued to develop through the Rhuddanian. Thus, rapid and substantial climate changes were associated with the beginning and end of the Hirnantian glacial episode.

Climate models suggest that a drop in atmospheric CO_2 was necessary for glaciation to occur in the Late Ordovician (Lenton et al., 2012). The overall drawdown has been attributed to increased weathering following intense orogenic activity and volcanic eruptions, enhanced by the presence of continents in the tropics. The origination of land plants and the later appearance of vascular plants may have resulted in two pulses of increased weathering and fluxes to the ocean. These pulses would have promoted marine productivity and burial of organic carbon, driving the onset of glaciation in the Late Ordovician and the major glacial episode in the Hirnantian.

Significant changes in the carbon cycle occurred during the Ordovician Period (Munnecke et al., 2010). An overall shift from relatively constant values of $\delta^{13}C_{carb}$ in the Early to mid Ordovician, to fluctuating values in the later Ordovician, seems to coincide with the onset of glacial conditions. There are a number of small, positive isotopic excursions in the Katian, and the Hirnantian Isotopic Carbon Excursion (HICE) is one of the most prominent in the entire Phanerozoic Eon (Figure 4d). Most if not all of these Ordovician excursions represent global perturbations of the carbon cycle, with the HICE corresponding to the major Hirnantian glacial episode (Smith et al., 2011). The positive excursions may have resulted from increased weathering of carbonate platforms during eustatic drops in sea level, which would have provided oceans with ^{13}C-enriched runoff. Another possibility is that oceanic productivity and burial of

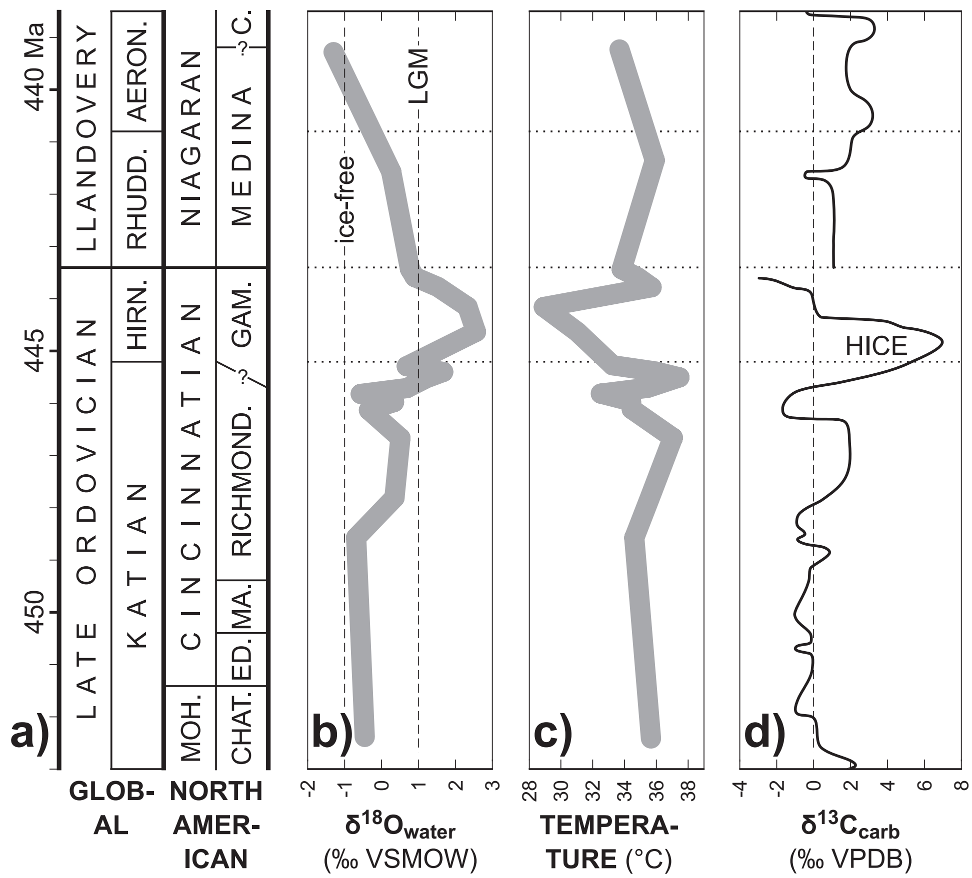

Figure 4: *Geochemical and climatic profiles in the Late Ordovician and Early Silurian.* ***a)*** *Time scale showing global epochs and ages from the Katian to Aeronian, and the corresponding North American divisions (based on Webby et al., 2004, Figure 2.2; Bergström et al., 2009; Cramer et al., 2011, Figure 1; International Commission on Stratigraphy, 2012). Abbreviations: global ages (chronological order), HIRN. = Hirnantian, RHUDD. = Rhuddanian, AERON. = Aeronian; North American epoch, MOH. = Mohawkian; North American ages (chronological order), CHAT. = Chatfieldian, ED. = Edenian, MA. = Maysvillian, RICHMOND. = Richmondian, GAM. = Gamachian, C. = Clinton.* ***b)*** *$\delta^{18}O_{water}$ trend, with dashed lines showing the expected value for an ice-free world and the value during the Pleistocene last glacial maximum (LGM) (based on Finnegan et al., 2011, Figure 3d).* ***c)*** *Tropical near-surface ocean temperature trend determined by carbonate clumped isotope paleothermometry (based on Finnegan et al., 2011, Figure 3a).* ***d)*** *Generalized $\delta^{13}C_{carb}$ profile, showing the Hirnantian Isotopic Carbon Excursion (HICE) (Katian–Hirnantian based on Munnecke et al., 2010, Figure 3; Rhuddanian–Aeronian based on Munnecke et al., 2010, Figure 4).*

isotopically light organic carbon were promoted during times of thermohaline circulation. For the significant positive excursion at the beginning of the Katian and the prominent HICE, pulses in the evolution of land plants may have enhanced weathering, productivity, and burial of organic carbon (Lenton et al., 2012). Positive $\delta^{13}C_{carb}$ excursions comparable in magnitude to the HICE do not occur in the Llandovery (Figure 4d).

Three important biotic events occurred during Ordovician to Early Silurian time: the Great Ordovician Biodiversification Event, the Late Ordovician mass extinction, and the Early Silurian recovery. They are discussed below.

Great Ordovician Biodiversification Event (GOBE)

The GOBE was of tremendous significance in the history of marine life (Harper, 2006; Servais et al., 2009; Figure 2). Within a span of about 25 million years, diversity below the phylum level rose more rapidly than at any other time. Diversity reached a plateau level that persisted for about 200 million years, until the greatest of all mass extinctions at the end of the Paleozoic Era. The Paleozoic Evolutionary Fauna, which rose to dominance during the GOBE, succeeded the Cambrian Evolutionary Fauna and remained the most significant faunal component for the rest of the Paleozoic.

In terms of paleoecological outcomes of the GOBE (Servais et al., 2010; Munnecke et al., 2010), the skeletonized portion of the Paleozoic Evolutionary Fauna was dominated by suspension feeders. New types of communities were developed, especially in association with reefs and in deeper water, and diversity rose within communities. There were increases in the occupation of ecospace and the complexity of ecological structures, involving food webs, tiering above and below the substrate surface, and exploitation of the water column. In addition to the diversification of benthic suspension-feeders, there were significant increases in the diversity of the pelagic fauna, zooplankton, and phytoplankton.

The GOBE was apparently caused by a combination of geological and possibly extraterrestrial factors, as well as biological processes (Servais et al., 2009, 2010; Munnecke et al., 2010). Rapid sea-floor spreading and maximum continental dispersal in the Ordovician promoted biogeographical differentiation. The high sea-level resulted in vast habitat areas of tropical shelves and epicontinental seas. Intense igneous activity produced volcanic islands that provided numerous habitats. Volcanism and the weathering of orogenic belts increased nutrient availability. The stable greenhouse state during the Early to mid Ordovician may have been especially favourable for the biosphere. Frequent meteoritic impacts may have enhanced environmental heterogeneity (Schmitz et al., 2008). In response to the extraordinary conditions of the Ordovician, the diversification of phytoplankton and zooplankton promoted diversification of pelagic and suspension-feeding benthic faunas (Servais et al., 2009, 2010).

Late Ordovician mass extinction

The first of the "big five" Phanerozoic mass extinctions occurred near the end of the Ordovician Period (Brenchley et al., 2001; Sheehan, 2001; Figure 2). Although it was not the largest in terms of diversity reduction, all of the major groups of benthic and pelagic taxa were affected. The extinctions, however, were concentrated at relatively low taxonomic levels. Estimated losses are about 25% of families, 60% of genera, and 85% of species. There were two pulses of extinction, the first occurring at the beginning of the Hirnantian, and the second later in the Hirnantian. Both pulses had a significant effect on groups such as brachiopods and trilobites. Graptolites and conodonts were primarily affected by the first and second pulses, respectively. Extinctions were most severe in the tropics.

Despite the substantial loss of taxonomic diversity, the Late Ordovician mass extinction was the least significant of the "big five" Phanerozoic mass extinctions in terms of ecologic severity (Brenchley et al., 2001; Sheehan, 2001; McGhee et al., 2004). Major components of the ecosystem were not lost permanently, the paleoenvironmental distribution of the Paleozoic and Modern evolutionary faunas remained unchanged (see Figure 2), and an ecologic structure like that of typical Ordovician communities was re-established during the Early Silurian recovery.

The Late Ordovician mass extinction was caused by factors related to rapid and substantial global climate change (Brenchley et al., 2001; Sheehan, 2001; Finnegan et al., 2011). The first and second pulses of extinction coincided with the beginning and end of the major Hirnantian glacial episode (Figure 4a, b). Biotas and their habitats were affected by both the drop and rise in sea level and water temperature (Figure 4c). During the first pulse of extinction, the effects of cooling and habitat loss due to the reduction of shallow seas were particularly significant in the tropics (Finnegan et al., 2012), where endemic faunas had become established in epicontinental seas. Nutrient enrichment and related environmental destabilization, as nutrients provided by runoff from expanding terrestrial areas became concentrated in the shrinking epicontinental seas, would have suppressed diversity and simplified the ecologic structure of communities (Elias and Young, 1998; Elias et al., in press). In the oceans, changes in circulation, structure of the water column, and nutrient fluxes apparently promoted extinction. The first pulse of extinction was driven by euxinic conditions and a steepened oxygen gradient when sea level dropped, whereas the second pulse occurred when anoxic water transgressed onto continental shelves during the sea-level rise (Hammarlund et al., 2012).

The plate-tectonic setting in latest Ordovician time may also have contributed to the mass extinction (Rasmussen and Harper, 2011). With contraction of the narrow Iapetus Ocean, there were losses of island-arc habitats and their endemic faunas as terranes accreted to Laurentia (Figure 3).

Early Silurian recovery

Following the Late Ordovician mass extinction, taxonomic diversity at the global scale recovered to the Paleozoic plateau level by the mid Silurian (Figure 2). At the continental scale, however, the time to reach pre-extinction levels of diversity seems to have varied from 5 million years to 15 million years. Some analyses suggest a faster recovery in Laurentia than in Baltica and Avalonia (Krug and Patzkowsky, 2007; Figure 3), whereas others indicate that the recovery in Laurentia was delayed (Rasmussen and Harper, 2011). In addition to geographically variable rates of recovery, there was also variation among taxonomic groups (Sheehan, 2001); graptolites, in particular, speciated rapidly. During the Early Silurian recovery of taxonomic diversity, ecologic complexity similar to that of typical Ordovician communities was restored (Brenchley et al., 2001; Sheehan, 2001).

The biotic recovery in the Early Silurian was promoted by relatively stable and favourable environmental conditions. Water temperature apparently remained elevated, despite the continued development of moderate-sized ice sheets through the Rhuddanian (Finnegan et al., 2011; Figure 4a–c). Widespread epicontinental seas returned with the rise in sea level (Munnecke et al., 2010). In Laurentia, the recovery benefitted from relatively high origination rates and from immigration, which promoted the shift from endemic faunas of the Ordovician to cosmopolitan faunas during the recovery (Krug and Patzkowsky, 2007). Terranes within the narrowing Iapetus Ocean provided migration pathways (Rasmussen and Harper, 2011; Figure 3).

The Hirnantian Stage and Ordovician-Silurian (O-S) boundary

Globally, the boundaries of the Ordovician System and its series and stages are placed at the bases of designated graptolite or conodont biozones (Cocks et al., 2010). The lower boundary of the latest Ordovician Hirnantian Stage (= top of Katian Stage) is defined as the first appearance of the graptolite *Normalograptus extraordinarius* at the Wangjiawan North section in China. The O-S boundary (= top of Hirnantian) is set at the base of the *Akidograptus ascensus* Biozone as recognized at Dob's Linn in Scotland. The Hirnantian Stage consists of the *N. extraordinarius* Biozone and the overlying *Normalograptus persculptus* Biozone.

In peripheral areas of North America, the Hirnantian Stage can be recognized by occurrences of *N. extraordinarius* and *N. persculptus* in central Nevada (Finney et al., 1999; Figure 5, location J), and by graptolites indicative of the *N. extraordinarius* and *N. persculptus* biozones on Truro and Cornwallis islands in Arctic Canada (Melchin and Holmden, 2006). Biostratigraphic interpretation of graptolites is problematic in the uppermost Ordovician to lowermost Silurian interval on Anticosti Island, Québec (Achab et al., 2011; Figure 5, location I). In the continental interior, graptolites diagnostic of the *N. extraordinarius*, *N. persculptus*, and *A. ascensus* biozones are absent. At some locations, other faunal groups such as corals, brachiopods, and conodonts suggest the presence of Hirnantian strata and the position of the O-S boundary, but they are not definitive (Bergström et al., 2012).

Carbon-isotope chemostratigraphy has become important for identifying Hirnantian strata and locating the O-S boundary, particularly where biostratigraphic data are absent or inconclusive. The distinctive HICE rises to high values in the *N. extraordinarius* and lower *N. persculptus* biozones, and ends in

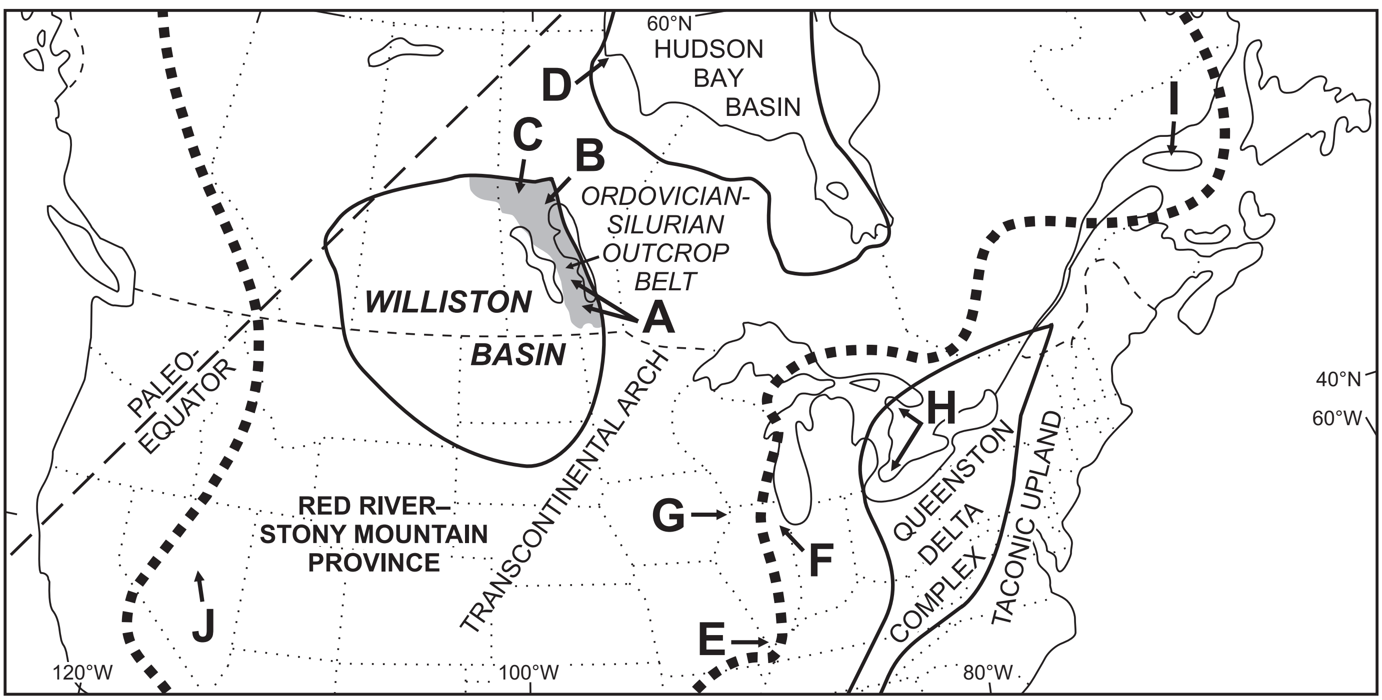

Figure 5: *Map of southern Canada and northern U.S.A., showing Late Ordovician–Early Silurian paleogeographic features (based on Elias and Young, 2004, Figure 15.2), the Ordovician-Silurian outcrop belt in the Williston Basin (based on Norford et al., 1994, Figure 9.22), the Late Ordovician paleoequator ca. 450 Ma (extrapolated from Cocks and Torsvik, 2002, Figures 5–7), and the Late Ordovician Red River–Stony Mountain biogeographic province (bold dotted outline; based on Elias and Young, 2004, Figure 15.2; Elias et al., in press). Locations in the Williston Basin: A = southern Manitoba (area of stops 1–3); B = Grand Rapids Uplands, Manitoba (area of stops 4–8); C = Cormorant Hill, Manitoba (area of stops 9–11). In addition to locations B and C, the Hirnantian Isotopic Carbon Excursion (HICE) has been reported from the following locations (see text for references): D = Airport Cove near Churchill, Manitoba; E = southeastern Missouri and southern Illinois; F = northeastern Illinois; G = eastern Iowa; H = southern Ontario; I = Anticosti Island, Québec; J = central Nevada.*

the middle *N. persculptus* Biozone (Bergström et al., 2009; see Figure 4d). It has been recognized in central Nevada (Finney et al., 1999; Figure 5, location J) and Arctic Canada (Melchin and Holmden, 2006). In the case of Anticosti Island, there is disagreement as to whether the HICE extends through the entire Ellis Bay Formation or begins in the upper part of the formation (Achab et al., 2011; Jones et al., 2011; Figure 5, location I). If the former interpretation is correct, the Hirnantian Stage is equivalent to the North American Gamachian Stage, but if the latter interpretation is correct, then the base of the Gamachian is lower than Hirnantian (Bergström et al., 2009; see Figure 4a). It has been suggested that the O-S boundary on Anticosti Island is located where the isotopic values return to baseline, in the lower Becscie Formation which overlies the Ellis Bay Formation (Jones et al., 2011).

In the North American interior, the HICE has been recognized at a few locations between the Taconic Upland and the Transcontinental Arch (Figure 5). These locations occur in the east-central U.S.A. (Bergström et al., 2012; Figure 5, locations E–G) and southern Ontario (Sharma and Dix, 2004; Bergström et al., 2011; Figure 5, location H). In the two major intracratonic basins on the other side of the Transcontinental Arch, the HICE has been reported from locations in Manitoba. One is in the Hudson Bay Basin (Demski et al., 2011a; Figure 5, location D) and two are in the Williston Basin (Demski et al., 2010; Figure 5, locations B and C). It seems that deposits of Hirnantian age are widely distributed across the continent.

The Williston Basin

Overview

Widespread deposition in the intracratonic Williston Basin began in Late Ordovician time (as currently defined), with maximum basinal subsidence in northwestern North Dakota (Norford et al., 1994; Figure 5). Deposition during the Ordovician and Silurian reflected eustatic and glacio-eustatic changes, and at times extended beyond the basin and across most of the continent (see e.g., Elias, 1991; Zhang, 2011). The first Late Ordovician transgression in the Williston Basin resulted in deposition of the siliciclastic Winnipeg Formation (Norford et al., 1994; Figure 6). Following a regressive event, subsequent Ordovician and Silurian sedimentation was dominated by carbonates. Deposition of the lower Red River Formation in Manitoba (Dog Head, Cat Head, and Selkirk members) and its lateral equivalents was initiated during a major transgression. The upper Red River Formation (Fort Garry Member) and its equivalents recorded three sedimentary cycles, the first two ending with anhydrite deposition in the central area of the basin. Deposition of the lower Stony Mountain Formation began during a major transgressive event, accompanied by the introduction of siliciclastic material into the southeastern part of the basin (Gunn and Penitentiary members). Higher in the Stony Mountain Formation, deposition of the Gunton Member concluded with anhydrite in the central part of the basin. Above the Stony Mountain Formation, a succession of sedimentary cycles resulted in the Stonewall Formation and lower Interlake Group (which includes the Fisher Branch Formation at its base in Manitoba). Some of these cycles were terminated by anhydrite deposition in the central area of the basin.

Marker beds and sedimentary cycles

Porter and Fuller (1959) and Fuller (1961) recognized a number of “non-sequential”, argillaceous to arenaceous marker beds in the Williston Basin. These relatively thin beds are associated with sedimentary cycles in the upper Red River Formation, and in the interval from the upper Stony Mountain Formation through lower Interlake Group. Unlike the anhydrite beds, the marker beds are areally extensive and permit basin-wide correlation. For example, the anhydrite at the top of the Gunton Member of the Stony Mountain Formation is overlain by a very widespread, argillaceous to arenaceous unit. This unit has been referred to as the top Gunton or basal Stonewall marker, and has been included either at the top of the Stony Mountain Formation or base of the Stonewall Formation (see Kendall, 1976). This deposit attains maximum thickness and grain size in southern Manitoba, where it is known as the Williams Member. In this guidebook, the Williams Member is retained in the Stony Mountain Formation (Figure 6). Within the overlying Stonewall Formation in the Williston Basin, the first depositional cycle is terminated by anhydrite and the relatively weakly developed, argillaceous, lower Stonewall marker bed (LS-marker in this guidebook). Higher in the Stonewall Formation, the argillaceous to arenaceous *t*-marker is prominent and very widespread. Toward the centre of the basin, the *t*-marker is represented by two closely spaced beds. At the top of the Stonewall Formation there is another marker bed, which is argillaceous and very widespread.

The Transcontinental Arch was probably a source area of siliciclastic material introduced into the Williston Basin (Porter and Fuller, 1959; Fuller, 1961; Witzke, 1980; Figure 5). This is indicated by the southeastward increase in thickness and grain size of the lower Stony Mountain Formation. Marker beds in the upper Stony Mountain and Stonewall formations also expand in the same direction. Frosted sand grains in the upper Stony Mountain Formation and in the *t*-marker bed of the Stonewall Formation were probably derived from exposures of the Winnipeg Formation (Andrichuk, 1959; Porter and Fuller, 1959).

Fully developed sedimentary cycles in the Ordovician of the Williston Basin each include a thin marker bed of argillaceous carbonate, which may contain quartz sand and carbonate clasts, and a succession of units as follows (Kendall, 1976): 1) fossiliferous carbonate wackestone to mudstone that is commonly burrow-mottled and forms the thickest part of the cycle, 2) thin-bedded to laminated, slightly argillaceous carbonate mudstone, and 3) anhydrite. Not all of the cycles are complete, but each records a change from deposition in relatively open marine environments to more restricted conditions. Various models have been proposed to explain these cycles (for discussions, see Kendall, 1976; Elias et al., 1988; Pratt and Haidl, 2008). Some workers have considered the cycles to represent periods of progradational sedimentation, with diachronous boundaries between cycles. However, the widespread distribution of the cycles and units within them suggests that environmental changes were basin-wide, with essentially synchronous boundaries between cycles. The succession of units within

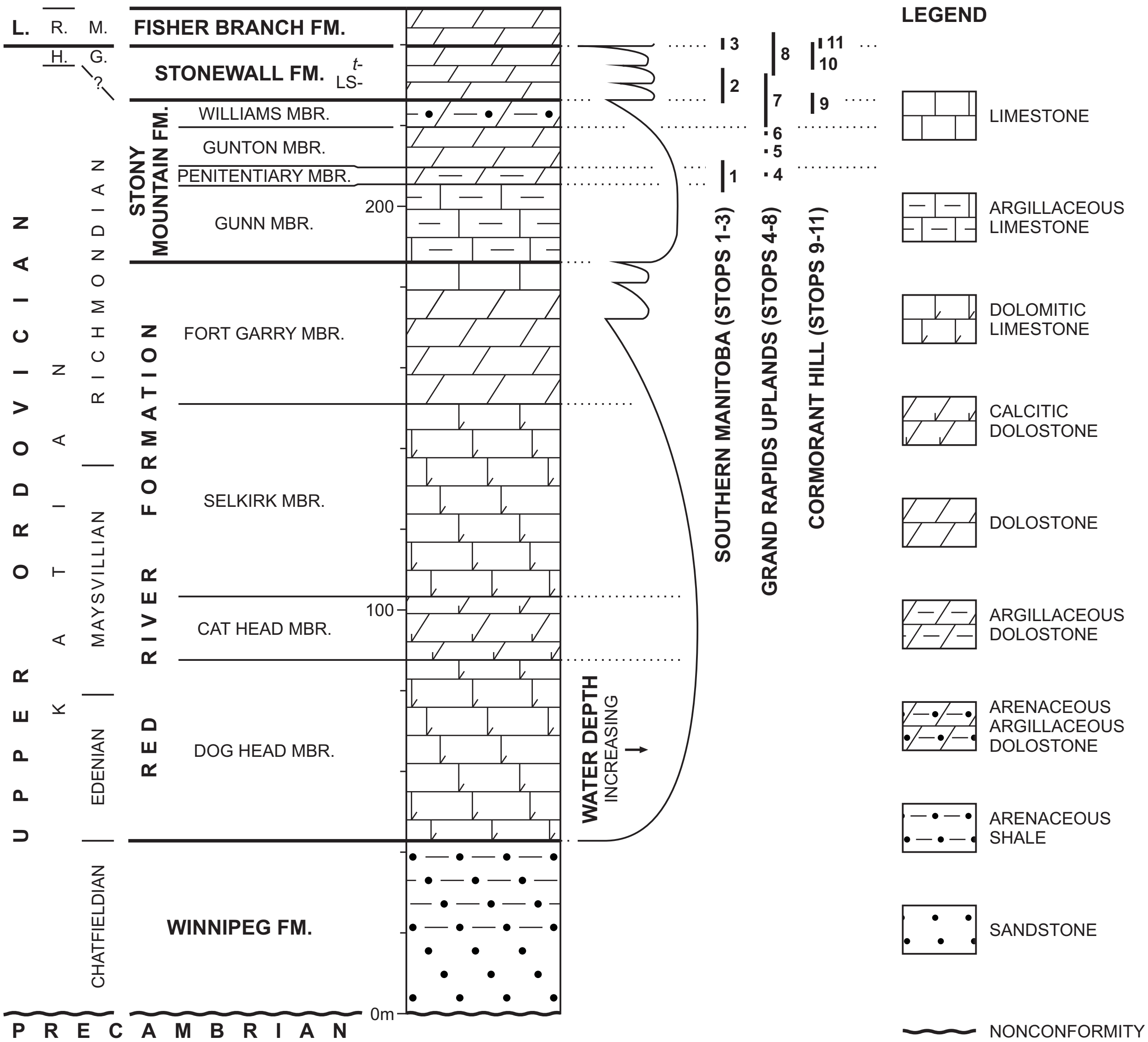

Figure 6: *Ordovician to lowermost Silurian lithostratigraphy of the Williston Basin outcrop belt in southern Manitoba, with a water-depth curve for the Red River through Stonewall formations, and showing the relative stratigraphic positions of Stops 1–11. Stratigraphic column shows thicknesses of units in the latitudinal range from Stop 1 (Stony Mountain) to Stop 2 (Stonewall) (see Figure 1), based on McCabe (1980, Figure GS-12-1) and Elias (1981, Figure 2). Relations between stratigraphic units and stages are based on extrapolations from Sweet (1982) for the Winnipeg Formation, extrapolations from Sweet (1979, p. 54, Figure 4) for the Red River to lower Stonewall formations (see Elias, 1991, Figure 2; Elias and Young, 2004, Figure 15.3), Demski et al. (2010) for the upper Stonewall Formation, and Jin et al. (1999) for the Fisher Branch Formation, which is the lowermost unit of the Interlake Group. In this guidebook, the Ordovician-Silurian boundary is placed at the contact between the Stonewall and Fisher Branch formations. Water-depth curve is based on Elias and Young (2004, Figure 15.3). Abbreviations: global series, L. = Llandovery; global stages (chronological order), H. = Hirnantian, R. = Rhuddanian; North American stages (chronological order), G. = Gamachian, M. = Medina.*

cycles may have been a response to shallowing upward, brining upward, and/or warming upward conditions. Some workers have considered the marker bed to represent subaerial exposure and nondeposition or erosion at the end of a depositional cycle. Others have considered the marker to represent reflooding of the basin at the start of a cycle, which may have followed subaerial exposure.

Holland and Patzkowsky (2012) interpreted Upper Ordovician lithofacies on the Bighorn carbonate platform of Wyoming, which are comparable to units within the Williston Basin. Their Facies 1, consisting of skeletal packstone alternating with argillaceous skeletal packstone beds, was considered to represent the deepest subtidal, open marine conditions. It is lithologically and faunally similar to, and equates stratigraphically with, the Gunn-Penitentiary facies of the Stony Mountain Formation. Facies 1 is overlain by Facies 2, composed of *Thalassinoides*-burrowed skeletal wackestone, which is comparable to the Gunton Member above the Gunn-Penitentiary interval in the Stony Mountain Formation. Facies 2 and the burrowed mudstone of Facies 3 were interpreted as open marine to restricted shallow subtidal deposits, respectively, and the laminated dolostone of Facies 4 was attributed to tidal-flat to sabkha environments.

Facies 2–4 typically occur in vertical succession, resembling the carbonate units between marker beds within sedimentary cycles in the Williston Basin. Repetitions of Facies 2–4 form a series of parasequences in strata that equate with the upper Red River, Stony Mountain, and lower Stonewall formations in the Williston Basin.

Holland and Patzkowsky (2012) suggested that changes in the nature of sedimentary cyclicity through the Bighorn succession were related to an increase in the amplitude and period of eustatic cyclicity, in response to climate change during the late Katian (see Figure 4a–c). The stratigraphic equivalent of the lower Red River Formation accumulated under greenhouse conditions, followed by widespread parasequences in equivalents of the upper Red River to lower Stonewall formations, which were deposited under transitional icehouse conditions. The stratigraphic succession in the Williston Basin provides a comparable record of global change, but is more complete. A major hiatus that begins in the upper part of the lower Red River equivalent and ends in the upper Red River equivalent on the Bighorn carbonate platform does not extend into the Williston Basin (Sweet, 1979; Elias, 1991).

In carbonate successions, carbon-isotope profiles can be useful for recognizing surfaces that were subaerially exposed, and can provide an indication of the duration of exposure and extent of erosional truncation (Theiling et al., 2007; Figure 7). This is particularly beneficial in the Ordovician, because features characteristic of exposure, such as paleosols and paleokarst, are seldom apparent (Railsback et al., 2003). The first application of this method in the Williston Basin suggested that the base of the *t*-marker bed in the Stonewall Formation of Manitoba was a subaerial exposure surface (Demski et al., 2010). Some of those data are presented in this guidebook (Stops 8, 10). Ongoing research in the Williston Basin is examining other marker beds and stratigraphic contacts. Results shown in this guidebook suggest that the LS-marker in the Stonewall Formation was associated with exposure toward the basin margin (Stop 7), but not at a more basinal location (Stop 2). Subaerial exposure is indicated at a surface considered to be the contact between the Williams Member of the Stony Mountain Formation and the overlying Stonewall Formation (Stops 2, 7, 9). As a result, the formational boundary at the type section of the Williams Member and Stonewall Formation is placed at a slightly higher position than that selected by previous workers (Stop 2). Recognition of this surface as a disconformity supports inclusion of the Williams Member in the Stony Mountain Formation.

Age of Stonewall Formation and position of O-S boundary

Kindle (1914) placed the O-S boundary at the base of the Stonewall Formation. Since then, the boundary has been repositioned a number of times, on the basis of faunal evidence and stratigraphic correlations. Okulitch (1943) raised the systemic boundary to a level that is in the lower part of the Stonewall Formation as currently recognized. Baillie (1951) pointed out that the Stonewall Formation may be equivalent to the Ellis Bay Formation on Anticosti Island, Québec (i.e., latest Ordovician, Gamachian in age). Stearn (1953, 1956) placed the O-S boundary at the top of the Stonewall Formation, and equated the formation with strata on Anticosti Island that are late Richmondian or Gamachian in age. Based on macrofossils in drillcore from Saskatchewan, Brindle (1960) suggested that the O-S boundary coincides with the *t*-marker in the upper Stonewall Formation, and that the underlying Stonewall strata are Richmondian. Using conodont-based graphic correlation and relative abundance logs, Sweet (1979) concluded that the uppermost Ordovician deposits on the Bighorn carbonate platform of Wyoming are post-Richmondian (i.e., Gamachian). He noted that those beds probably equate with strata in the lower Stonewall Formation of the Williston Basin.

Based on conodont studies in the Williston Basin area of Saskatchewan and Manitoba (Norford et al., 1998), the O-S boundary was located in an interval associated with the *t*-marker bed in the upper Stonewall Formation. The boundary was placed where a Late Ordovician conodont fauna is succeeded abruptly by one of Early Silurian aspect including *Ozarkodina hassi*. It was recognized that the latter fauna ranges into the latest Ordovician in some areas near the continental margin. In the Williston Basin, however, the appearance of the *Ozarkodina* fauna was considered to be Silurian, because it was thought that latest Ordovician (Gamachian) to earliest Silurian

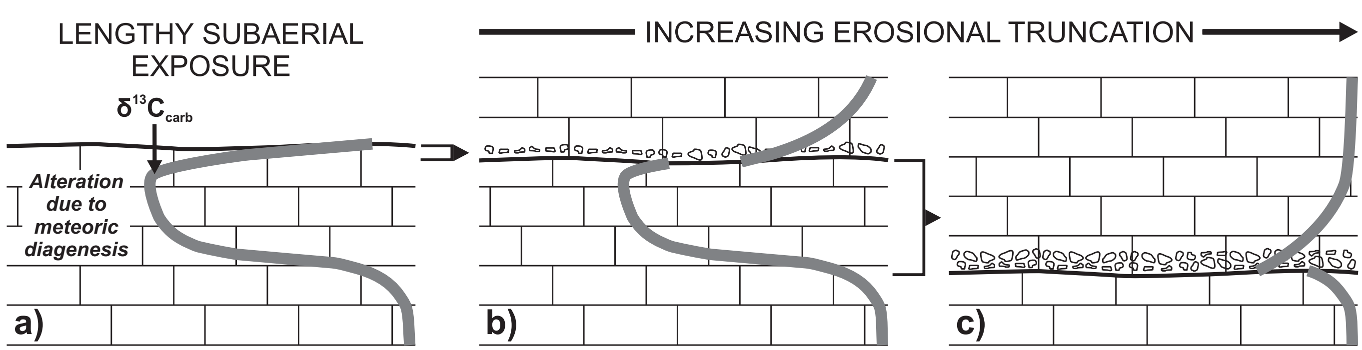

***Figure 7:** Characteristic $\delta^{13}C_{carb}$ profiles related to alteration and truncation as a result of subaerial exposure (modified from Theiling et al., 2007, Figure 7). **a)** During subaerial exposure, meteoric diagenesis results in a negative excursion beneath the surface, which increases in magnitude and depth with increasing duration of exposure. **b)** Minor erosional truncation and subsequent deposition yields this pattern, as the amount of reworked material diminishes upward. **c)** Significant truncation and subsequent deposition yields this pattern.*

(early Rhuddanian) strata were probably absent in the cratonic interior due to the major glacio-eustatic regression.

Recently, it was discovered that a positive isotopic-carbon excursion begins at the base of the *t*-marker, rises to a peak at the position of the conodont turnover, and then decreases in the uppermost Stonewall Formation in Manitoba (Demski et al., 2010). Some of those data are presented in this guidebook (Stops 8, 10). On Anticosti Island, Québec, and in central Nevada, northeastern Illinois, and southern Ontario, the *Ozarkodina* fauna appears in association with an isotopic excursion that has been identified as the HICE (Finney et al., 1999; Bergström et al., 2011, 2012). In Manitoba, the coincidence of the isotopic excursion with the appearance of *Ozarkodina* suggests that this excursion represents the HICE, and that strata in the upper Stonewall Formation above the base of the *t*-marker are latest Ordovician, Hirnantian in age (Demski et al., 2010; Figure 6).

The peak values of $\delta^{13}C_{carb}$ in the upper Stonewall Formation are relatively low (+2‰), similar to most other occurrences of the HICE in the continental interior. In such cases, the isotopic excursion may represent only the upper, mid-Hirnantian part of the complete HICE, where values are decreasing (see Figure 4d), and the deposits may record an interglacial transgression (Demski et al., 2011b; Bergström et al., 2012). The base of the *t*-marker in the Stonewall Formation was possibly a surface of subaerial exposure during the major, early Hirnantian glacio-eustatic regression (Demski et al., 2011b). The isotopic excursion in the overlying strata returns to a background level at the top of the Stonewall Formation. In this guidebook, the O-S boundary is placed at the disconformable contact between the Stonewall Formation and the succeeding Fisher Branch Formation (Figure 6; Stops 3, 8, 10, 11). The Fisher Branch Formation contains the brachiopod *Virgiana decussata*, considered to indicate an Early Silurian (Llandovery, late Rhuddanian) age (Jin et al., 1999).

Biota

In Upper Ordovician strata of the Williston Basin, the faunas of highest diversity occur within the Red River and Stony Mountain formations (Young et al., 2008). These faunas arose during the GOBE. It has long been recognized that faunal assemblages like those in the Red River and Stony Mountain formations are widespread in North America, and they have been collectively referred to as the “Arctic fauna” (e.g., Nelson, 1959a, b). Characteristic taxa include receptaculitids (*Fisherites*), solitary and colonial corals (e.g., *Bighornia*, *Manipora*), and large molluscs representing gastropods (e.g., *Maclurina*) and cephalopods (e.g., *Lambeoceras*). Elias (1981) defined the Red River–Stony Mountain biogeographic province on the basis of this distinctive biota, and delineated its geographic extent using corals. The province ranges from northern Greenland to northern Mexico and from eastern Québec to eastern Alaska, occupying much of Canada and the central and western U.S.A. (Elias and Young, 2004; Elias et al., in press; Figure 5). Overall, the Red River–Stony Mountain Province included much of the vast epicontinental sea and stable continental shelf areas of Laurentia.

Within the Williston Basin and beyond, changes in the geographic distribution, diversity, and composition of coral assemblages were related to environmental cyclicity, and resulted from differences in environmental conditions among cycles and changing conditions within cycles (Elias, 1991; Young and Elias, 1999; Elias and Young, 2004; Elias et al., in press). In the Williston Basin, the greatest diversity is observed in the upper part of the lower Red River Formation (Selkirk Member), which was deposited during greenhouse conditions. Diversity was lower, but at times substantial, in the subsequent Ordovician cycles that represent transitional icehouse, to icehouse conditions. This is recorded in the upper Red River, Stony Mountain, and Stonewall formations. Brachiopods in the Red River and lower Stony Mountain formations show a similar pattern of diversity (Jin and Zhan, 2001).

Southwest of the Williston Basin, on the Bighorn carbonate platform of Wyoming, Holland and Patzkowsky (2009) recognized five biofacies in strata that correspond to the Red River and Stony Mountain formations. Those authors placed the biofacies along an environmental gradient, which is useful in the interpretation of faunal assemblages within the Williston Basin. In the Bighorn succession, the deep subtidal brachiopod biofacies is confined to deposits that correlate with the Gunn-Penitentiary facies of the Stony Mountain Formation. The gastropod and crinoid biofacies occur at various levels in the succession, with the gastropod biofacies being shallow subtidal, and the crinoid biofacies approaching the transition to more restricted, inner, shallow subtidal conditions. The dasyclad biofacies, characterized by *Fisherites*, occurs in certain shallow subtidal deposits within the interval that corresponds to the lower Red River Formation. The coral biofacies is represented in open, shallow subtidal deposits at the base of two cycles in the upper Red River–Stony Mountain interval.

In the Williston Basin, some of the characteristic Red River–Stony Mountain corals range into the Stonewall Formation (Elias, 1989; Elias and Young, 2004; Elias et al., in press). They were joined in the lower Stonewall Formation by a few exotic taxa, including genera that came from the continental margin (e.g., *Tryplasma*) and species that may have been derived from continental margin forms (e.g., *Streptelasma*? *hindi*). These arrivals are considered to reflect cooling of the epicontinental sea, leading up to the Hirnantian glacial maximum. New data, some of which are presented in this guidebook, place the disappearance of characteristic Red River–Stony Mountain macrofossils a short distance below the *t*-marker bed in the Stonewall Formation. This is considered to represent the first pulse of the Late Ordovician mass extinction, associated with the onset of the major Hirnantian glaciation. Additional new data indicate that the coral-dominated assemblage in the Stonewall Formation above the *t*-marker, which includes *Streptelasma* and *Propora*, resembles the Edgewood Assemblage that occurs in Hirnantian-age strata in the east-central U.S.A. (Elias and Young, 1998; Elias et al., in press). Above the Stonewall Formation, the macrofauna of the Fisher Branch Formation is best known through the work of Stearn (1956). This Rhuddanian-age fauna is the first record of the Early Silurian biotic recovery in the Williston Basin. In the stratigraphic section at Grand Rapids, Manitoba, Johnson and Lescinsky (1986) and Jin et al. (1999) reported assemblages that vary in taxonomic diversity, composition, and relative abundance, including two intervals in which the brachiopod *Virgiana decussata* is strongly dominant.

The Williston Basin outcrop belt

Overview

Ordovician and Silurian strata are exposed in an outcrop belt on the northeastern side of the Williston Basin (Figure 5). This belt extends from southern to west-central Manitoba and into adjacent east-central Saskatchewan. The history of stratigraphic studies and nomenclature in Manitoba has been summarized by Andrichuk (1959), McCabe and Bannatyne (1970), McCabe (1971), Cowan (1971), Johnson and Lescinsky (1986), and Young et al. (2008). For work conducted in Saskatchewan, refer to Kupsch (1952) and Haidl (1992). The stratigraphic column in southern Manitoba, as recognized in this guidebook, is shown in Figure 6. Interpretations of depositional environments have been provided in a number of stratigraphic and paleontologic studies (e.g., Andrichuk, 1959; Cowan, 1971; Elias, 1982, 1991; Westrop and Ludvigsen, 1983; Johnson and Lescinsky, 1986; Elias et al., 1988; Young and Elias, 1999; Jin and Zhan, 2001; Young et al., 2007, 2008, 2012). The history of systematic paleontologic studies has been summarized by Stearn (1956), Elias (1983), Elias et al. (1988), Lobdell (1992), Jin and Zhan (2001), and Young et al. (2008). Faunal lists have been provided in a number of stratigraphic studies (e.g., Baillie, 1951, 1952).

In Manitoba, the erosional edge of the Williston Basin outcrop belt parallels structure contours within the basin, giving the impression that the strata were deposited on the basin margin (Bezys and McCabe, 1996; Nicolas and Barchyn, 2008; Figures 1, 5). However, the isopach trends of Ordovician units are east-west, indicating that the outcrop belt exposes a dip section with more basinal deposits in the south (Stops 1–3, core-hole 69-2) and more marginal deposits in the north (Grand Rapids Uplands, Stops 4–8, core-hole M-6-79; Cormorant Hill, Stops 9–11, core-hole M-9-86). The amount of basinward thickening and facies variation decreased during the Ordovician, and Silurian strata are relatively uniform throughout southwestern Manitoba. On this field trip, we will examine the Upper Ordovician Stony Mountain and Stonewall formations, and the Fisher Branch Formation at the base of the Lower Silurian Interlake Group (Figure 6).

Stratigraphic and depositional features

The Stony Mountain Formation decreases in thickness northward (Bezys and McCabe, 1996). In the southern area, it has a thickness of 38.4 m in core-hole 69-2 (Cowan, 1977; this guidebook; for location see Figure 1). In the north, its thickness is 31.4 m in core-hole M-6-79 (McCabe, 1979) and 31.5 m in core-hole M-9-86 (McCabe, 1986). The lower part of the formation (i.e., below the Gunton Member; Figure 6) has a thickness of 22.6 m in core-hole 69-2 (Cowan, 1977), 13.8 m in core-hole M-6-79 (McCabe, 1979), and 8.4 m in core-hole M-9-86 (McCabe, 1986). At the type section of the Stony Mountain Formation in the south (Stop 1), the lower part of the formation comprises argillaceous limestone with limestone interbeds in the Gunn Member, overlain by argillaceous dolostone of the Penitentiary Member. The Gunn Member is the most basinal facies, with relatively deep, subtidal deposits that formed under open marine conditions during the last major transgressive event in the Ordovician (Elias, 1991; Figure 6). The lithology of the Gunn Member changes rapidly northward, becoming like that of the Penitentiary Member (Cowan, 1971; McCabe, 1980; Bezys and McCabe, 1996). The significant argillaceous content of the lower Stony Mountain Formation in the south decreases northward, disappearing midway between the southern and northern ends of the outcrop belt (Porter and Fuller, 1959, Figure 11). In the northern part of the belt, strata in the lower Stony Mountain Formation are referred to in this guidebook as Gunn/Penitentiary equivalent (Stop 4).

Compared with the lower Stony Mountain Formation, the upper part of the formation was deposited under shallower, more restricted and fluctuating conditions (Figure 6). The mottled and nodular dolostone of the Gunton Member is relatively uniform in lithology throughout the outcrop belt (Bezys and McCabe, 1996; Stops 1, 5, 6). It represents deposition in shallow subtidal, somewhat open to restricted conditions. This member thickens northward in the outcrop belt (see McCabe, 1980, Figure GS-12-1). Its thickness is 10.9 m in core-hole 69-2 (Cowan, 1977; this guidebook), 14.1 m in core-hole M-6-79 (this guidebook), and 18.1 m in core-hole M-9-86 (McCabe, 1986). Dolostone of the overlying Williams Member is more argillaceous and arenaceous at the type section in the south (Stop 2) than in the north (Stops 7, 9). Deposition occurred under very shallow, restricted, intertidal conditions, ending with subaerial exposure. The uppermost bed of the Williams Member is arenaceous dolostone in the south (Stop 2), and thrombolitic dolostone in the north (Stops 7, 9). This member has a thickness of 4.9 m in core-hole 69-2 (this guidebook), 3.5 m in core-hole M-6-79 (this guidebook), and 5.0 m in core-hole M-9-86 (McCabe, 1986).

The Stonewall Formation has a relatively uniform thickness and lithology throughout the outcrop belt (Bezys and McCabe, 1996). Its thickness is 11.3 m in core-hole 69-2 (Cowan, 1977; this guidebook), 15.3 m in core-hole M-6-79 (this guidebook), and 12.1 m in core-hole M-9-86 (this guidebook). The formation can be divided into lower, middle, and upper intervals of dolostone, which are separated by comparatively thin, argillaceous to arenaceous, dolomitic marker beds. The marker between the lower and middle dolostone intervals is thinner and less prominent than the marker between the middle and upper intervals. The lower of these two markers is equated with the lower Stonewall marker bed known elsewhere in the Williston Basin, and is referred to as the LS-marker in this guidebook. The thickness of the LS-marker is 0.4 m at the type section of the Stonewall Formation (Stop 2), 0.7 m in core-hole 69-2, 0.3 m at Stop 7, 0.2 m in core-hole M-6-79, and 0.4 m in core-hole M-9-86 (this guidebook). The upper marker bed is the *t*-marker, which has a thickness of 1.6 m in core-hole 69-2, 0.7 m at Stop 8, 0.8 m in core-hole M-6-79, 0.5 m at Stop 10, and 0.7 m in core-hole M-9-86 (this guidebook). Strata at the top of the Stonewall Formation consist of argillaceous dolostone at Stop 3, and dolofloatstone at Stops 8, 10, and 11. It is uncertain whether these deposits represent the top Stonewall marker bed known elsewhere in the Williston Basin. The lower, middle, and upper parts of the Stonewall Formation as recognized in this guidebook represent depositional cycles. Each cycle attained shallow subtidal, somewhat open conditions in the dolostone interval, and ended with shallow, restricted conditions or usually subaerial exposure (Figure 6).

Assuming that the uppermost Stonewall Formation is Hirnantian in age and the Fisher Branch Formation is late Rhuddanian, the formational/systemic boundary may represent a hiatus of up to about 2 million years (see Figure 4a). The entire Lower Silurian Interlake Group displays little evidence of basin differentiation or geographic variability in lithologies (Bezys and McCabe, 1996). Dolostone of the Fisher Branch Formation was deposited during the first Silurian transgressive cycle, which reached water depths exceeding fair-weather wave base (Johnson and Lescinsky, 1986). In the southern part of the outcrop belt, at a location about 20 km west of Stop 2, the Fisher Branch Formation is 8.2 m thick (core-hole M-1-86; McCabe, 1986). In the northern part of the belt, its thickness is 8.1 m in core-hole M-6-79 (Stewart, 2012). The lower part of the Fisher Branch Formation is exposed at the type section in the southern part of the outcrop belt (Stop 3), and at Stops 8, 10, and 11 in the north.

Biogeographic and biostratigraphic features

In subsequent sections of this guidebook, data on macrofossil occurrences in the Stony Mountain, Stonewall, and Fisher Branch formations are presented for southern Manitoba (including Stops 1–3) and for new exposures in the Grand Rapids Uplands (including Stops 4–8). These data provide an opportunity for biogeographic and biostratigraphic comparisons between the southern, more basinal part of the Williston Basin outcrop belt and the northern, more marginal area. The biotic patterns that are revealed are a reflection of geographic variations in environmental conditions within the basin, and regional and global environmental changes through time.

Four solitary rugose coral genera occur in the lower Stony Mountain Formation in southern Manitoba (*Bighornia*, *Deiracorallium*, *Lobocorallium*, *Salvadorea*). *Lobocorallium* had the strongest preference for relatively deep, high energy, open marine conditions (Elias, 1982, 1991). It is the only one of these genera that has not been found in the lower Stony Mountain Formation in the Grand Rapids Uplands. Its absence probably reflects the overall environmental gradient from deeper water in the south to shallower in the north. Total faunal diversity decreases from the lower Stony Mountain Formation to the overlying Gunton Member, in both the south and north. This is attributed to the general temporal change toward shallower, more restricted conditions during deposition of this formation.

Within the Gunton Member at a northern location (Stop 5), there is an interval of intense *Thalassinoides* bioturbation mottling. Associated macrofossils include the gastropod *Maclurina*, up to 9 cm across, and the cyclocrinitid alga *Pasceolus*, reaching 3 cm in diameter. In southern Manitoba, the Selkirk Member of the Red River Formation (Figure 6) is famous for the stratigraphic and geographic continuity of *Thalassinoides* mottling (Young et al., 2008; Jin et al., 2012). In the Selkirk Member, giant *Maclurina* shells reach widths of more than 20 cm, and receptaculitids (morphologically comparable to cyclocrinitids) are represented by *Fisherites*, which can exceed 30 cm in diameter. Recurrences of the *Thalassinoides* facies in the Gunton Member of the Stony Mountain Formation, but with less vertical and lateral continuity than in the Selkirk Member of the Red River Formation, may reflect changes in the nature of deposition, biotas, and biotic activity from greenhouse conditions (Selkirk Member) to transitional icehouse conditions (Gunton Member).

The Williams Member at the top of the Stony Mountain Formation lacks macrofossils, except for a remarkable occurrence in the Grand Rapids Uplands (Young et al., 2007, 2012). The diverse biota in this Konservat-Lagerstätte includes groups that had mineralized shells (e.g., brachiopods, bivalves, gastropods, cephalopods) or skeletons of organic composition (e.g., eurypterids, pycnogonids, xiphosurids), as well as soft-bodied organisms (e.g., cnidarian medusae). Preservation of this biota involved rapid burial under anoxic and/or hypersaline conditions, in a restricted lagoon or tidal flat.

In the Stonewall Formation, solitary rugose corals are absent in the southern part of the outcrop belt. However, the widespread Stony Mountain genera *Bighornia*, *Deiracorallium*, and *Salvadorea* occur in the middle dolostone interval of the Stonewall Formation in the Grand Rapids Uplands. Some of the colonial corals show the same pattern. The rugosan *Palaeophyllum* and the tabulates *Calapoecia*, *Catenipora*, and *Ellisites* are present in the Stony Mountain Formation in the south and north. They are known from the Stonewall Formation only in the north, where *Palaeophyllum* occurs in the lower dolostone interval and all four genera are represented in the middle dolostone interval. The marginal area of the Williston Basin may have served as a refugium for some of the Stony Mountain corals, as the epicontinental sea cooled prior to the major Hirnantian glacial episode. The disappearance of these corals and the associated macrofauna a short distance below the *t*-marker in the Stonewall Formation is attributed to the first pulse of the Late Ordovician mass extinction event.

Exotic colonial corals unrelated to the Stony Mountain fauna began to arrive in the Williston Basin during deposition of the Stonewall Formation. The rugosan *Tryplasma* appears in the lower dolostone interval in the Grand Rapids Uplands. In the middle dolostone interval, *Tryplasma* and the tabulate *Angopora* occur in both the northern and southern areas of the outcrop belt, while the rugosan *Pycnostylus* is present in the north. The arrival of these corals is thought to reflect cooling of the epicontinental sea before the icehouse conditions of the Hirnantian. In the north, the conodont turnover from a Late Ordovician fauna, including *Aphelognathus*, to the *Ozarkodina* fauna is recorded in the upper part of the Stonewall Formation. A coral-dominated macrofauna occurs in the upper dolostone interval in the Grand Rapids Uplands. It includes the solitary rugosans *Streptelasma* and *Rhegmaphyllum*, and tabulates representing favositids and *Propora*. This fauna is considered to be a Hirnantian assemblage, which may have been introduced during an interglacial transgression.

The fauna of the Fisher Branch Formation includes the brachiopod *Virgiana decussata*, which occurs abundantly in the Grand Rapids Uplands and in the southern area of the outcrop belt (see also Johnson and Lescinsky, 1986; Jin et al., 1999). This genus dispersed widely in open marine conditions during the first major transgressive cycle in the Silurian. In the Williston Basin, the Fisher Branch fauna of Rhuddanian age is the earliest record of the Early Silurian biotic recovery.

Stop 1: Stony Mountain quarries, west pit

Overview

Stop 1 is at the west pit of the former City of Winnipeg quarries, on the north side of the town of Stony Mountain, Manitoba (Figures 1, 8a; UTM [NAD83/WGS84] 627357mE, 5550781mN; lat. 50°05′44″N, long. 97°13′09″W). We will examine the north side of this pit, and in particular, the exposures in the northwest area of the pit. The stratigraphic section includes the upper part of the Gunn Member, the Penitentiary Member, and the lower part of the Gunton Member of the Stony Mountain Formation (Figure 6).

The Stony Mountain Formation was named by Dowling (1900). His measured section of the exposure at Stony Mountain, based on the Gunn quarry, was quoted "from Mr. Tyrrell's notes for 1897" (Dowling, 1900, p. 88–89). The Gunn quarry can therefore be taken as the type section of the formation. Based on the location of the Gunn quarry as stated by Goudge (1945, p. 35–36), that quarry has been incorporated into the southwest area of the west pit of the former City of Winnipeg quarries. The northwest area of the west pit currently provides the best nearby reference section.

Okulitch (1943) divided the Stony Mountain Formation into members. He called the lower member the Stony Mountain Shale, and referred to the exposure near the crusher and office of the City of Winnipeg quarries. The crusher and office no longer exist, but were located at the west end of the west pit of the former City of Winnipeg quarries (see Elias, 1982, Figure 1). Currently, the northwest area of that pit provides the best nearby reference section. The Stony Mountain Shale was renamed the Gunn Member by Sinclair and Leith (1958). Okulitch (1943) identified the overlying unit as the Penitentiary Member. He noted that it was well exposed in the City of Winnipeg quarries, and that its entire thickness was preserved at Stony Mountain. The uppermost unit that occurs at Stony Mountain was named the Gunton Member by Okulitch (1943).

The stratigraphic section exposed at Stop 1 is illustrated in Figure 9. The stratigraphic distribution of macrofossils in the Stony Mountain Formation at Stony Mountain and vicinity is depicted in Figure 10.

Gunn Member, Stony Mountain Formation

The Gunn Member is reddish purple to greenish gray in colour. It consists predominantly of recessive, argillaceous, burrow mottled, fossiliferous mudstone to wackestone (Figure

Figure 8: *Satellite views of stops in southern Manitoba (base images from Google Maps, August 24, 2012).* ***a)*** *Stop 1 (circled) in the west pit of the former City of Winnipeg quarries, Stony Mountain.* ***b)*** *Stop 2 (circled) in Stonewall Quarry Park, Stonewall.* ***c)*** *Stop 3 (circled), 6 km northwest of Fisher Branch.*

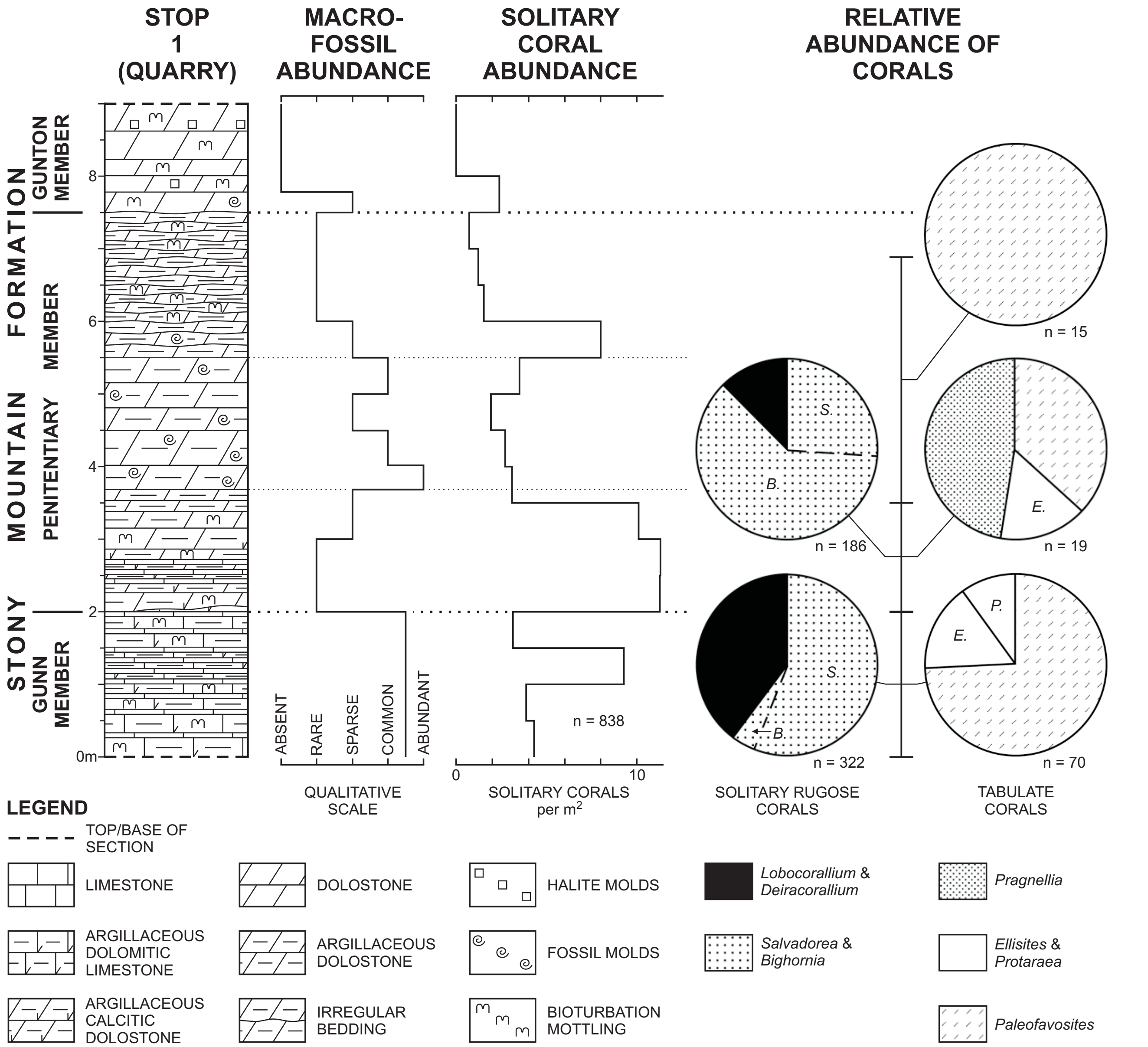

***Figure 9:** Lithostratigraphic section at Stop 1 (Stony Mountain quarries), and plots showing the abundance of macrofossils and solitary rugose corals, and the relative generic abundance of solitary rugose corals and the main tabulate corals in the indicated stratigraphic intervals (based on Elias, 1982, 1991; Young and Elias, 1999).*

11). Thin, hard interbeds, discontinuous beds, and lenses are composed of bioclastic packstone to grainstone. The packstone to grainstone beds typically have a sharp, scoured basal surface (Elias, 1982; Lukie, 1996; Figure 12). The types of bioclasts that are dominant vary among beds (e.g., brachiopods, trilobites). Some beds show lateral variation in relative abundance of the bioclast types. Common features within beds include normal grading and planar or cross laminations. Some of the beds are amalgamated. Bioturbation is less extensive than in the mudstone to wackestone intervals. The upper surface of packstone to grainstone beds may be encrusted by epifauna, penetrated by borings, and eroded. Some of the beds have undulatory surfaces representing megaripples.

The Gunn Member at Stony Mountain is widely known for the excellent preservation, abundance, and diversity of macrofossils (Figures 9, 10). The majority of specimens were buried in depositional positions, rather than possible life orientations (e.g., Elias, 1982). Some show little to no evidence of abrasion, but most were abraded to highly abraded prior to final burial. Some of the brachiopods and almost all of the trilobites and echinoderms were disarticulated. The most conspicuous fossils are brachiopods, followed by solitary rugose corals and bryozoans. Faunal diversity is very high (Figure 10). Brachiopods represent the *Diceromyonia storeya* community (Jin and Zhan, 2001). The dominant solitary rugosan is *Salvadorea* and the dominant tabulate coral is *Paleofavosites* (Elias, 1982; Young and Elias, 1999; Figure 9).

Deposition of the Gunn Member occurred under normal, open marine, subtidal conditions during a major transgression that was accompanied by a substantial influx of siliciclastic material (Elias, 1991; Figure 6). Water depth was relatively great, but above storm wave-base. The mudstone to wackestone

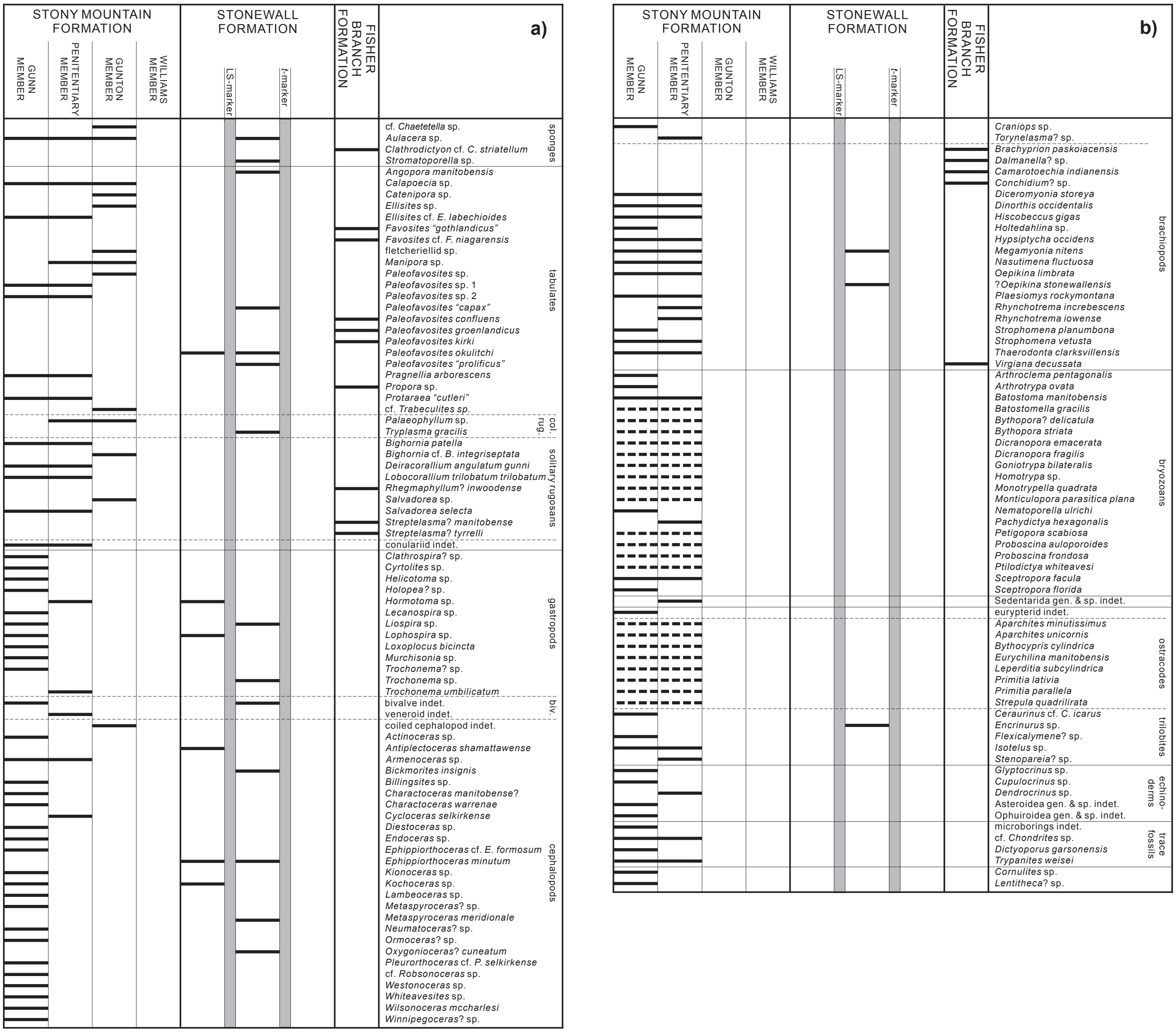

***Figure 10:** Stratigraphic distribution of macrofossils in southern Manitoba; part **a)** is continued in part **b)**. Data are based on the Stony Mountain Formation at Stony Mountain and vicinity (Young et al., 2008 and references cited on p. 97 therein), Stonewall Formation at Stonewall quarries (Stearn, 1956), and Fisher Branch Formation in the Fisher Branch area and the Narcisse area about 45 km south of Fisher Branch (Stearn, 1956). Range bars indicate presence within, but not necessarily throughout, a stratigraphic interval; dashed range bars indicate presence in the Gunn and/or Penitentiary members of the Stony Mountain Formation. Thin horizontal lines separate major fossil groups (solid) and subgroups (dashed). Abbreviations: col. rug. = colonial rugosans, biv. = bivalves.*

intervals are considered to represent relatively slow, lower energy, background sedimentation (Elias, 1982; Lukie, 1996). The packstone to grainstone interbeds, discontinuous beds, and lenses are interpreted as high-energy storm deposits that commonly underwent comparatively rapid cementation. The contact between the Gunn Member and the overlying Penitentiary Member is placed at the uppermost surface of the interval with typical Gunn lithology (Elias, 1982; Figure 13a).

Penitentiary Member, Stony Mountain Formation

The entire thickness of the dolomitic Penitentiary Member is exposed at Stop 1 (Figures 11, 13, 14). This member is generally yellowish orange, but colours in areas near the base may resemble those of the underlying Gunn Member, and there are commonly two intervals near the top with irregular reddish colouration. Three units can be recognized within the Penitentiary Member at this location (Elias, 1982; Young and Elias, 1999).

The lower, 1.7-m-thick unit of the Penitentiary Member is mainly argillaceous mudstone to wackestone, with several thin interbeds of bioclastic packstone to grainstone (Figure 9). There is a thin, discontinuous bed at the base of the member. In places, this bed features inclined laminae, reworked fossils, and a bored, encrusted upper surface overlain by a seam

Figure 11: *Northwest corner of the pit at Stop 1, with a person pointing to the contact between the Gunn Member and the overlying Penitentiary Member of the Stony Mountain Formation (photographed in 2012; see Figure 9).*

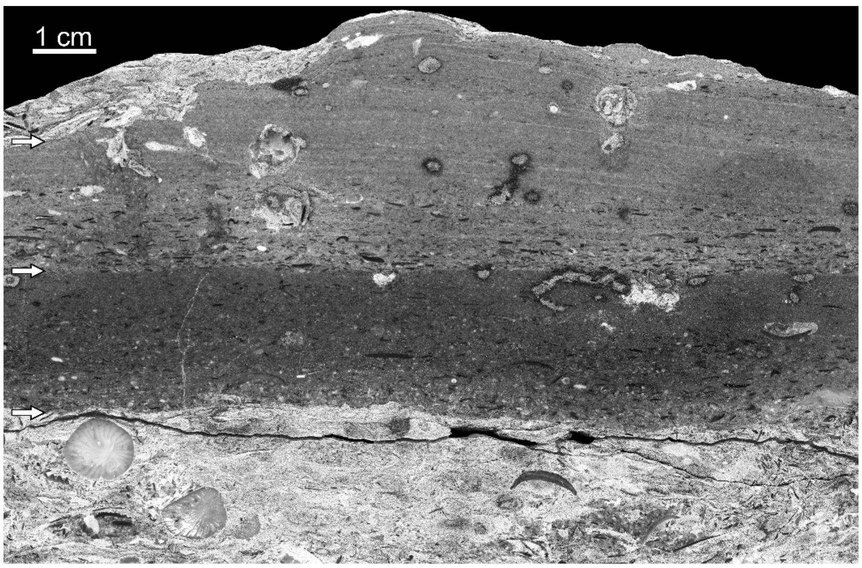

Figure 12: *Vertical polished slab (stratigraphic "up" toward top of figure) showing an amalgamated storm bed within argillaceous, fossiliferous deposits of the Gunn Member, Stony Mountain Formation (from east pit of former City of Winnipeg quarries, Stony Mountain). On left side, lower arrow points to the scoured basal surface of the amalgamated bed. Middle arrow points to the planar boundary between the lower graded interval and the upper interval, which is graded and has inclined laminations; note bioturbation within the amalgamated bed. Upper arrow points to the top of the amalgamated bed, which in places retained its original undulatory surface (right side to centre of figure), but in other places was eroded prior to subsequent deposition (left side of figure).*

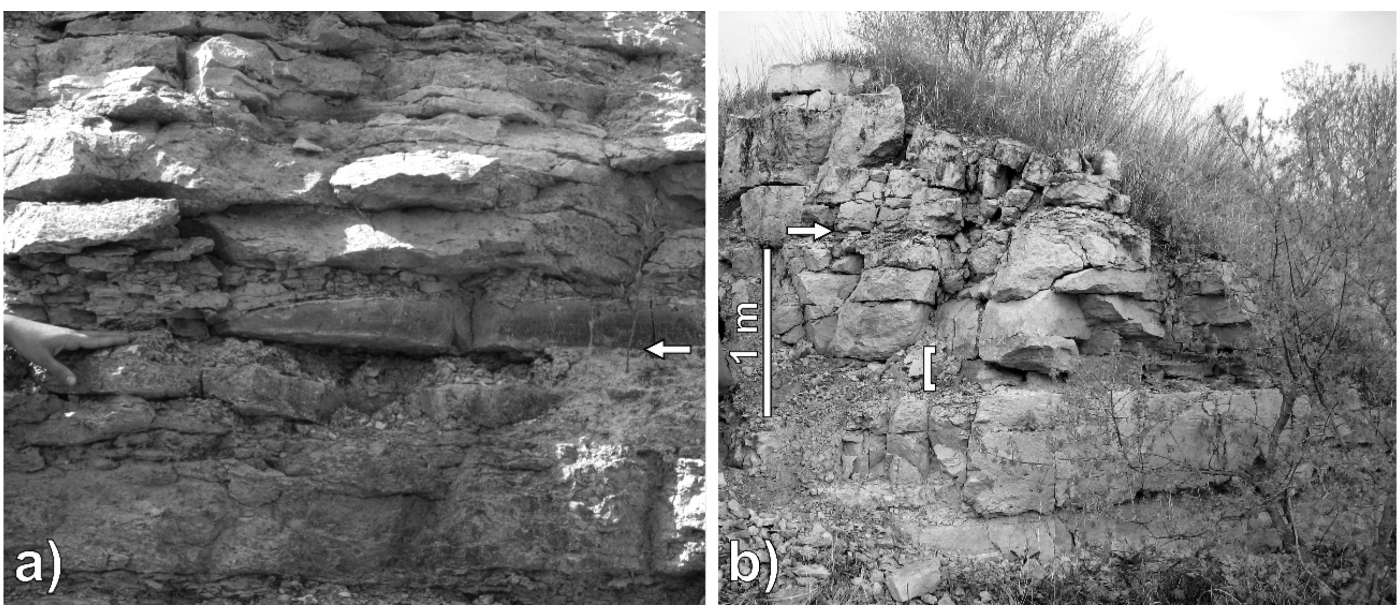

Figure 13: *Contacts between members of the Stony Mountain Formation at Stop 1 (see Figure 9). **a)** Contact between the Gunn Member and the overlying Penitentiary Member (indicated by arrow and hand) in the northwest corner of the pit (photographed in 1980); note the discontinuous basal bed of the Penitentiary Member, which is present above the arrow but pinches out to the left and is absent at the hand. **b)** Contact between the Penitentiary Member and the overlying Gunton Member (indicated by arrow) at the top of the knoll in the northwest area of the pit (photographed in 2009); bracket indicates the uppermost reddish interval in the Penitentiary Member.*

Figure 14: *Northwest area of the pit at Stop 1, showing the Penitentiary Member of the Stony Mountain Formation (photographed in 2012; see Figure 9). Two reddish intervals (brackets in upper centre) occur in the upper Penitentiary Member.*

of greenish clay. Macrofossils, dominated by brachiopods, are rare to sparse in the lower unit of the Penitentiary Member, but solitary rugose corals show their greatest abundance. The dominant solitary rugosan is *Bighornia*, and *Pragnellia* is the most abundant tabulate coral. This unit was deposited under environmental conditions that restricted overall faunal abundance, compared with the underlying Gunn Member.

The middle, 1.8-m-thick unit of the Penitentiary Member consists of thickly bedded, argillaceous, fossiliferous dolostone that was originally mostly wackestone with some mudstone and packstone (Figure 9). Macrofossils, preserved as molds (Figure 15a), are mainly brachiopods, solitary rugose corals, and bryozoans. Overall abundance is generally greater than in the underlying unit of the Penitentiary Member, but solitary corals are less common. The dominant colonial coral is *Paleofavosites*. This unit represents a return to more favourable, open marine, subtidal conditions that promoted overall faunal abundance.

The upper, 2-m-thick unit of the Penitentiary Member consists of argillaceous dolostone in thinner, irregular beds (Figure 9). Some intervals show bioturbation mottling. Macrofossils, preserved as molds, show an upward decrease in overall abundance from sparse to rare, although there is a peak in the abundance

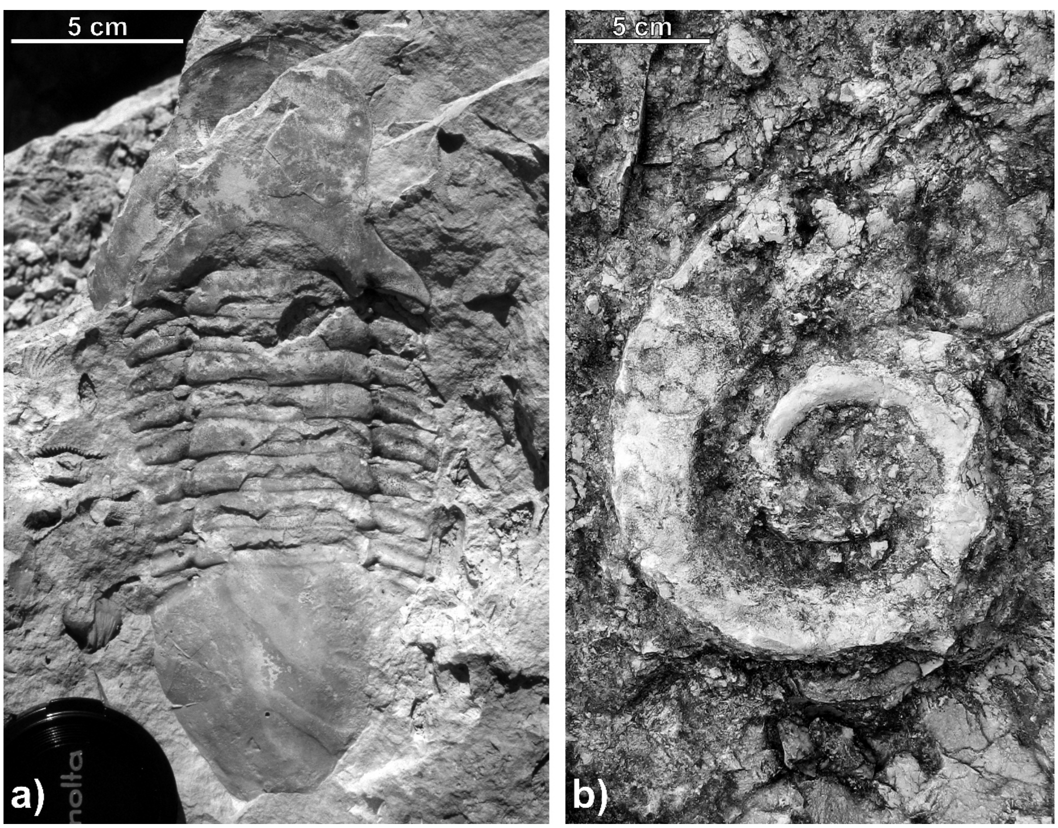

Figure 15: *Fossils in the Stony Mountain Formation at Stop 1.* ***a)*** *Molds are common in the middle interval of the Penitentiary Member (see Figure 9), but this large, articulated specimen of the trilobite* Isotelus *sp. is unique.* ***b)*** *Macrofossils are generally absent above the basal interval of the Gunton Member (see Figure 9); this coiled cephalopod is therefore unusual.*

of solitary rugose corals at the base of the unit. This unit was deposited under conditions of increasing environmental restriction.

Overall biodiversity is lower in the Penitentiary Member than in the underlying Gunn Member (Figure 10). Most taxa in the Penitentiary Member also occur in the Gunn Member, but differences in relative abundance have been documented for the *Diceromyonia storeya* brachiopod community (Jin and Zhan, 2001) and for solitary and colonial coral associations (Elias, 1982, 1991; Young and Elias, 1999; Figure 9). Differences in the coral associations reflect environmental conditions such as water depth, degree of restriction, and substrate conditions. The Penitentiary Member is thought to record the transition from generally deeper, open marine, subtidal conditions during deposition of the lower Stony Mountain Formation, to more restricted and shallower conditions in the upper part of the formation (Figure 6). Within this overall pattern, however, there was an abrupt change in conditions at the contact between the Gunn and Penitentiary members, and there were environmental variations during deposition of the Penitentiary Member.

Argillaceous dolostone of the Penitentiary Member grades upward into dolostone of the Gunton Member over several 10s of centimetres (Figure 13b). The contact is placed where the typical Gunton lithology becomes predominant.

Gunton Member, Stony Mountain Formation

The Gunton Member at Stop 1 is composed of extremely hard, thickly bedded, coarsely mottled, pale grayish orange dolostone (Figure 13b). Molds of macrofossils, including corals, are sparse in the basal, transitional interval of the member, but are essentially absent above that (Figures 9, 15b). The very low faunal abundance and diversity, and presence of halite molds, indicate deposition under restricted conditions. Higher in the Gunton Member at other locations in the vicinity of Stony Mountain, fossiliferous strata that contain a diversity of corals record the final return of relatively favourable subtidal conditions during deposition of the Stony Mountain Formation (Cowan, 1971; Young et al., 2008; Figures 6, 10).

Stop 2: Stonewall Quarry Park

Overview

Stop 2 is at Stonewall Quarry Park, on the north side of the town of Stonewall, Manitoba (Figures 1, 8b; UTM [NAD83/WGS84] 619760mE, 5555692mN; lat. 50°08′29″N, long. 97°19′26″W). We will examine strata in the test pit, as well as the main quarry beds (Figure 16). The stratigraphic section includes the uppermost part of the Williams Member of the Stony Mountain Formation, and the lower to middle portion of the overlying Stonewall Formation (Porter, 2011; Figure 6).

The Williams Member, with its type section in the test pit, was proposed by Smith (1963). The first published reference to the Williams Member was by Cowan (1971). The Stonewall Formation was established by Kindle (1914), to include all of the strata in southern Manitoba that he considered Silurian in age. He described the section in a quarry on the north side of Stonewall, which has always been taken as the type section of the formation (Stearn, 1956). That site is now preserved in Stonewall Quarry Park. Baillie (1951) restricted the Stonewall Formation to the lower part of his Interlake Group, and Stearn (1953) removed this formation from the group. Stearn (1956, Figure 2) showed where various authors placed the lower boundary of the Stonewall Formation at the type section.

Figure 17 illustrates the stratigraphic section exposed at Stop 2, the position of the boundary between the Stony Mountain and Stonewall formations as recognized in this guidebook, the carbon-isotope profile, and correlation of the section with core-hole 69-2. Figure 10 shows the stratigraphic distribution of macrofossils in the Stonewall Formation, based on the quarries at Stonewall. Note that macrofossils are unknown from the Williams Member of the Stony Mountain Formation in southern Manitoba.

Williams Member, Stony Mountain Formation

The Williams Member consists of argillaceous to arenaceous dolostone. The entire thickness of this lithology (as measured in core-hole 69-2; Figure 17) may once have been visible

Figure 16: *Overview of Stop 2, showing the test pit (left side) and the main quarry beds (right side) (photographed in 2009).*

in the pit at the Stonewall quarry, but the exposure was reduced by infilling over the years (Goudge, 1945, section described near bottom of p. 38; Baillie, 1951, p. 9–12; Stearn, 1956, p. 10–11). At present, only the uppermost part of the Williams Member can be seen at the bottom of the test pit (Figures 17, 18).

Stearn (1956, p. 11, Figure 2) placed the upper boundary of the Stony Mountain Formation at the top of his unit E, which consists of recessive, argillaceous and arenaceous dolomudstone. He included the hard, arenaceous dolostone of unit F at the base of the Stonewall Formation. The contact between units E and F is sharp and slightly undulatory (Figure 19a). Unit F contains rounded, sand-size carbonate clasts and frosted quartz grains (Figure 20a), and was described as “obscurely crossbedded” by Stearn (1956, p. 11). The contact between unit F and the overlying dolostone of unit G is sharp and irregular (Figure 19a).

The carbon-isotope profile for the section at Stop 2 shows a negative trend in units E and F, with a minimum value at the base of unit G, and rising values through units G and H to a stable baseline beginning a short distance above the bottom of unit J (Figure 17). This pattern suggests that the contact between units F and G may represent a period of subaerial exposure and significant erosional truncation (see Figure 7c). Considering also that unit F resembles the underlying strata in containing clastic material, the boundary between the Williams Member of the Stony Mountain Formation and the overlying Stonewall Formation is raised to the top of Stearn’s unit F (Figure 17).

Smith (1963) considered deposition to have been continuous from the Gunton Member to the Williams Member, with the change marked by termination of the upper Gunton coral fauna and an influx of terrigenous material in the Williams. The Williams Member lacks macrofossils in southern Manitoba (Figure 10). It is interpreted as the final regressive phase during deposition of the Stony Mountain Formation (Figure 6), under very shallow, restricted conditions that ended with subaerial exposure.

Stonewall Formation

The entire thickness of Stearn’s (1956) unit G is exposed in the test pit at Stop 2 (Figures 17, 18). This unit represents the lower dolostone interval of the Stonewall Formation. It is extremely hard, thickly bedded, coarsely mottled, and vuggy. Some of the vugs can be identified as molds of tabulate corals, and gastropods and cephalopods have also been reported (Figure 10). This unit records relatively open, shallow subtidal conditions during the first depositional cycle in the Stonewall Formation (Figure 6). The contact between unit G and the overlying unit H is sharp and irregular (Figure 19b).

Unit H of Stearn (1956) is recessive, occurring within the upper part of the test pit (Figure 18) and forming the quarry floor in much of the surrounding area (Figure 21). Except for a thin seam of brownish gray shale at the top, this unit consists of rubbly, argillaceous dolomudstone (Figure 19b). The dolomudstone is whitish gray to olive gray, with a reddish zone in the middle. The dolomudstone contains lighter coloured, spherical dolomitic nodules up to about 2 mm in diameter, which in some cases are intergrown with one another (Figure 20b).

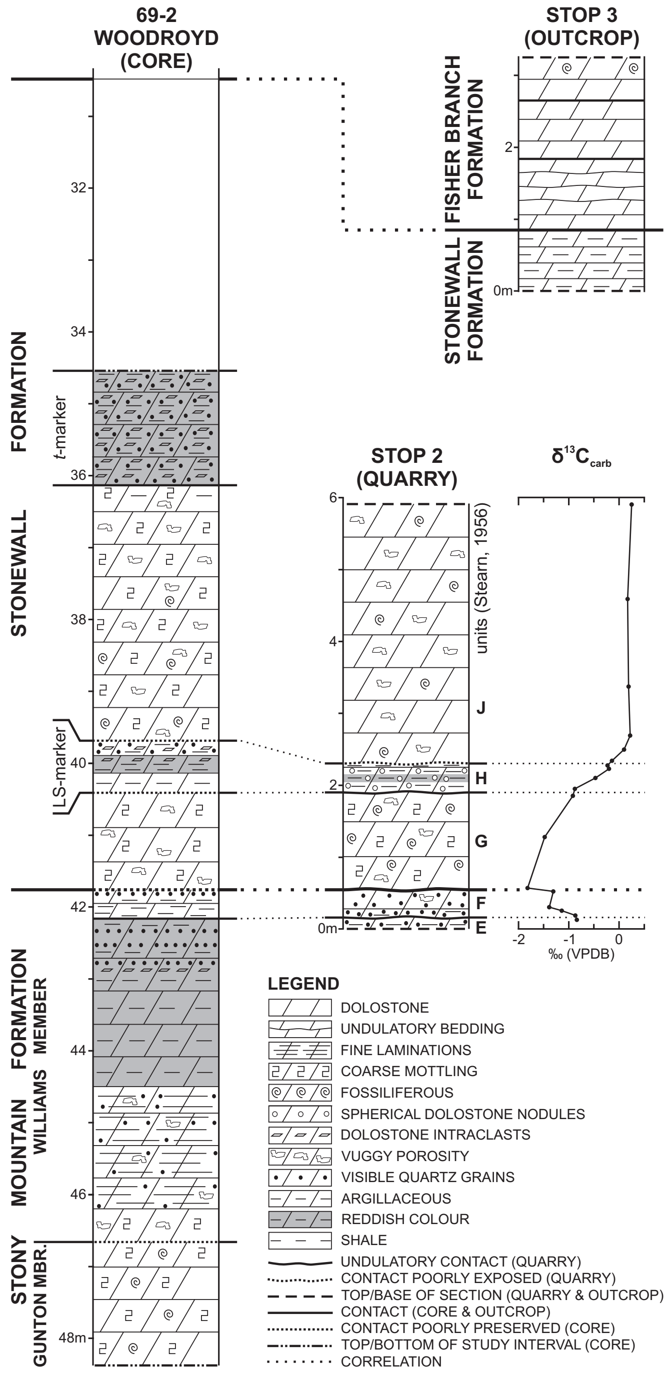

***Figure 17:** Lithostratigraphic sections and correlation of Stop 2 (Stonewall Quarry Park), Stop 3 (outcrops near Fisher Branch), and core-hole 69-2 (Woodroyd; Figure 1; UTM [NAD83/WGS84] 607980mE, 5568007mN; lat. 50°15'16"N, long. 97°29'07"W). For Stop 2, the section is based on Porter (2011) and shows the lettered stratigraphic units of Stearn (1956, p. 10–11, Figure 2); the $\delta^{13}C_{carb}$ profile is new. The section at Stop 3 is based on new data. Placement of the Stony Mountain–Stonewall formational contact at the top of Stearn’s unit F (rather than at the bottom) is new, as is recognition of the LS-marker in southern Manitoba. For core-hole 69-2, the study interval is based on Porter (2011) and the top of the Stonewall Formation is placed according to Cowan (1977).*

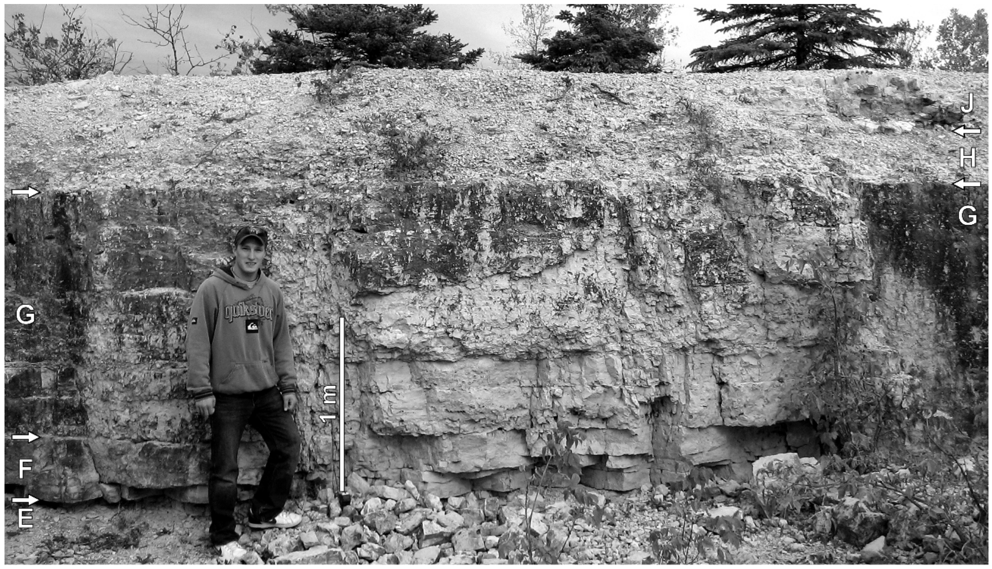

Figure 18: *Test pit at Stop 2 (photographed in 2010). Arrows on the left and right sides indicate contacts between the lettered units of Stearn (1956; see Figure 17). In this guidebook, the boundary between the Williams Member of the Stony Mountain Formation and the overlying Stonewall Formation is placed at the contact between units F and G; unit H is considered to represent the LS-marker in the Stonewall Formation.*

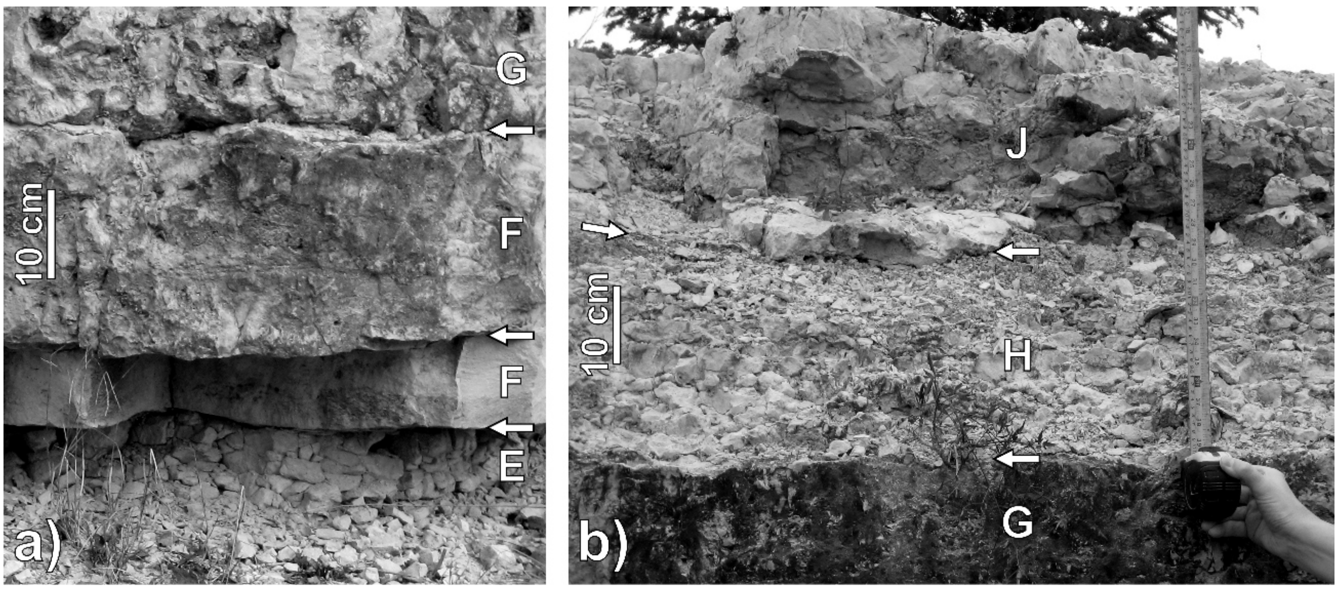

Figure 19: *Contacts in the test pit at Stop 2.* ***a)*** *Lower strata (photographed in 2010; area shown is in lower left of Figure 18). Lower arrow indicates the undulatory contact between units E and F of Stearn (1956); middle arrow indicates a contact within unit F; upper arrow indicates the irregular contact between units F and G of Stearn (1956), considered in this guidebook to represent the Stony Mountain–Stonewall formational boundary.* ***b)*** *Upper strata (photographed in 2010; area shown is in upper right of Figure 18). Lower, left-pointing arrow indicates the irregular contact between units G and H of Stearn (1956); upper, left-pointing arrow indicates the poorly exposed, apparently irregular contact between units H and J of Stearn (1956); position of the scale bar indicates the reddish zone in the middle of unit H; right-pointing arrow indicates the thin shale seam at the top of unit H. In this guidebook, unit H is considered to represent the LS-marker in the Stonewall Formation.*

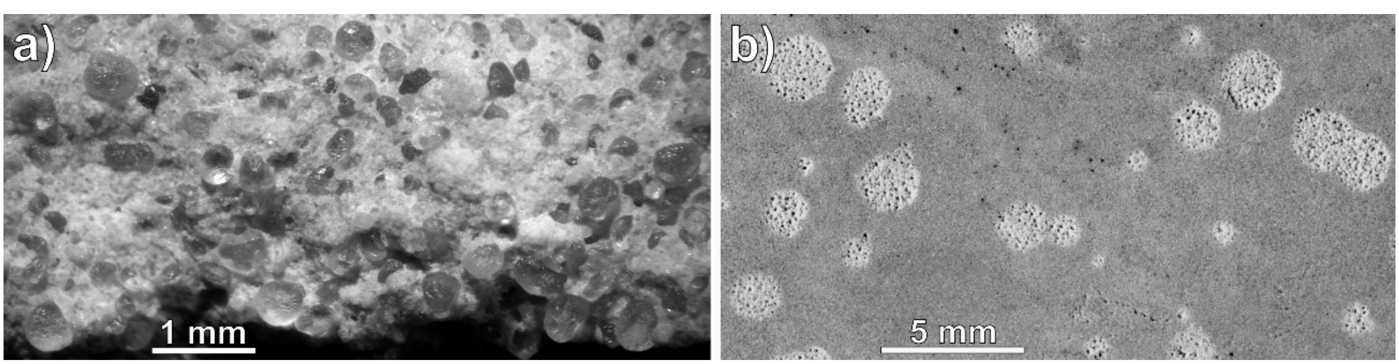

Figure 20: *Samples from the test pit at Stop 2.* ***a)*** *Frosted, rounded quartz sand grains on the basal surface of unit F of Stearn (1956; assigned in this guidebook to Williams Member, Stony Mountain Formation).* ***b)*** *Polished surface showing spherical dolostone nodules in unit H of Stearn (1956; considered in this guidebook to represent LS-marker in Stonewall Formation).*

Figure 21: *Main quarry beds of the Stonewall Formation at Stop 2 (photographed in 2009). Bottom of the 1-m scale bar is at the contact between unit H and the overlying unit J of Stearn (1956; see Figure 17). In this guidebook, unit H is considered to represent the LS-marker in the Stonewall Formation.*

This feature is common in some dolomudstones of the Silurian Interlake Group in the Williston Basin (Porter and Fuller, 1959; Cowan, 1971; Johnson and Lescinsky, 1986, Figure 4b). Porter and Fuller (1959, p. 165) used the term "pseudo-oölitic" for these "micrograined carbonate bodies, structureless or nearly so, of oölitic dimensions."

The main quarry beds at Stop 2 are unit J of Stearn (1956; Figures 17, 21). These strata represent the middle dolostone interval and the second depositional cycle of the Stonewall Formation (Figure 6). This dolostone is hard, thickly bedded, slightly mottled, and slightly vuggy. Macrofossils are more diverse than in the lower dolostone interval of the formation (unit G), and include stromatoporoids, colonial rugose and tabulate corals, gastropods, bivalves, cephalopods, brachiopods, and trilobites (Figure 10). The middle dolostone interval records the most open, normal marine, shallow subtidal conditions attained during deposition of the Stonewall Formation.

Based on correlation of the strata at Stop 2 with core-hole 69-2, the top of the quarry section is just a short distance below the projected position of the *t*-marker (Figure 17). Exposures of the *t*-marker bed of the Stonewall Formation are unknown in the southern part of the Williston Basin outcrop belt.

Stop 3: outcrops near Fisher Branch

Overview

Stop 3 is at a series of outcrop exposures along a northwest-facing ridge, 6 km northwest of the town of Fisher Branch, Manitoba (Figures 1, 8c). We will examine two exposures: site 3a (UTM [NAD83/WGS84] 593946mE, 5665518mN; lat. 51°08′00″N, long. 97°39′26″W) and site 3b (UTM [NAD83/WGS84] 593841mE, 5665437mN; lat. 51°07′58″N, long. 97°39′32″W). The stratigraphic section includes the uppermost part of the Stonewall Formation and the lower portion of the overlying Fisher Branch Formation (Figure 6). In this guidebook, the contact between these formations is considered to be the O-S systemic boundary.

The Fisher Branch Formation was proposed by Stearn (1956, p. 16) "for the medium-grained, thick-bedded dolomite that overlies the Stonewall formation." Stop 3 is at the type section that he designated. The stratigraphic section and its correlation with core-hole 69-2 are illustrated in Figure 17. Occurrences of macrofossils in the Fisher Branch Formation, based on the Fisher Branch area and the Narcisse area (about 45 km south of Fisher Branch), are depicted in Figure 10.

Stonewall Formation

The upper portion of the upper dolostone interval of the Stonewall Formation is exposed at Stop 3. It is recessive, and consists of argillaceous, "pseudo-oölitic" (see Stop 2) dolomudstone that lacks macrofossils (Figure 22). Deposition probably occurred under restricted, shallow marine conditions, during the regressive phase of the third cycle in the formation (Figure 6). It has not been determined whether these strata represent the top-Stonewall marker bed known elsewhere in the Williston Basin.

Fisher Branch Formation

The Fisher Branch Formation at Stop 3 is composed of hard dolostones. Dolomudstone occurs near the base, but the predominant lithology is bioturbated dolowackestone. Bedding in the basal 30-cm-thick interval is locally inclined, impinging on the presumably disconformable contact with the underlying Stonewall Formation (Figure 22b). Beds are undulatory in the overlying 65-cm-thick interval, and massive in the upper part of the exposures (Figures 22, 23). Macrofossils reported from the

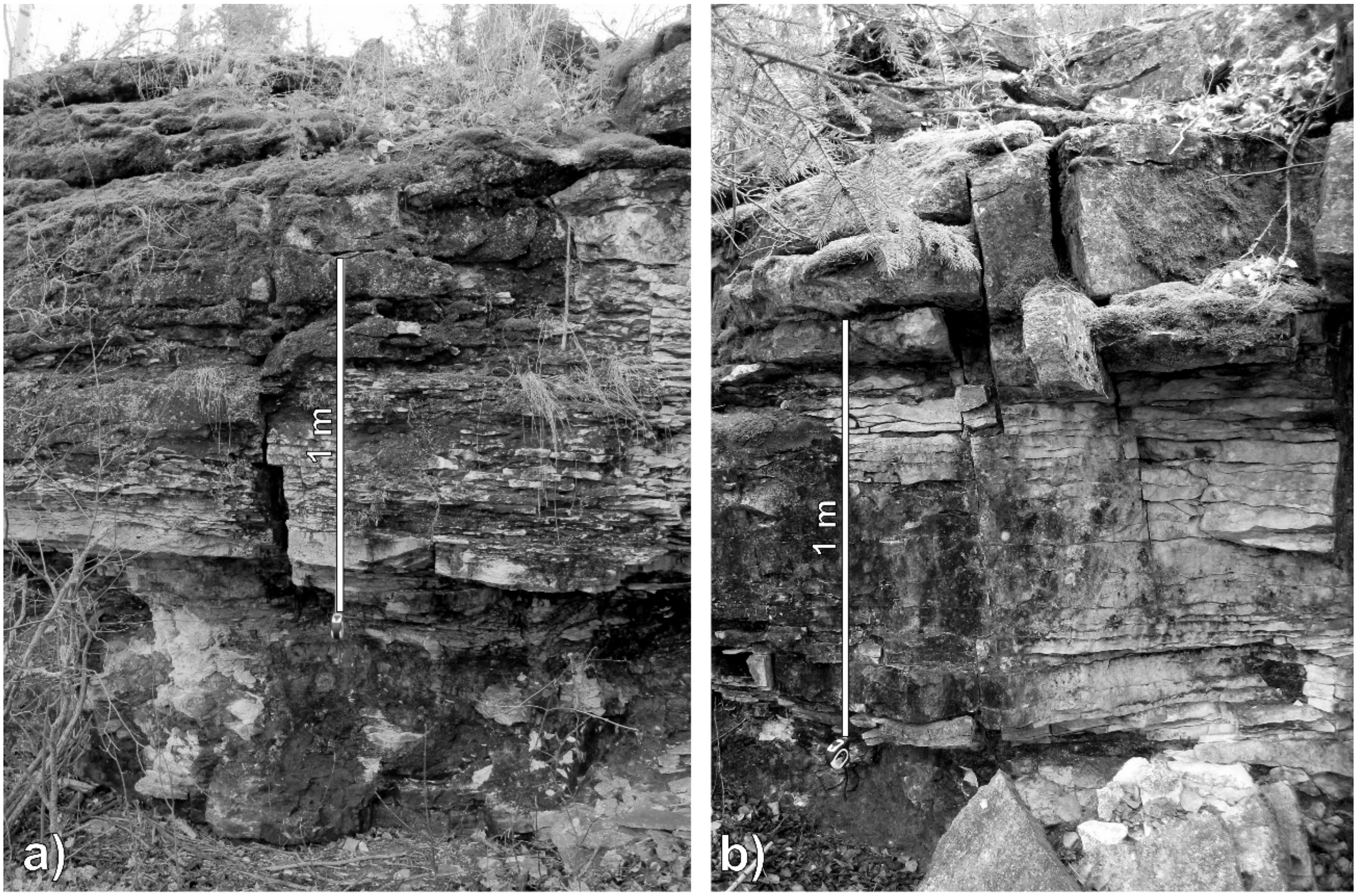

Figure 22: *Contact between the Stonewall Formation and the overlying Fisher Branch Formation in outcrops at Stop 3 (photographed in 2012; see Figure 17).* ***a)*** *Outcrop 45 m northeast of site 3a (contact is at bottom of 1-m scale bar).* ***b)*** *Outcrop at site 3a (contact is at bottom of 1-m scale bar). In the Fisher Branch Formation, bedding in the basal 30-cm interval is locally inclined (right half of figure b), bedding in the overlying 65-cm interval is undulatory, and bedding in the upper part of the exposures is massive.*

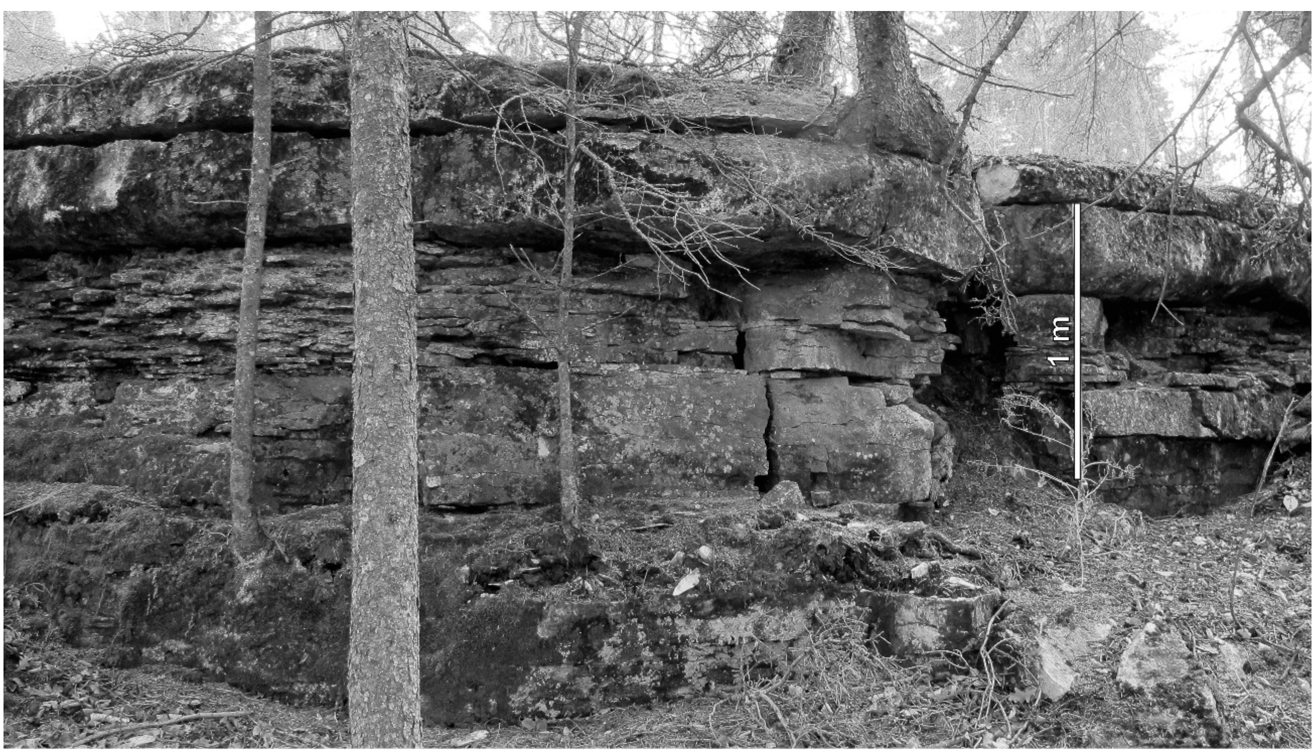

Figure 23: *Outcrop of the Fisher Branch Formation at Stop 3, site 3b (photographed in 2012; see Figure 17). Uppermost bed (above top of 1-m scale bar) contains fossils of the brachiopod* Virgiana *sp.*

Fisher Branch Formation at Stop 3 include solitary rugose corals, tabulate corals, and brachiopods (Stearn, 1956, column 4 in chart on p. 20). Stearn (1956, p. 17) noted that "Brachiopods and corals are present in abundance throughout the section and *Virgiana decussata* is especially abundant in the upper beds." The Fisher Branch Formation records the first transgression in the Silurian Period (Figure 6), which brought normal, open marine, shallow subtidal conditions to this area.

Stop 4: exposure beside Highway 6, 101.0 km north of Grand Rapids

Overview

Stop 4 is at a surface exposure on the east side of Provincial Trunk Highway 6, opposite a paved roundabout on the west side, in the Grand Rapids Uplands at a highway distance of 101.0 km north of the town of Grand Rapids, Manitoba (Figures 1, 24a; UTM [NAD83/WGS84] 488920mE, 5989160mN; lat. 54°03′02″N, long. 99°10′09″W). This exposure of the Stony Mountain Formation is in the upper part of the Gunn/Penitentiary equivalent (Figure 6).

A series of surface exposures on the east side of the highway, between 1.4 km north and 1.4 km south of Stop 4, reveals a succession of strata in the upper half of the Gunn/Penitentiary equivalent (Stewart, 2012). The stratigraphic position of each exposure, with respect to the base of the LS-marker bed in the vicinity of Stop 7, was determined using laser-aided surveying and was correlated with core-hole M-6-79 (Figures 24a, 25). Occurrences of macrofossils in the Gunn/Penitentiary equivalent at these exposures are shown in Figure 26.

Gunn/Penitentiary equivalent, Stony Mountain Formation

A large area of strata that are typical of the Gunn/Penitentiary equivalent is exposed on horizontal surfaces at Stop 4 (Figure 27). This unit consists of highly fossiliferous, bioturbated, dolomitic mudstone, approaching wackestone in places. Some of the bioturbation is identifiable as *Thalassinoides*. The

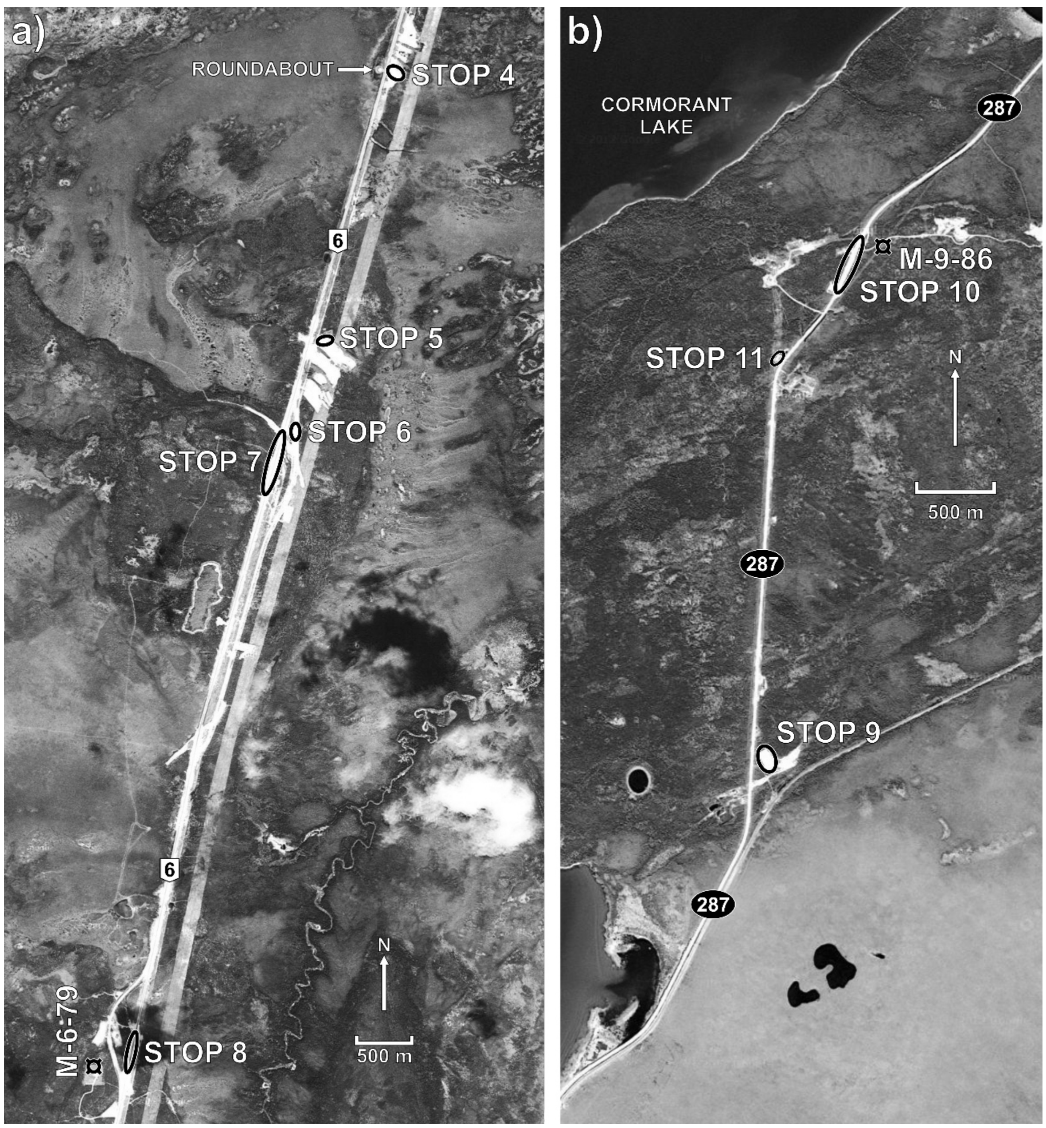

***Figure 24:** Satellite views of stops and core holes in west-central Manitoba. **a)** Stops 4–8 (circled) and core-hole M-6-79 (¤) along Provincial Trunk Highway 6 in the Grand Rapids Uplands (base image from Google Maps, August 22, 2012). Stop 8 is 91.9 km (highway distance) north of Grand Rapids. **b)** Stops 9–11 (circled) and core-hole M-9-86 (¤) along Provincial Road 287 at Cormorant Hill (base image from Google Maps, August 23, 2012). Stop 10 is 3.6 km (road distance) southwest of Cormorant.*

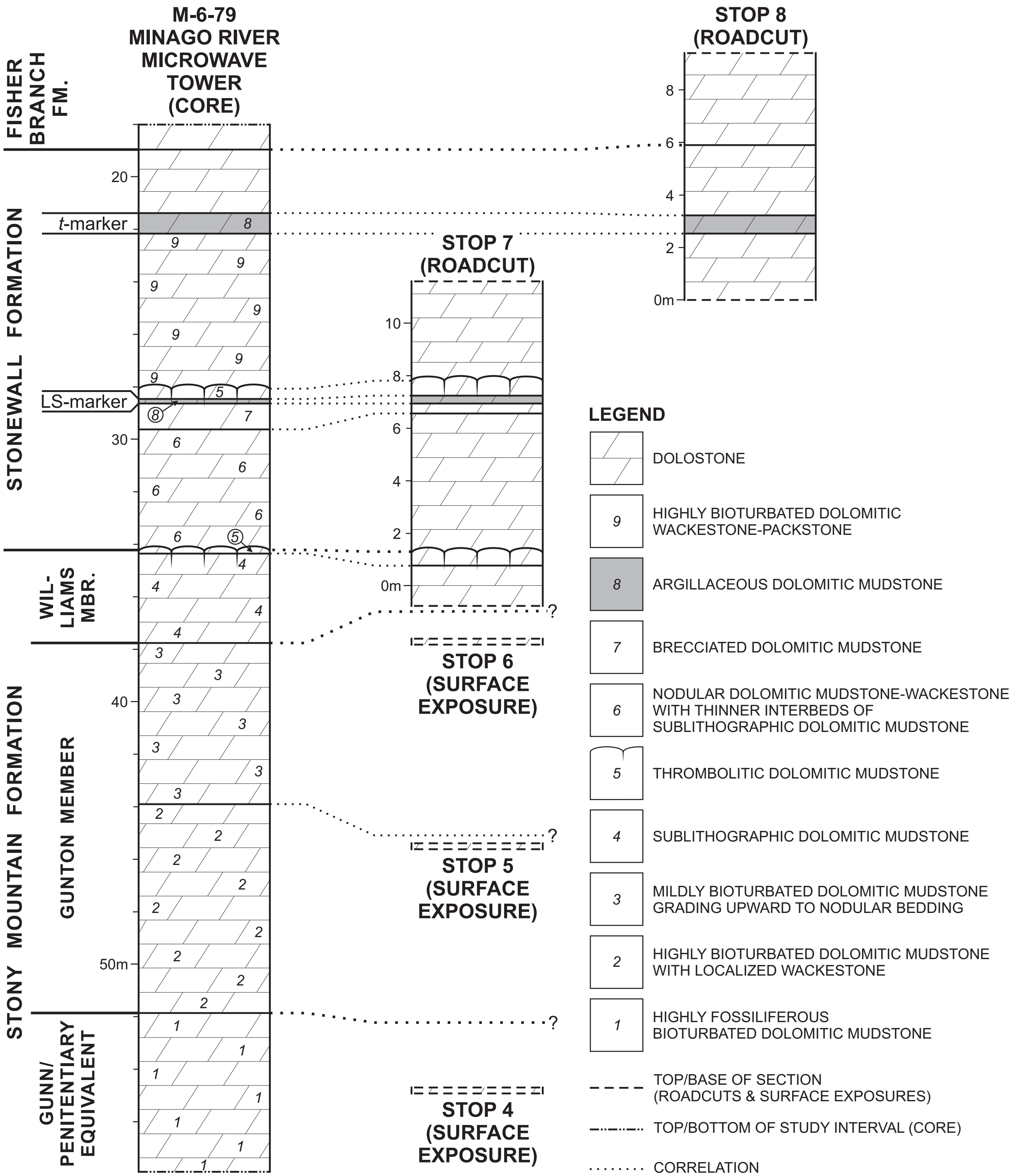

***Figure 25:** Lithostratigraphic sections and correlation of Stops 4–8 (Grand Rapids Uplands) and core-hole M-6-79 (Minago River Microwave Tower; Figure 24a; UTM [NAD83/WGS84] 486162mE, 5980110mN; lat. 53°58'09"N, long. 99°12'39"W). Stops 4–7 and the study interval in core-hole M-6-79 are based on Stewart (2012), and Stop 8 is based on Demski (2010).*

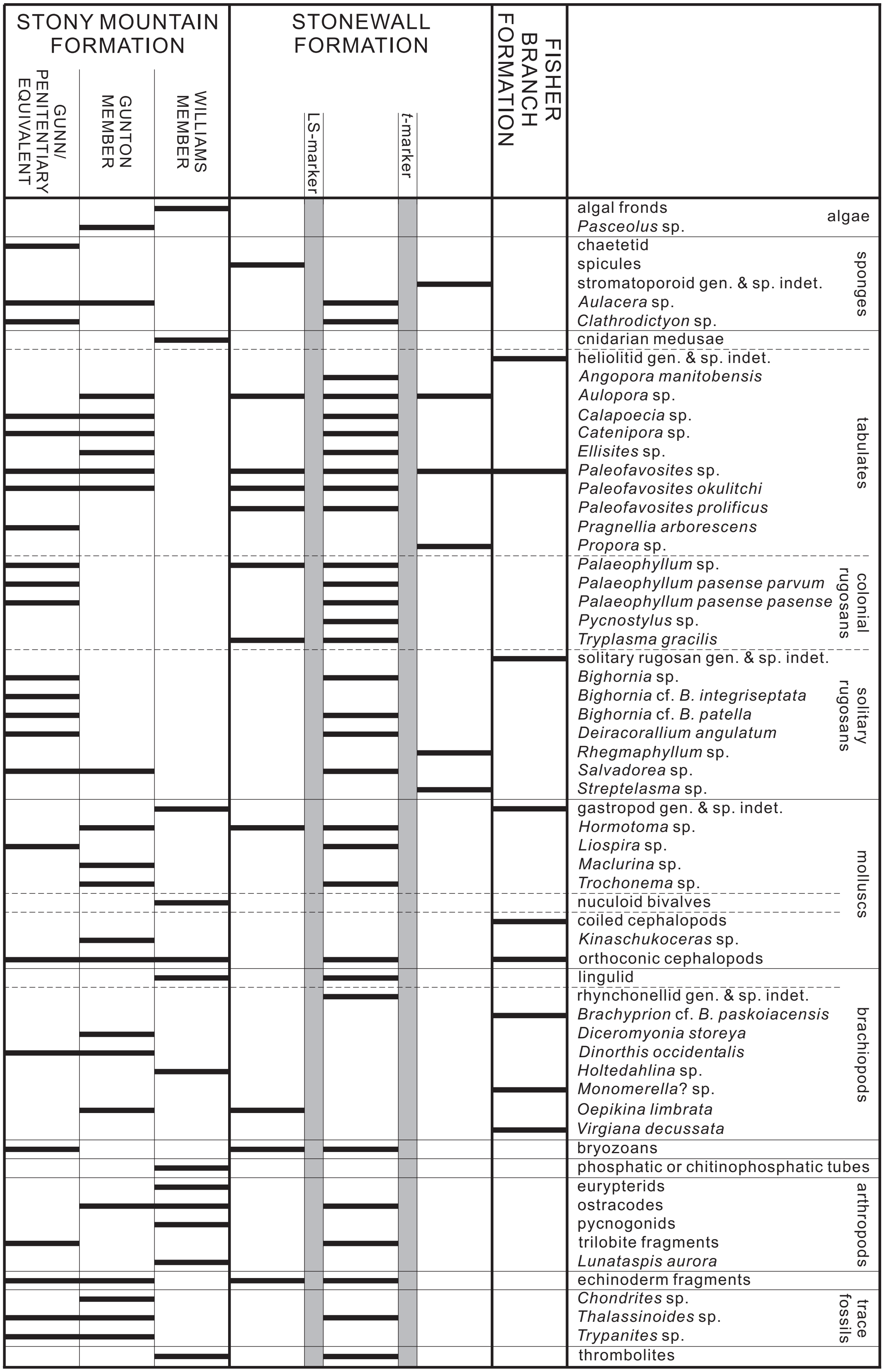

***Figure 26:** Stratigraphic distribution of macrofossils in the Grand Rapids Uplands, based on Stewart (2012) for the Stony Mountain Formation and Stonewall Formation below the t-marker, with additional data for the Williams Member of the Stony Mountain Formation from Young et al. (2007, 2012) and Rudkin et al. (2008), and on Demski (2010) and new information for the Stonewall Formation above the t-marker and the Fisher Branch Formation. Range bars indicate presence within, but not necessarily throughout, a stratigraphic interval. Thin horizontal lines separate major fossil groups (solid) and subgroups (dashed).*

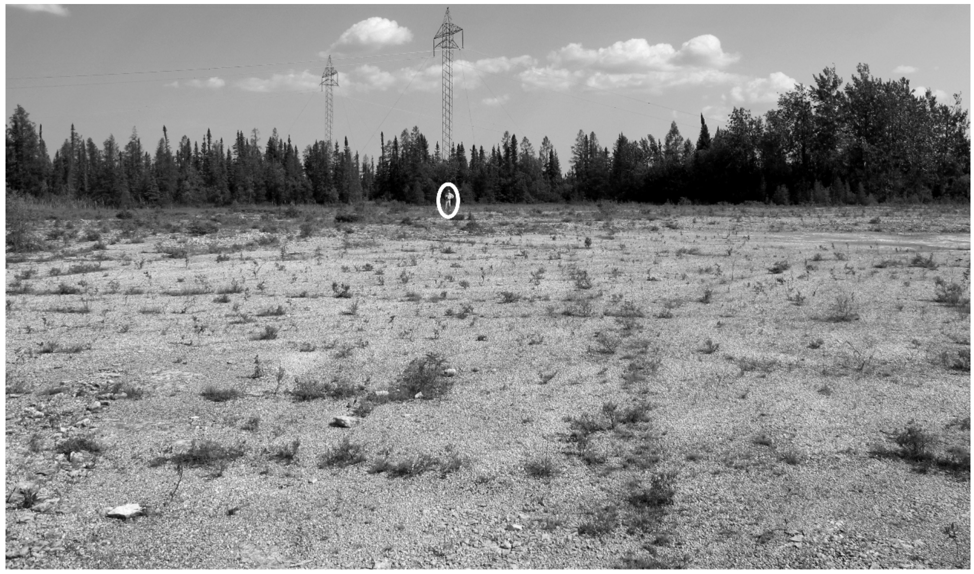

***Figure 27:** Surface exposure of strata in the lower Stony Mountain Formation (Gunn/Penitentiary equivalent) at Stop 4 (photographed in 2012; see Figure 25). Person (circled) is standing at the eastern extremity of the exposure.*

macrofauna is diverse (Figure 26), with solitary and colonial rugose corals and tabulate corals being especially conspicuous (Figure 28).

These strata generally represent normal, open marine, low to moderate energy, subtidal conditions. Occasional very small halite molds suggest that there were fluctuations in salinity or water circulation. The Gunn/Penitentiary equivalent is considered to be the deepest water deposit within the Stony Mountain Formation (Figure 6). However, water depth was probably somewhat shallower than in southern Manitoba, where more basinal deposits of the Gunn and Penitentiary members accumulated (e.g., Stop 1).

The contact between the Gunn/Penitentiary equivalent and the overlying Gunton Member is not exposed, but in core-hole

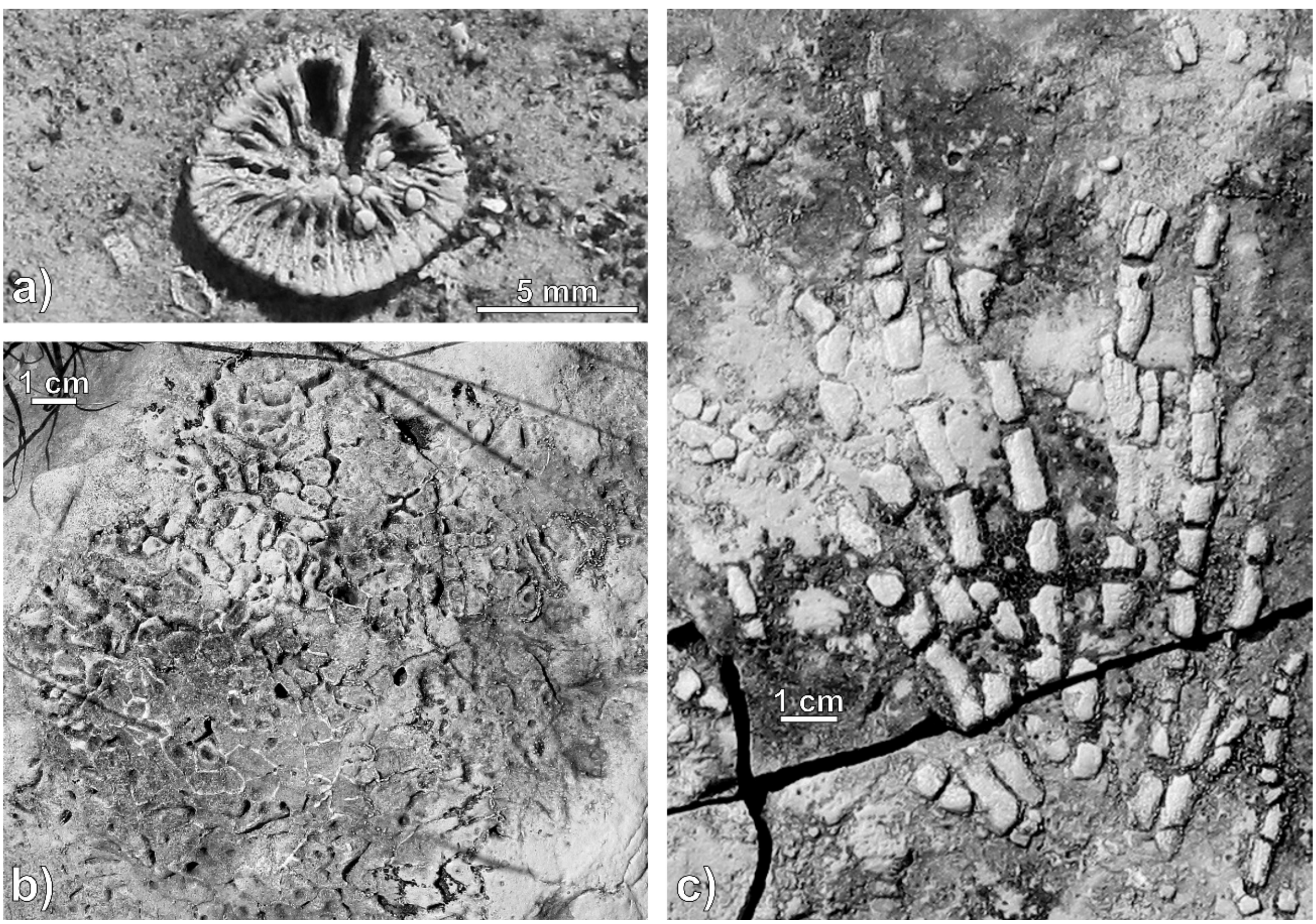

***Figure 28:** Fossils on bedding surfaces in the lower Stony Mountain Formation (Gunn/Penitentiary equivalent) at Stop 4. **a)** Solitary rugose coral* Bighornia *cf.* B. patella*. **b)** Tabulate coral* Catenipora *sp.* ***c)** Tabulate coral* Pragnellia arborescens.

M-6-79 it is gradational. There is an upward increase in the pervasiveness of *Thalassinoides*-type bioturbation and a decrease in the abundance of macrofossils.

Stop 5: exposure beside Highway 6, 98.4 km north of Grand Rapids

Overview

Stop 5 is at a surface exposure on the east side of Provincial Trunk Highway 6, in the Grand Rapids Uplands at a highway distance of 98.4 km north of the town of Grand Rapids, Manitoba (Figures 1, 24a; UTM [NAD83/WGS84] 488220mE, 5986660mN; lat. 54°01′41″N, long. 99°10′47″W). This exposure of the Stony Mountain Formation is near the top of the lower part of the Gunton Member (Figure 6).

Stop 5 and several nearby surface exposures reveal a succession of strata near the top of the lower part of the Gunton Member (Stewart, 2012). The stratigraphic position of each exposure, with respect to the base of the LS-marker bed in the vicinity of Stop 7, was determined using laser-aided surveying and was correlated with core-hole M-6-79 (Figures 24a, 25). A combined tabulation of macrofossil occurrences in the lower and upper parts of the Gunton Member is shown in Figure 26.

Gunton Member, Stony Mountain Formation

A large surface area of strata that are typical of the lower part of the Gunton Member is exposed at Stop 5 (Figure 29a). The lower part of the member consists of highly bioturbated, dolomitic mudstone with wackestone in places. Bioturbation identifiable as *Thalassinoides* is characteristic, and is spectacularly exposed at this stop (Figure 29b). Unfortunately, the surface is undergoing degradation due to weathering.

Macrofossils are sparse on the extensive *Thalassinoides* surface at Stop 5. Most are gastropods, including large shells of *Maclurina* up to 9 cm across (Figure 29c). Specimens of the cyclocrinitid alga *Pasceolus*, up to about 3 cm in diameter, occur a short distance below the *Thalassinoides* surface.

Compared with the Gunn/Penitentiary equivalent, the lower part of the Gunton Member contains less bioclastic material and has lower macrofossil abundance and overall biodiversity (Figure 26). There is a reduction in the diversity of solitary rugose corals, and a complete loss of colonial rugosans. Deposition probably occurred under somewhat more restricted and shallower, subtidal conditions. The lower part of the Gunton Member marks the beginning of the overall regressive phase during deposition of the upper Stony Mountain Formation (Figure 6).

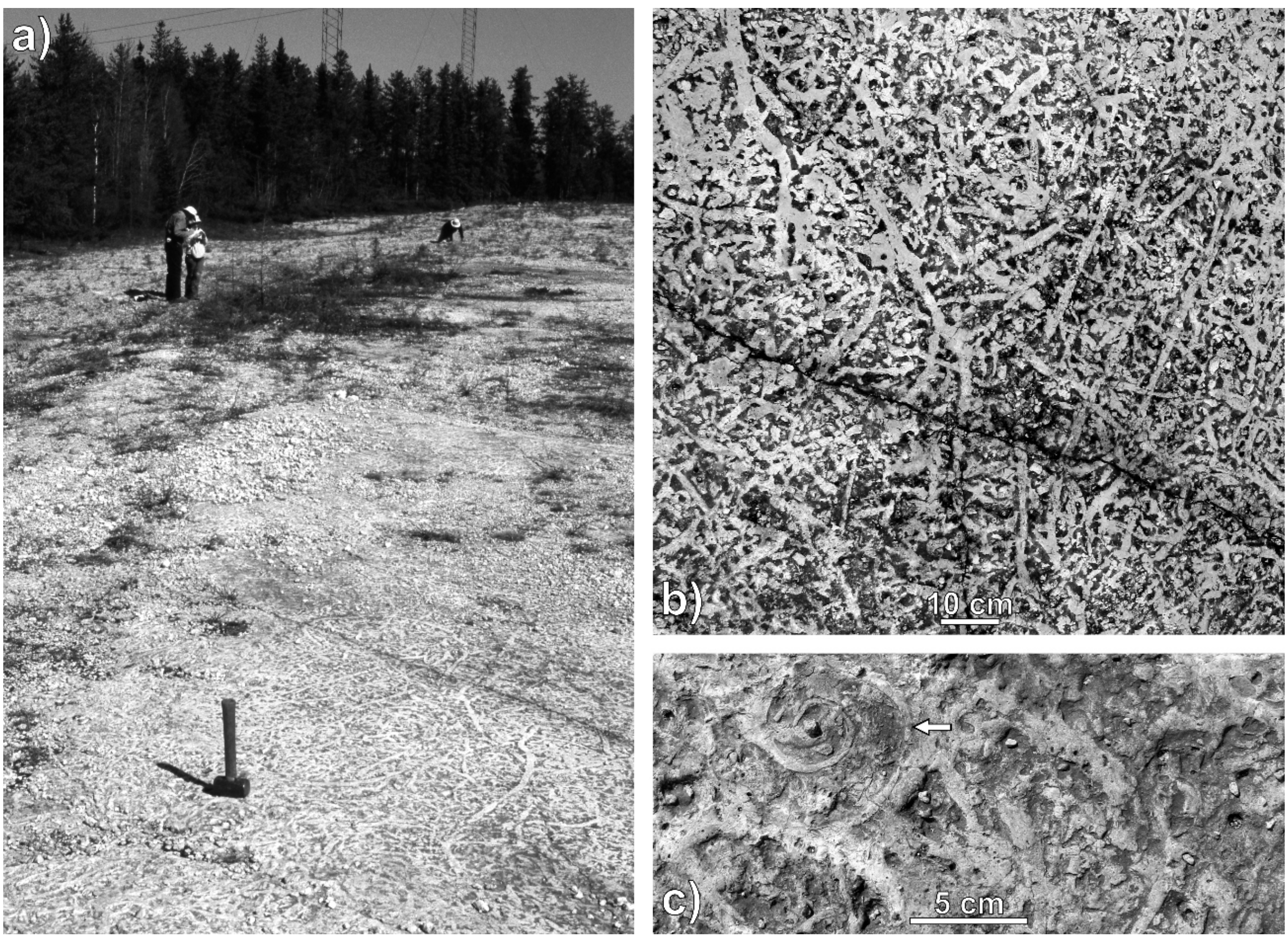

Figure 29: *Surface exposure of strata in the lower Gunton Member of the Stony Mountain Formation at Stop 5 (see Figure 25).* ***a)*** *Trace fossil* Thalassinoides *sp. is prominent on the bed in the foreground (photographed in 2005; hammer is 25 cm long).* ***b)*** Thalassinoides *sp. (photographed in 2004).* ***c)*** *Gastropod* Maclurina *sp. (at arrow) and* Thalassinoides *sp. (photographed in 2012).*

The contact between the lower and upper parts of the Gunton Member is not exposed, but in core-hole M-6-79 it is gradational. An upward decrease in *Thalassinoides*-type bioturbation is accompanied by a change to nodular bedding.

Stop 6: exposure near Highway 6, 97.6 km north of Grand Rapids

Overview

Stop 6 is at a surface exposure 100 m east of Provincial Trunk Highway 6, in the Grand Rapids Uplands at a highway distance of 97.6 km north of the town of Grand Rapids, Manitoba (Figures 1, 24a; UTM [NAD83/WGS84] 487993mE, 5985873mN; lat. 54°01′16″N, long. 99°11′00″W). This exposure of the Stony Mountain Formation is near the top of the upper part of the Gunton Member (Figure 6).

A series of surface exposures on the east side of the highway, from just south of Stop 5 to just south of Stop 6, reveals a succession of strata in the upper part of the Gunton Member (Stewart, 2012). The stratigraphic position of each exposure, with respect to the base of the LS-marker bed in the vicinity of Stop 7, was determined using laser-aided surveying and was correlated with core-hole M-6-79 (Figures 24a, 25). A combined tabulation of macrofossil occurrences in the lower and upper parts of the Gunton Member is shown in Figure 26.

Gunton Member, Stony Mountain Formation

Several beds in the upper part of the Gunton Member are exposed at Stop 6 (Figure 30). The upper part of the member consists of mildly bioturbated, dolomitic mudstone grading gradually upward into dolomitic mudstone with nodular bedding. Evaporite molds, some resembling halite crystals, are common near the top of the member.

Overall biodiversity in the Gunton Member is relatively low (Figure 26). Most taxa occur rarely, but a few appear in abundance at particular stratigraphic positions. Examples at Stop 6 include a surface with locally abundant rhynchonelliformean brachiopods, and another surface with the coiled cephalopod *Kinaschukoceras* (Figure 31). Compared with the lower part of the Gunton Member, the upper part was probably deposited in increasingly restricted and shallower marine environments, with occasional pulses of conditions that were more favourable for certain organisms. This part of the Gunton Member represents a continuation of the overall regressive phase during deposition of the upper Stony Mountain Formation (Figure 6). The contact between the Gunton Member and overlying Williams Member is marked by a change from nodular bedded dolomudstone to laminated dolomudstone.

Stop 7: roadcut on Highway 6, 97.6 km north of Grand Rapids

Overview

Stop 7 is at a major roadcut along Provincial Trunk Highway 6, in the Grand Rapids Uplands at a highway distance of 97.6 km north of the town of Grand Rapids, Manitoba (Figures 1, 24a). We will examine the roadcut on the east side of the highway, beginning at the bottom (UTM [NAD83/WGS84] 487936mE, 5985892mN; lat. 54°01′16″N, long. 99°11′03″W) and proceeding to the top (UTM [NAD83/WGS84] 487770mE, 5985307mN; lat. 54°00′57″N, long. 99°11′12″W). The stratigraphic section includes the Williams Member of the Stony Mountain Formation, and the lower dolostone interval, LS-marker bed, and most of the middle dolostone interval of the overlying Stonewall Formation (Stewart, 2012; Figure 6).

The stratigraphic section at Stop 7 and its correlation with core-hole M-6-79 are illustrated in Figure 25. Lithologic details, plots of selected conodont data, and the carbon-isotope

Figure 30: *Surface exposure of strata in the upper Gunton Member of the Stony Mountain Formation at Stop 6 (photographed in 2012, looking south; see Figure 25).*

***Figure 31:** Bedding surface in the upper Gunton Member of the Stony Mountain Formation at Stop 6, with three specimens of the coiled cephalopod* Kinaschukoceras *sp. (at arrows; photographed in 2012).*

profile are presented in Figure 32. Figure 26 shows the stratigraphic distribution of macrofossils in the Williams Member of the Stony Mountain Formation and in the lower and middle dolostone intervals of the Stonewall Formation, based on the roadcut at Stop 7 and surface exposures in this area.

The spectacular roadcut at Stop 7 was created in 2006, in order to straighten Provincial Trunk Highway 6. Recent work has further extended the lower part of the roadcut, probably down to the base of the Williams Member of the Stony Mountain Formation (Figure 33). Strata in the main part of the roadcut belong to the Stonewall Formation (Figure 34). This roadcut provides the best exposure of the LS-marker in the Williston Basin outcrop belt.

Williams Member, Stony Mountain Formation

The Williams Member consists primarily of sublithographic, dolomitic mudstone with platy to more massive bedding (Figure 33). It is argillaceous, with fine, subrounded quartz sand grains at some horizons. Sedimentary features that occur within this member include fine planar laminations, symmetrical ripples, crossbeds, channels, and molds of halite crystals. Macrofossils are generally absent, but a Konservat-Lagerstätte has been reported from an interval within the Williams Member at another location in this area (Young et al., 2007, 2012). That site has yielded a diverse biota including cnidarians, molluscs, brachiopods, arthropods, and other groups (Figure 26). At the top of the Williams Member, there is an interval of thrombolitic, dolomitic mudstone (Figures 25, 32, 35a). The thrombolitic mounds of clotted mudstone are interspersed with argillaceous to sublithographic mudstone.

Strata of the Williams Member are considered to represent restricted lagoonal or tidal-flat environments. Water energy was generally low but occasionally higher, and salinity ranged from relatively normal to hypersaline. *Rhipidognathus* is the dominant conodont in this member (Figure 32). The *Rhipidognathus* biofacies indicates extremely shallow water (Nowlan and Haidl, 2001).

The carbon-isotope profile for the section at Stop 7 shows a negative trend in the upper part of the Williams Member, with minimum values at the top of the thrombolitic interval and rising values in the overlying strata (Figure 32). This pattern suggests that there may have been subaerial exposure but minimal erosional truncation following deposition of the thrombolitic interval (see Figure 7a, b). This pattern also ties the thrombolitic interval to underlying strata of the Williams Member, and supports placement of the boundary between the Stony Mountain and Stonewall formations at the top of the thrombolitic interval (Figures 25, 32).

The Williams Member is interpreted as the final regressive phase during deposition of the Stony Mountain Formation (Figure 6). Very shallow, restricted marine conditions may have been followed by subaerial exposure.

Stonewall Formation

Strata in the Stonewall Formation below the LS-marker belong to the lower dolostone interval (Figures 32, 34). This interval consists mainly of thick, nodular, dolomitic mudstone to wackestone beds, with four thin interbeds of darker coloured, sublithographic, dolomitic mudstone. Macrofossils and irregular bioturbation occur in the thick beds, but are rare in the interbeds. Tabulate corals are the most common macrofossils; overall biodiversity is low (Figure 26). At the top of the lower dolostone interval, there is a thin unit of dolomitic mudstone with localized areas of brecciation (Figures 25, 32). The intraclasts are subangular, mostly 4 mm or less in size, account for up to 10% of the rock volume, and appear to have been derived from this unit. Macrofossils are absent.

The alternations of dolomitic mudstone-wackestone and sublithographic mudstone in the lower dolostone interval suggest a series of similar depositional cycles, possibly related to oscillations in water depth, energy, or circulation. Other evidence suggests that conditions also changed during an overall transgressive-regressive cycle. In the lower part of the interval, there is a general upward decrease in the relative abundance

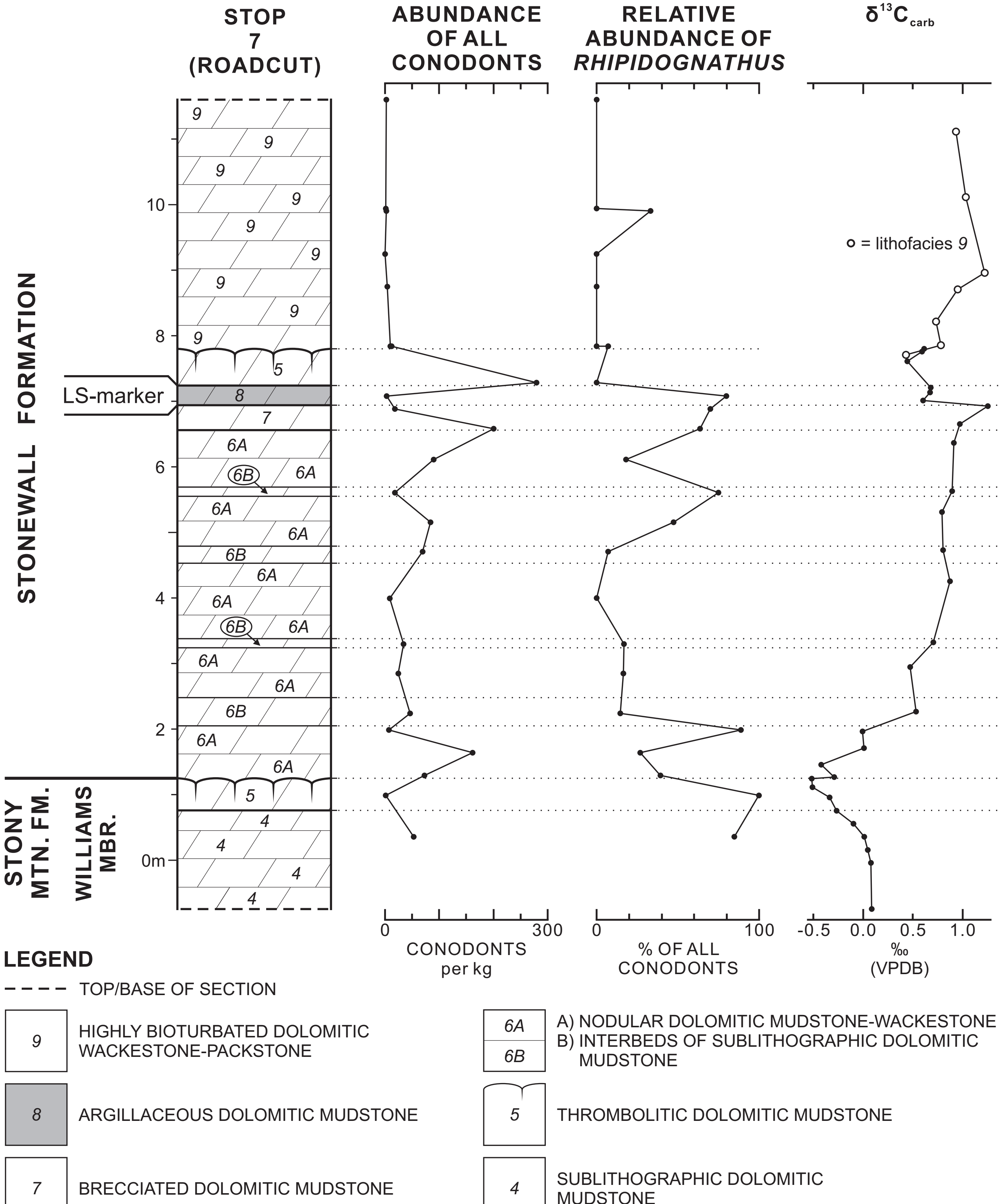

Figure 32: *Lithostratigraphic section at Stop 7 in the Grand Rapids Uplands, and plots of conodont abundance, relative abundance of* Rhipidognathus*, and $\delta^{13}C_{carb}$. Isotope samples were obtained immediately below and above the base of lithofacies 9, at stratigraphically low and high places along this undulatory contact; to distinguish these samples, a different symbol is used for data points from lithofacies 9. Based on Stewart (2012; conodont data from Nowlan, 2008, 2009a), with the addition of new isotopic-carbon data from the Williams Member of the Stony Mountain Formation and base of the Stonewall Formation.*

Figure 33: *Stop 7, looking south from the bottom of the roadcut on the east side of Provincial Trunk Highway 6 (photographed in 2012). Lowermost bedding surface (left foreground at arrow) is probably the top of the Gunton Member of the Stony Mountain Formation (slightly lower stratigraphically than base of section in Figures 25, 32). It is overlain by the light-coloured Williams Member of the Stony Mountain Formation, which in turn is overlain by the Stonewall Formation in the more distant low exposures along the roadcut. The main roadcut in the distance (right of centre) exposes the Stonewall Formation (see Figure 34).*

Figure 34: *Main roadcut at Stop 7, on the east side of Provincial Trunk Highway 6 (photographed in 2007, looking south). Strata represent the Stonewall Formation and include the gray, argillaceous LS-marker (indicated by bracket in upper centre above 1-m scale bar; see Figure 32).*

of the conodont *Rhipidognathus*, suggesting a change from very shallow to somewhat deeper water (Figure 32). The rising isotopic-carbon values would be expected during a transgression following subaerial exposure (see Figure 7b). The exotic colonial rugose coral *Tryplasma* was introduced during this event (Figure 26), likely in response to cooling of the epicontinental sea prior to icehouse conditions in the Hirnantian. The greatest abundance and diversity of macrofossils, and the lowest relative abundance of *Rhipidognathus*, occur in the middle part of the lower dolostone interval. The macrofossil assemblage, dominated by colonial corals, indicates relatively open, normal marine, shallow subtidal conditions. In the upper part of the interval, macrofossil abundance and diversity decrease, and there is a general upward increase in the relative abundance of *Rhipidognathus*, indicating increasingly restricted and shallower marine conditions.

The LS-marker bed consists of recessive, argillaceous, dolomitic mudstone (Figures 32, 34, 35b). This marker is variably bluish gray in colour, with gradation from reddish brown to bluish green to yellowish green to greenish gray. The contact with the underlying, brecciated, dolomitic mudstone unit is sharp and undulatory. There is a sharp discontinuity in the carbon-isotope pattern at the contact, with a shift to lower values (Figure 32). Upward in the LS-marker, there is gradation in character from finely arenaceous and argillaceous, to crumbly and fissile, to more coherent, shaly, sublithographic beds. There is an upward decrease in the amount of terrigenous material, including quartz. Macrofossils are absent, and the fragmentary, abraded nature of the conodonts is suggestive of active reworking.

The final regression during deposition of the lower dolostone interval of the Stonewall Formation may have ended with subaerial exposure, brecciation, and erosional truncation of the surface. The lack of a negative isotopic-carbon excursion below the surface could indicate that exposure was brief and/or that strata affected by meteoric diagenesis were truncated before

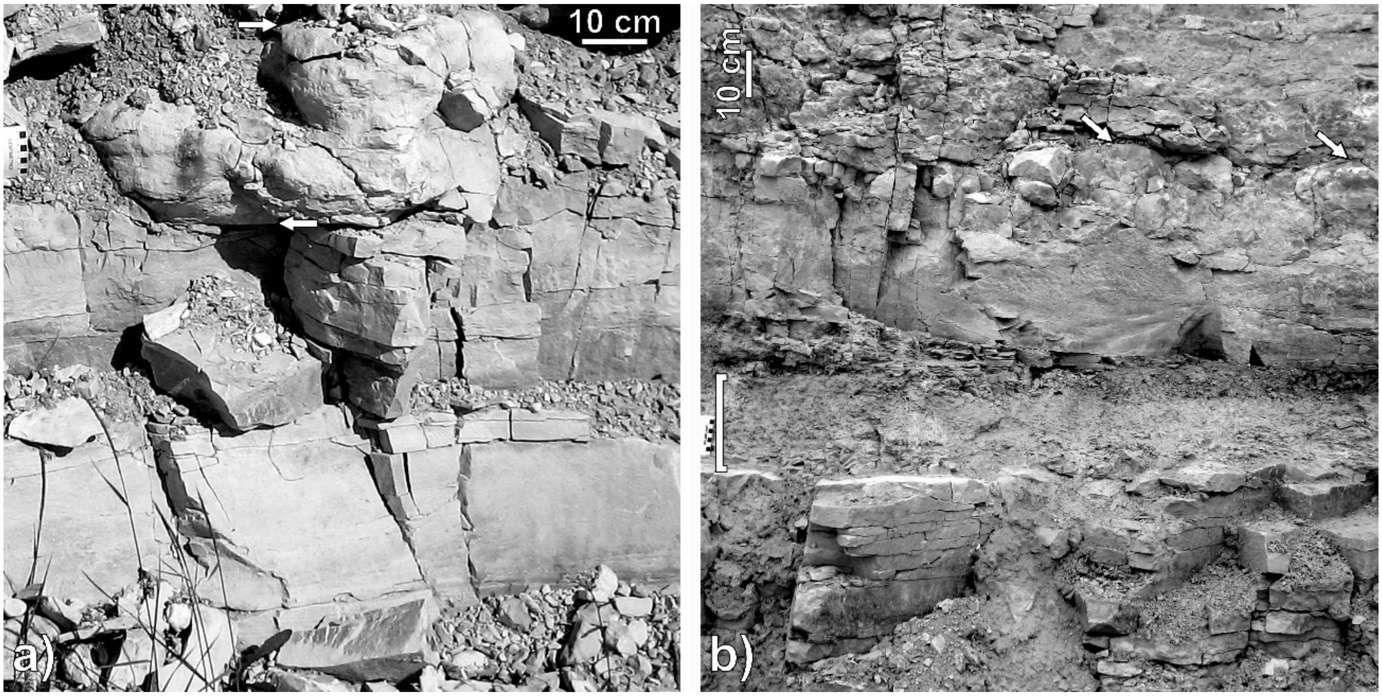

Figure 35: *Thrombolitic intervals at Stop 7 (see Figure 32).* ***a)*** *Thrombolitic mounds (between lower and upper arrows in upper centre) at the top of the Williams Member of the Stony Mountain Formation (photographed in 2012).* ***b)*** *Thrombolitic mounds (tops indicated by arrows in upper centre and upper right) above the gray, argillaceous LS-marker (indicated by bracket on left side) in the Stonewall Formation (photographed in 2007).*

deposition resumed (see Figure 7). The LS-marker bed above the surface may record subaerial processes and/or deposition of terrigenous and reworked material during a transgressive event.

The LS-marker is in relatively sharp contact with the overlying, middle dolostone interval of the Stonewall Formation. The basal unit of this interval consists of sublithographic, dolomitic mudstone featuring thrombolitic textures and mounds (Figures 25, 32, 35b). Only one macrofossil, a lingulid brachiopod, was found in the thrombolitic unit. The high abundance of conodonts and absence of *Rhipidognathus* suggest a rapid deepening event, with favourable conditions in the water column for conodonts. On the sea-floor, microbes flourished and formed thrombolites, but conditions were unfavourable for animals.

The thrombolitic unit is sharply overlain by a unit of dolostone that extends to the top of the roadcut (Figures 25, 32, 34, 35b). The latter unit consists primarily of highly bioturbated, dolomitic wackestone with zones of packstone. Near the base, however, there is less bioturbation and the rock is almost a dolomitic mudstone, which may be laminated where it onlaps thrombolitic mounds. Isotopic-carbon values rise above the thrombolitic unit, reaching a background level comparable to that in the lower dolostone interval of the Stonewall Formation (Figure 32). Such a pattern would be expected during a transgression following subaerial exposure (see Figure 7). Isotope data for the lower to middle portion of the thrombolitic unit are not yet available. It is hoped that they will clarify the relation between the thrombolitic unit and the underlying LS-marker and overlying bioturbated, dolomitic wackestone-packstone unit, with respect to possible subaerial exposure.

Macrofossils appear at the bottom of the bioturbated, dolomitic wackestone-packstone unit. They are very common from about 0.5 to 2.0 m above the base of the unit, and then disappear. Overall diversity in this unit is very high (Figure 26). The assemblage is coral dominated, including an abundance of tabulates as well as colonial and solitary rugosans. Some distinctive taxa that are characteristic of the Stony Mountain Formation recur in this unit, such as the solitary rugosans *Bighornia* and *Deiracorallium*. There were also introductions of exotic taxa, including the tabulate *Angopora* and colonial rugosan *Pycnostylus* (Figure 36). Their arrival likely indicates further cooling of the epicontinental sea, near the onset of icehouse conditions in the Hirnantian. In addition to corals, there is an abundance of brachiopods and bryozoans. Stromatoporoids, gastropods, and cephalopods are common. Some areas of bioturbation are identifiable as *Thalassinoides*. Conodonts are scarce, and *Rhipidognathus* is rare (Figure 32).

Based on its lithology and biota, the highly bioturbated, dolomitic wackestone-packstone unit is considered to represent an open, normal marine, moderate energy, shallow subtidal environment. These favourable conditions promoted the highest biodiversity attained at any time during deposition of the Stonewall Formation. The disappearance of the macrofauna in the upper part of this unit is considered to record the first pulse of the Late Ordovician mass extinction event in this area.

Stop 8: roadcut on Highway 6, 91.9 km north of Grand Rapids

Overview

Stop 8 is at a major roadcut along Provincial Trunk Highway 6, in the Grand Rapids Uplands at a highway distance of 91.9 km north of the town of Grand Rapids, Manitoba (Figures 1, 24a). We will examine the roadcut on the west side of

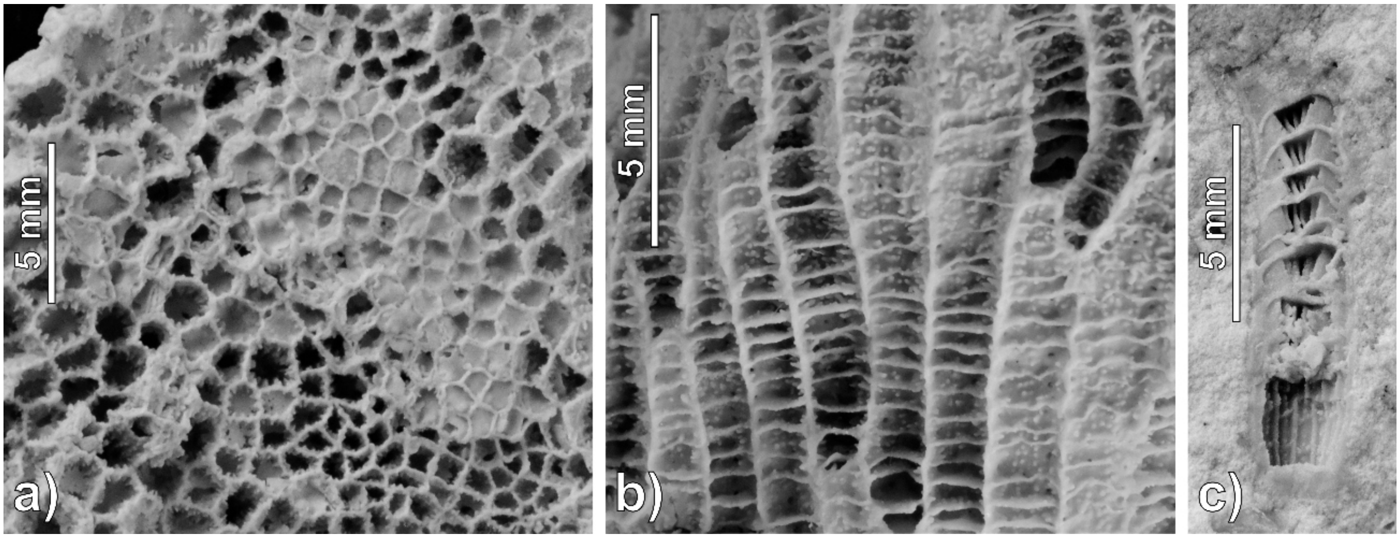

***Figure 36:** Fossils from the Stonewall Formation, above the thrombolitic interval that overlies the LS-marker at Stop 7 (see Figure 32). **a, b)** Tabulate coral* Angopora manitobensis*; interior of broken corallum, transverse and longitudinal views, respectively.* ***c)** Colonial rugose coral* Pycnostylus *sp.; interior of broken corallite, longitudinal view.*

the highway, beginning at the bottom (UTM [NAD83/WGS84] 486525mE, 5980407mN; lat. 53°58′19″N, long. 99°12′20″W) and proceeding to the top (UTM [NAD83/WGS84] 486443mE, 5980022mN; lat. 53°58′06″N, long. 99°12′24″W). The stratigraphic section includes the upper part of the middle dolostone interval, the *t*-marker bed, and the upper dolostone interval of the Stonewall Formation, and the lower part of the overlying Fisher Branch Formation (Demski, 2010; Figure 6).

The stratigraphic section at Stop 8 and its correlation with core-hole M-6-79 are illustrated in Figure 25. Lithologic details, the carbon-isotope profile, and plots of selected conodont data are presented in Figure 37. Figure 26 shows the stratigraphic distribution of macrofossils in the upper dolostone interval of the Stonewall Formation and in the Fisher Branch Formation at Stop 8.

The roadcut at Stop 8 was created in 2006, in order to straighten Provincial Trunk Highway 6. It provides the best exposure of the *t*-marker in the Williston Basin outcrop belt (Figure 38).

Stonewall Formation

Strata exposed below the *t*-marker represent the upper part of the middle dolostone interval of the Stonewall Formation (Figures 25, 37, 38, 39a). These strata are composed of sublithographic to lithographic dolomudstone. Some of the lower beds contain fine planar laminations. Higher in the interval, a bed with undulatory lower and upper contacts is overlain by an argillaceous unit. At the top of the middle dolostone interval, there is a thick bed with a mottled texture. The basal contact of this bed is undulatory (top of scale bar in Figure 39a). The top of the bed is an irregular, scoured surface, which is overlain by the *t*-marker.

The exposed strata of the middle dolostone interval lack macrofossils, but contain conodonts including *Aphelognathus* (Figure 37). Deposition likely occurred under restricted, shallow marine conditions, with occasional influxes of terrigenous material. These strata probably record the regressive phase of an overall depositional cycle represented by the entire middle dolostone interval of the Stonewall Formation. Strata deposited during the initial transgression and open-marine phase were seen in the upper part of the section at Stop 7 (Figures 25, 32).

The carbon-isotope profile through the middle dolostone interval of the Stonewall Formation shows a negative excursion beginning 1 m below the *t*-marker, followed by a slight rise in values near the marker (Figure 37). This pattern suggests that deposition of the dolostone interval may have been followed by a period of subaerial exposure and minimal erosional truncation (Demski et al., 2010; see Figure 7a, b).

The *t*-marker bed consists of recessive, argillaceous dolomudstone (Figures 25, 37, 38, 39a). The colour is gray, with a thick part in the middle of the bed distinguished by large, irregular, discontinuous, reddish areas. Dolomudstones in the lower and upper parts of the bed are relatively massive and homogeneous. They are gradational with the middle part of the bed, which has areas that may be intraclastic or bioturbated, and areas with planar laminations. Fine, subrounded to subangular quartz sand grains occur throughout the *t*-marker bed, decreasing upward in size and abundance. The total amount of insoluble residue also decreases upward through the marker bed. Macrofossils are absent, but fragmentary to moderately well-preserved conodonts occur throughout the bed. *Aphelognathus* is present in the lower part, and *Ozarkodina* appears in the middle (Figure 37). The contact between the *t*-marker bed and the overlying upper dolostone interval of the Stonewall Formation appears to be sharp and conformable.

The lower, approximately 2 m of the upper dolostone interval consists of a succession of sublithographic to lithographic dolomudstone units (Figures 37, 39a). Some of the beds are finely laminated, burrowed, or mottled. A short distance above the base of this succession, there is an arenaceous zone with fine, rounded to subrounded quartz sand grains. In the middle of this succession, a vuggy unit with an undulatory upper surface is present.

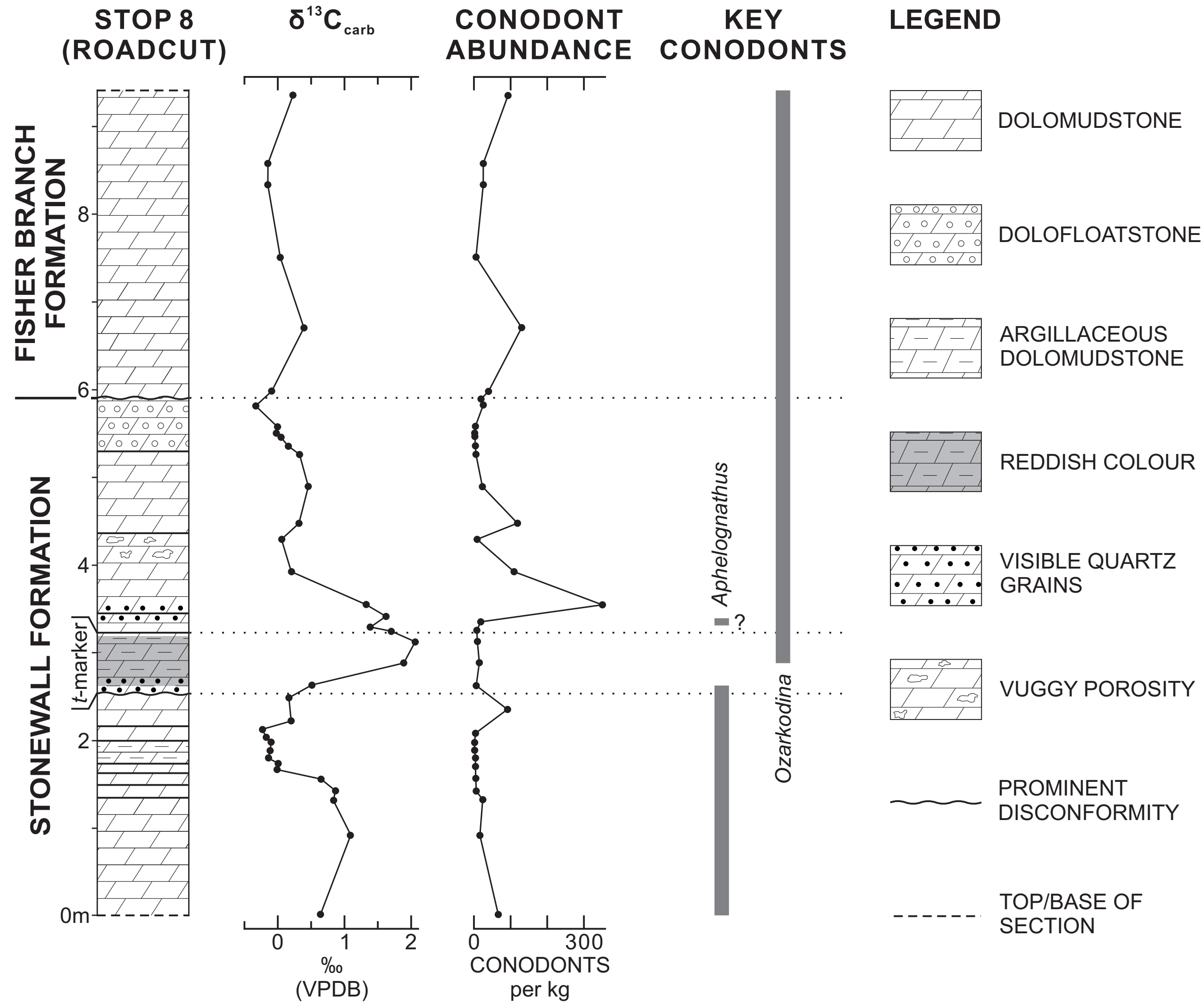

Figure 37: *Lithostratigraphic section at Stop 8 in the Grand Rapids Uplands, and plots showing $\delta^{13}C_{carb}$, conodont abundance, and ranges of two biostratigraphically significant conodont genera. Based on Demski (2010; conodont data from Nowlan, 2009b), with the addition of one conodont datum (Nowlan, 2013) and one isotope datum.*

Figure 38: *Roadcut at Stop 8, on the west side of Provincial Trunk Highway 6 (photographed in 2008, looking south). Strata represent the Stonewall Formation and the overlying Fisher Branch Formation (see Figures 25, 37); arrow (centre) indicates the red and gray* t*-marker in the Stonewall Formation (for detail and scale, see Figure 39a); Stonewall–Fisher Branch contact is exposed in the distance (for detail see Figure 40).*

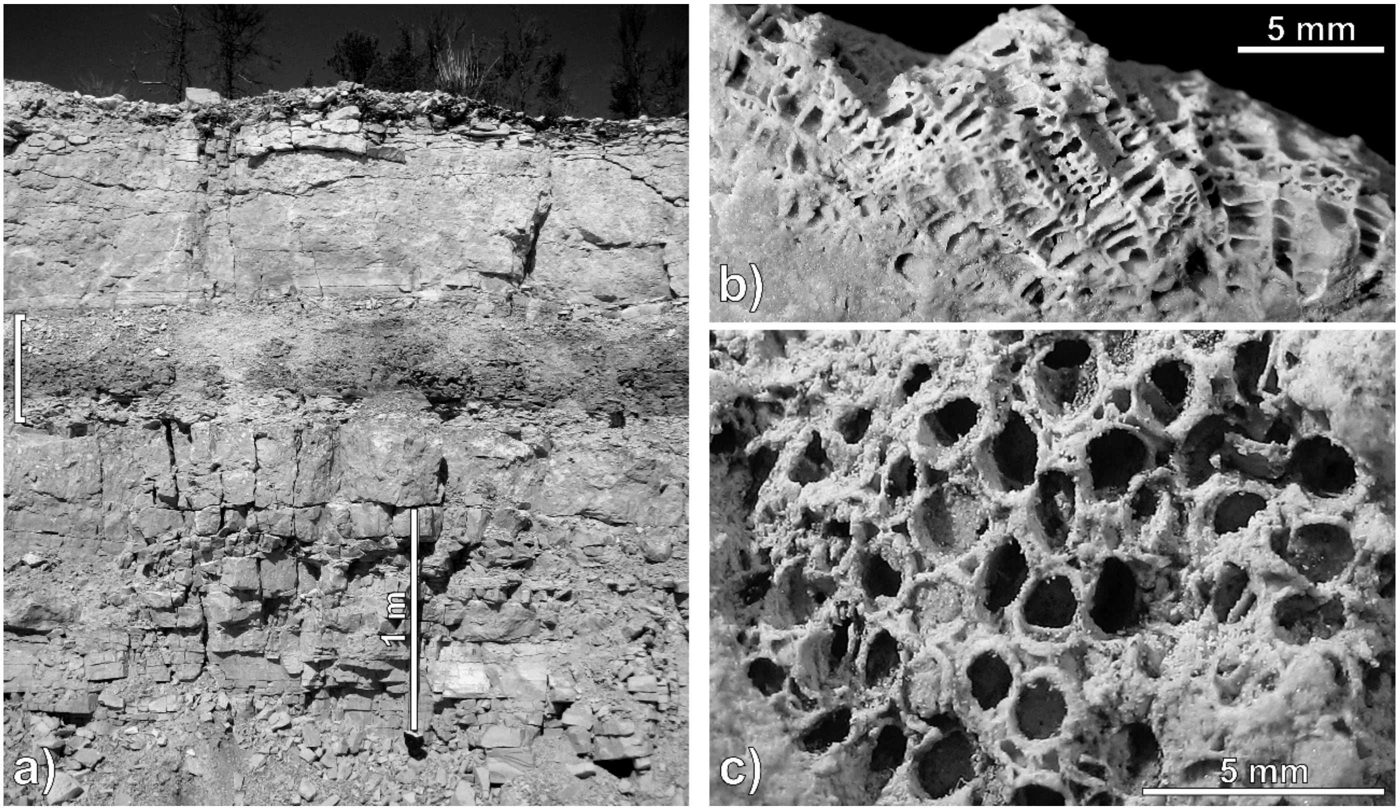

Figure 39: *Stonewall Formation at Stop 8 (also see Figures 37, 38).* ***a)*** *Red and gray, argillaceous* t-*marker is indicated by the bracket on the left side (photographed in 2008).* ***b, c)*** *Tabulate coral* Propora *sp. from 55–75 cm above the top of the* t-*marker; interiors of two broken coralla, longitudinal and transverse views, respectively.*

Figure 40: *Undulatory contact (indicated by arrows on left and right sides, and top of 50-cm scale bar at centre) between the Stonewall Formation and the overlying Fisher Branch Formation at Stop 8 (photographed in 2010; see Figure 37).*

The upper unit in the upper dolostone interval is about 60–70 cm thick. This unit has a sharp, irregular base, and includes beds of sublithographic dolomudstone and intraclastic dolofloatstone. Some of the dolomudstone beds show fine planar laminations or mottling. Intraclasts in the dolofloatstone beds are subangular to rounded. The largest intraclasts, up to 3 cm in size, occur at the base of the unit. It has not been determined whether this unit represents the top-Stonewall marker bed known elsewhere in the Williston Basin. The contact between the upper dolostone interval of the Stonewall Formation and the overlying Fisher Branch Formation is sharp, disconformable, and broadly undulatory (Figure 40).

Scarce macrofossils occur between 55 and 75 cm above the base of the upper dolostone interval. This coral-dominated assemblage includes the first appearances of the tabulate *Propora* (Figure 39b, c) and the solitary rugosans *Rhegmaphyllum* and *Streptelasma* (Figure 26). Conodonts, including *Ozarkodina*, range through the upper dolostone interval (Figure 37). A sample from about 15 cm above the base of the interval includes moderately well-preserved as well as worn elements that likely represent *Aphelognathus*, together with *Ozarkodina*. The maximum abundance of conodonts occurs just above that stratigraphic position.

Beginning at the base of the *t*-marker, the carbon-isotope profile shows an increase in values (Figure 37). This is not simply a return to background level, as might be expected above a surface of subaerial exposure (see Figure 7). Rather, it is a positive excursion that rises beyond the background level of about +1‰ seen lower in the Stonewall Formation, reaching a peak value of +2‰ near the top of the *t*-marker bed (Figure 37). This peak is followed by an overall decrease in values in the upper dolostone interval of the Stonewall Formation, with a minimum at the top of the formation.

The coincidence of this positive isotopic excursion with the turnover from *Aphelognathus* to *Ozarkodina* conodont faunas suggests that this excursion represents the HICE, and that strata in the upper Stonewall Formation above the base of the *t*-marker are latest Ordovician, Hirnantian in age (Demski et al., 2010; Figure 6). This interpretation is strengthened by the coral fauna found in the upper dolostone interval of the Stonewall Formation, which is comparable to faunas that have been documented from strata of Hirnantian age in the east-central U.S.A. (Elias and Young, 1998; Elias et al., in press).

The *t*-marker bed is interpreted as a transgressive deposit during a time of substantial terrigenous input. Succeeding strata in the upper dolostone interval of the Stonewall Formation represent fluctuating, generally restricted, shallow marine conditions. A macrofaunal assemblage including exotic coral taxa made a brief appearance when the most open, normal marine conditions were attained. Deposition from the base of the *t*-marker to the top of the Stonewall Formation may have occurred during an interglacial phase, with a disconformity at the base of the *t*-marker possibly representing the major glacioeustatic regression during the early Hirnantian (Demski et al., 2011b).

Fisher Branch Formation

Strata exposed above the Stonewall Formation in the upper part of the roadcut represent the lower portion of the Fisher Branch Formation (Figures 25, 37, 38, 40). Immediately above the broadly undulatory base of the formation, there is a 4- to 5-cm-thick bed of bioturbated, sublithographic dolomudstone, which lacks macrofossils, but contains cubic halite molds up to 12 mm wide. Above that, the remaining, approximately 3.4 m of section consists of relatively homogeneous, extensively bioturbated, fossiliferous dolomudstone with dolowackestone in places. The poorly preserved macrofauna includes tabulate and solitary rugose corals, gastropods, cephalopods, and brachiopods (Figure 26). Corals are usually predominant. The brachiopod *Virgiana decussata* occurs in distinct beds, each about 5 cm thick, situated approximately 2.5 and 2.7 m above the base of the formation. This species is considered to indicate an Early Silurian (Llandovery, late Rhuddanian) age (Jin et al., 1999). Conodonts, including *Ozarkodina*, range from the bottom to the top of the exposed Fisher Branch Formation (Figure 37).

The exposed portion of the Fisher Branch Formation is considered to have been deposited during a transgressive event. The initial, restricted conditions were soon followed by normal, open marine, shallow subtidal environments. The macrofauna that was introduced represents the earliest record of the Early Silurian biotic recovery in this area.

In this guidebook, the O-S boundary is placed at the sharp, broadly undulatory contact between the Stonewall and Fisher Branch formations (Figures 6, 40). Assuming that the uppermost Stonewall Formation is Hirnantian in age and the Fisher Branch Formation is late Rhuddanian, the disconformity between these formations may represent a hiatus of up to about 2 million years. It is uncertain whether decreasing isotopic-carbon values beginning about 1 m below the formational boundary (Figure 37) are an indication of subaerial exposure followed by erosional truncation (see Figure 7), or are part of the falling limb of the HICE (see Figure 4d).

Stop 9: quarry beside Road 287, south side of Cormorant Hill

Overview

Stop 9 is at a quarry on the east side of Provincial Road 287, on the south side of Cormorant Hill at a road distance of 7.3 km southwest of the town of Cormorant, Manitoba (Figures 1, 24b; UTM [NAD83/WGS84] 392290mE, 6003888mN; lat. 54°10′18″N, long. 100°39′00″W). The stratigraphic section includes the upper portion of the Williams Member of the Stony Mountain Formation, and the lower portion of the lower dolostone interval of the Stonewall Formation (Figure 6). The stratigraphic section, carbon-isotope profile, and correlation of the section with core-hole M-9-86 are illustrated in Figure 41.

Williams Member, Stony Mountain Formation

The Williams Member is composed of slightly argillaceous, sublithographic to lithographic dolomudstone (Figures 41, 42, 43a). Macrofossils are absent. Reddish, skeletal halite molds have been illustrated from the base of the section (Bezys, 1991, p. 61, Figure GS-14-6). Planar laminations and some cross

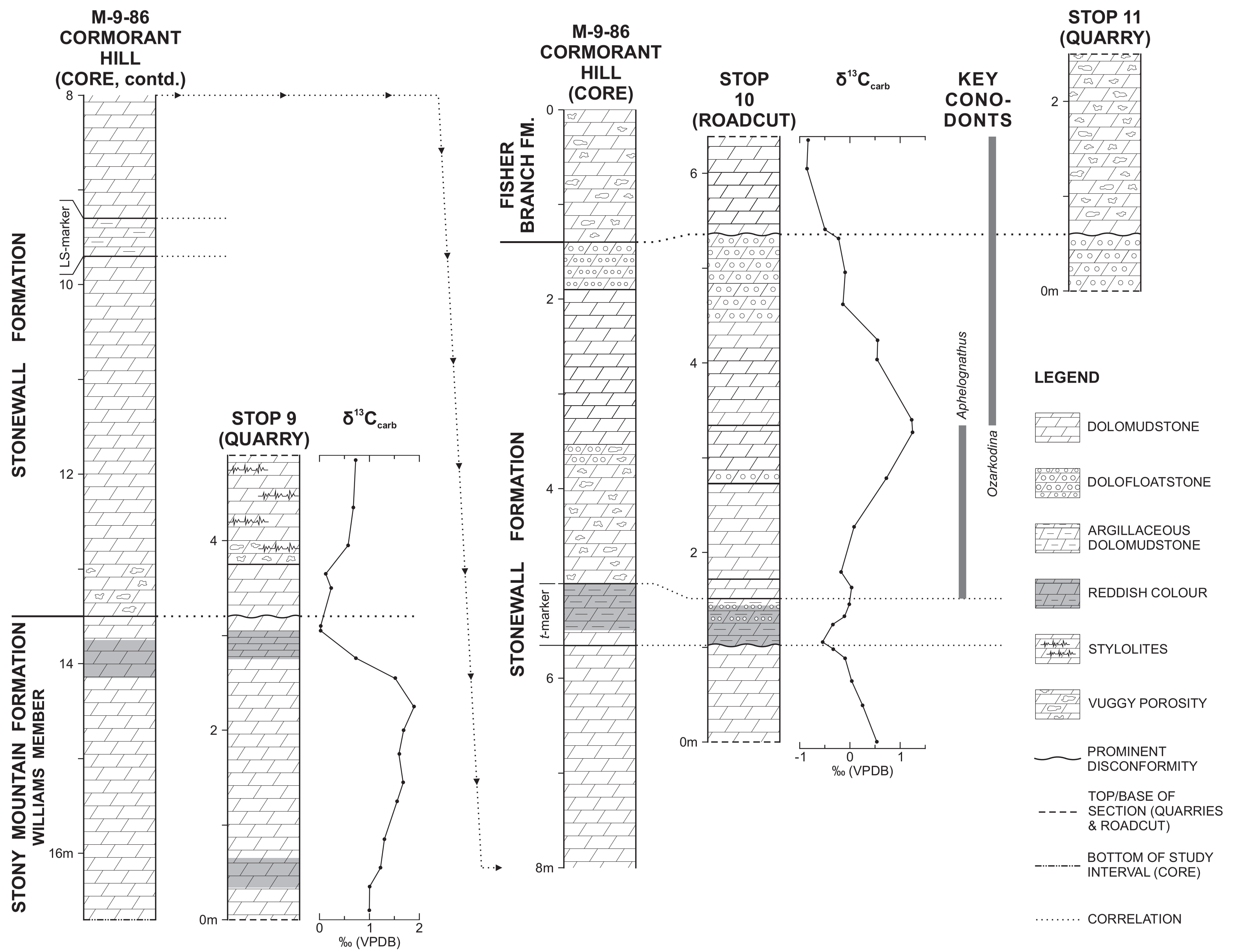

Figure 41: *Lithostratigraphic sections and correlation of Stops 9–11 (Cormorant Hill) and core-hole M-9-86 (Cormorant Hill; Figure 24b; UTM [NAD83/WGS84] 393113mE, 6007175mN; lat. 54°12'05"N, long. 100°38'19"W). New data are illustrated for Stop 9, including the $\delta^{13}C_{carb}$ profile, and for core M-9-86, including recognition of the LS-marker. For Stop 10, the section and plots showing $\delta^{13}C_{carb}$ and ranges of two biostratigraphically significant conodont genera (shown above the* t-*marker only) are based on Demski (2010; conodont data from Nowlan, 1989). The section for Stop 11 is based on Demski (2010) and new information.*

Figure 42: Williams Member of the Stony Mountain Formation and the overlying Stonewall Formation in the quarry at Stop 9 (photographed in 2012; see Figure 41). Formational contact (arrow on left side) occurs above a reddish zone (bracket on left side) near the top of the Williams Member.

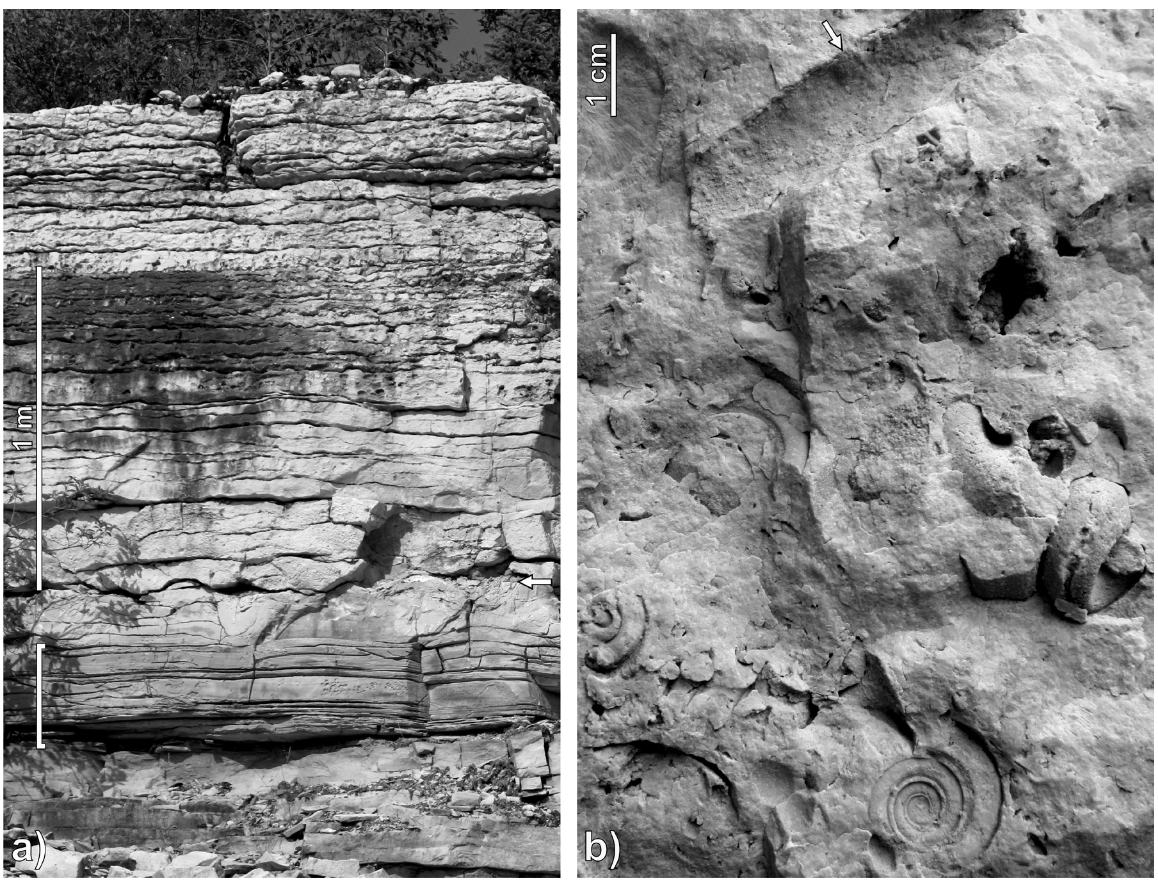

*Figure 43: Strata and fossils at Stop 9. **a)** Undulatory contact (indicated by bottom of 1-m scale bar on left and arrow on right) between the Williams Member of the Stony Mountain Formation and the overlying Stonewall Formation (photographed in 2012; see Figure 41). Reddish zone (bracket on left side) occurs near the top of the Williams Member; in places, the uppermost part of the Williams Member is thrombolitic and contains infilled channels. **b)** Molds of an orthoconic cephalopod (arrow at top centre) and gastropods in the Stonewall Formation.*

laminations are especially conspicuous in a prominent reddish zone, from about 15 to 45 cm below the top of the member. In places, the upper 15 cm of the member is thrombolitic and includes infilled channels. This interval is conformable with underlying strata of the Williams Member, and is considered correlative with the thrombolitic unit at the top of the Williams Member in the Grand Rapids Uplands (Stop 7; Figures 25, 32).

Deposition of the Williams Member at Stop 9 occurred under very shallow, restricted marine conditions, during the final regressive phase of the Stony Mountain Formation (Figure 6). The upper surface of the member is sharp and undulatory (Figure 43a), with an overlying thin seam of greenish gray clay preserved in some places. The carbon-isotope profile shows a negative trend in the upper metre of the Williams Member, followed by rising values in the lower part of the overlying Stonewall Formation (Figure 41). This pattern resembles the one for the same stratigraphic interval in the Grand Rapids Uplands (Figure 32). It may reflect subaerial exposure and minor erosional truncation following deposition of the thrombolitic unit of the Williams Member (see Figure 7a, b).

Stonewall Formation

The lower portion of the lower dolostone interval of the Stonewall Formation, below the level of the LS-marker, is exposed at Stop 9 (Figures 41, 42, 43a). The basal 55 to 60 cm comprises undulatory beds of dolomudstone to dolowackestone containing small echinoderm columnals and other fossils, including corals. The rest of the section, to the top of the exposure, consists of highly stylolitized, irregular beds of dolomudstone with wisps of greenish clay. In this part of the section, the lower beds are fossiliferous, with many echinoderm columnals and abundant corals.

Macrofossils in the Stonewall Formation at Stop 9 include tabulate corals (*Paleofavosites*), brachiopods (*Megamyonia nitens*, *Oepikina*? *stonewallensis*), coiled cephalopods (*Bickmorites insignis*, *Discoceras*?), orthoconic cephalopods (*Actinoceras*), and gastropods (*Hormotoma*, *Liospira*, *Trochonema*) (Figure 43b). Deposition of the formation began during a transgressive event that brought open, normal marine, shallow subtidal conditions to this area.

Stop 10: roadcut on Road 287, north side of Cormorant Hill

Overview

Stop 10 is at a major roadcut along Provincial Road 287, on the north side of Cormorant Hill at a road distance of 3.6 km southwest of the town of Cormorant, Manitoba (Figures 1, 24b; UTM [NAD83/WGS84] 392945mE, 6007156mN; lat. 54°12′05″N, long. 100°38′28″W). We will examine the cut on the northwest side of the road. The stratigraphic section includes the upper part of the middle dolostone interval, the *t*-marker bed, and the upper dolostone interval of the Stonewall Formation, and the lower part of the overlying Fisher Branch Formation (McCabe, 1988; Bezys, 1991, Figure GS-14-5, Table GS-14-2; Norford et al., 1998, Figure 6; Demski, 2010; Figure 6). The stratigraphic section, carbon-isotope profile, plots of selected conodont data, and correlation of the section with core-hole M-9-86 are illustrated in Figure 41.

Stonewall Formation

Strata exposed below the *t*-marker represent the upper part of the middle dolostone interval of the Stonewall Formation, above the level of the LS-marker (Figures 41, 44). These strata are composed of sublithographic dolomudstone. Fine planar laminations, slight bioturbation, and sparse sand-size intraclasts occur in some beds. There are no macrofossils, but conodonts are present. Deposition likely occurred under restricted, shallow marine conditions, during the regressive phase of the depositional cycle represented by the middle dolostone interval of the Stonewall Formation.

Irregular fractures extend downward from the contact with the overlying *t*-marker bed, and are infilled from above. The carbon-isotope profile shows a negative trend leading up to the contact, and a lower value at the bottom of the *t*-marker followed by rising values (Figure 41). This pattern may have resulted from a period of subaerial exposure and erosional truncation, between deposition of the middle dolostone interval and the *t*-marker bed of the Stonewall Formation (see Figure 7c).

The *t*-marker bed is composed of recessive, argillaceous, sublithographic dolomudstone and dolofloatstone (Figures 41, 44). The lower to middle portion has a reddish colour, and the uppermost part is gray. Dolomudstone layers in the lower part of the marker contain fine laminations. The upper part of the marker is dolofloatstone, with sand- to granule-size, subrounded to rounded, variably coloured dolostone clasts. Visible quartz grains are rare in the marker. The total amount of insoluble residue decreases upward. Macrofossils are absent, but conodonts are present. Some dolostone concretions, up to 75 cm wide and 50 cm thick, are present in the marker bed, with underlying and overlying layers displaced around them. The *t*-marker bed may represent transgressive deposition under restricted conditions, with an influx of siliciclastics and a substantial amount of reworked carbonate material.

There is a sharp, undulatory contact between the *t*-marker bed and the overlying upper dolostone interval of the Stonewall Formation (Figures 41, 44, 45). The lower, 20-cm-thick unit in this interval consists of bioturbated, sublithographic dolomudstone. It is overlain at a sharp, conformable contact by about 1 m of mottled, sublithographic dolomudstone, with a sharp, possibly disconformable upper contact. The overlying unit is about 60 cm thick. Coarse, conglomeratic dolofloatstone occurs in the lower part. The variably coloured dolostone clasts are subangular to subrounded and up to 4 cm across at the base of the unit, decreasing upward in size and becoming subrounded to rounded. This is followed by dolomudstone toward the top of the unit. The upper contact is sharp and conformable. It is overlain by about 1 m of mottled, sublithographic dolomudstone, followed by about 1 m of dolofloatstone at the top of the Stonewall Formation. Clasts in the lower part of this dolofloatstone are up to 2 cm across, subangular to subrounded, and randomly oriented. Grain size decreases upward, where clasts are variably coloured and subrounded. It has not been determined whether this dolofloatstone represents the top-Stonewall marker bed known elsewhere in the Williston Basin.

Macrofossils have not been found in the upper dolostone interval of the Stonewall Formation at Stop 10. Conodonts, however, are present (Figure 41). *Amorphognathus* occurs in the lower part of the interval (units 3a and 3b of Norford et al., 1998), whereas *Ozarkodina* appears in the upper part (units 3c and 2 of Norford et al., 1998) (see Figure 45). Deposition of the upper dolostone interval seems to have occurred under restricted, fluctuating, shallow marine conditions, with occasional episodes of reworking and accumulation of carbonate clasts.

In the carbon-isotope profile, the overall increase in values that begins at the base of the *t*-marker reaches a peak value of +1.3‰ in the middle of the upper dolostone interval (Figure 41). This is not simply a return to background level, as might be expected above a surface of subaerial exposure (see Figure 7). Rather, it is a positive excursion that rises beyond the background level of about +0.5‰ in the lower and middle dolostone intervals of the Stonewall Formation at Stops 9 and 10, respectively (confirmed by data from core-hole M-9-86). The peak of this excursion is followed by a trend of decreasing values, with values at the top of the upper dolostone interval matching those at the bottom of the interval (Figure 41).

As at Stop 8, the coincidence of this positive isotopic excursion with the turnover from *Aphelognathus* to *Ozarkodina* conodont faunas suggests that this excursion represents the HICE, and that strata in the upper Stonewall Formation above the base of the *t*-marker are latest Ordovician, Hirnantian in age (Demski et al., 2010; Figure 6). Deposition may have occurred during an interglacial phase, with a disconformity at the base of the *t*-marker possibly representing the major glacio-eustatic regression during the early Hirnantian (Demski et al., 2011b).

Fisher Branch Formation

Strata exposed above the Stonewall Formation in the upper part of the roadcut represent the lower portion of the Fisher Branch Formation (Figures 41, 44, 45). The sharp, broadly undulatory formational contact is overlain by highly mottled and bioturbated, sublithographic dolomudstone that extends to the top of the exposure (Figure 46). Macrofossils were not found in the Fisher Branch Formation at Stop 10 (but occur at nearby Stop 11). Conodonts including *Ozarkodina* are present (unit 1 of Norford et al., 1998) (see Figures 41, 45). The exposed portion of the Fisher Branch Formation is considered to have been deposited during a transgressive event that brought normal, open marine, shallow subtidal conditions to this area.

In this guidebook, the O-S boundary is placed at the contact between the Stonewall and Fisher Branch formations (Figures 6, 46). The overall trend of decreasing isotopic-carbon values, following the positive peak in the upper dolostone interval of the Stonewall Formation, reaches a baseline of about -0.8‰ in the lower Fisher Branch Formation (Figure 41).

Stop 11: quarry beside Road 287, top of Cormorant Hill

Overview

Stop 11 is at a small quarry on the northwest side of Provincial Road 287, at the top of Cormorant Hill at a road distance of 4.6 km southwest of the town of Cormorant, Manitoba (Figures 1, 24b; UTM [NAD83/WGS84] 392426mE, 6006447mN; lat. 54°11′41″N, long. 100°38′56″W). The stratigraphic section includes the uppermost part of the upper dolostone interval of the Stonewall Formation, and the lower part of the overlying

Figure 44: *Roadcut at Stop 10, on the northwest side of Provincial Road 287 (photographed in 2012, looking southwest). Strata represent the Stonewall Formation and the overlying Fisher Branch Formation (see Figure 41). Base of the* t*-marker in the Stonewall Formation is at the top of the 1-m scale bar (lower right); red and gray, argillaceous* t*-marker is indicated by the bracket (centre); Stonewall–Fisher Branch contact is indicated by the arrow (upper centre).*

Figure 45: *Stonewall Formation overlain by the Fisher Branch Formation at Stop 10 (photographed in 2010; see Figure 41). Top of the* t*-marker in the Stonewall Formation is at the bottom of the 1-m scale bar (lower left) and at the right-pointing arrow (lower centre); arrows (lower centre and right side) indicate contacts between the numbered units of Bezys (1991, Figure GS-14-5) and Norford et al. (1998, Figure 6); units 3a–c and 2 are in the Stonewall Formation, and unit 1 is the lower portion of the Fisher Branch Formation.*

Fisher Branch Formation (Demski, 2010; Figure 6). In this guidebook, the contact between the Stonewall and Fisher Branch formations is considered to be the O-S systemic boundary. The stratigraphic section and its correlation with Stop 10 and core-hole M-9-86 are illustrated in Figure 41.

Stonewall Formation

Only the uppermost strata of the Stonewall Formation are exposed at Stop 11 (Figures 41, 47a). They resemble the uppermost dolofloatstone unit at Stop 10. Just below the top of the formation at Stop 11, the dolostone clasts are up to 5 mm across, variably coloured, subrounded to rounded, and randomly oriented. There are no macrofossils. It has not been determined whether these strata represent the top-Stonewall marker bed known elsewhere in the Williston Basin. The top of the formation is a sharp, smoothly irregular surface of truncation, representing a prominent disconformity.

Fisher Branch Formation

As at Stop 10, the exposed, lower part of the Fisher Branch Formation consists of highly mottled and bioturbated, sublithographic dolomudstone (Figures 41, 47a). Unlike Stop 10, macrofossils are present. Corals, including tabulates and solitary rugosans (Figure 47b), are predominant, and gastropods are also represented. These strata of the Fisher Branch Formation were deposited during a transgressive event accompanied by normal, open marine, shallow subtidal conditions. The macrofauna that was introduced is the earliest record of the Early Silurian biotic recovery in this area. The brachiopod *Virgiana* has not been found here (see also McCabe, 1988). At Stop 8, the lowest *Virgiana* bed is 2.5 m above the base of the formation. Less than 2 m of the formation is exposed at Stop 10, so these strata are likely below the level of *Virgiana*.

Travel details and instructions

Day 1: Saturday, May 25, 2013

- MANDATORY SAFETY ORIENTATION SESSION in front of main entrance to Winnipeg Convention Centre (375 York Ave., between Carlton St. and Edmonton St.).
  - **7:45 a.m.**
- DEPARTURE from driveway in front of Winnipeg Convention Centre.
  - **depart 8:00 a.m.**
- Turn right (N) onto one-way Edmonton St., travel 0.15 km to St. Mary Ave.
- Turn left (W) onto one-way St. Mary Ave., travel 0.7 km to its end at Portage Ave.
- Turn left (W) onto Portage Ave., travel 2.1 km to Wall St.

Figure 46: *Undulatory contact (indicated by arrow on left and top of 1-m scale bar at centre) between the Stonewall Formation and the overlying Fisher Branch Formation at Stop 10 (photographed in 2012; see Figure 41).*

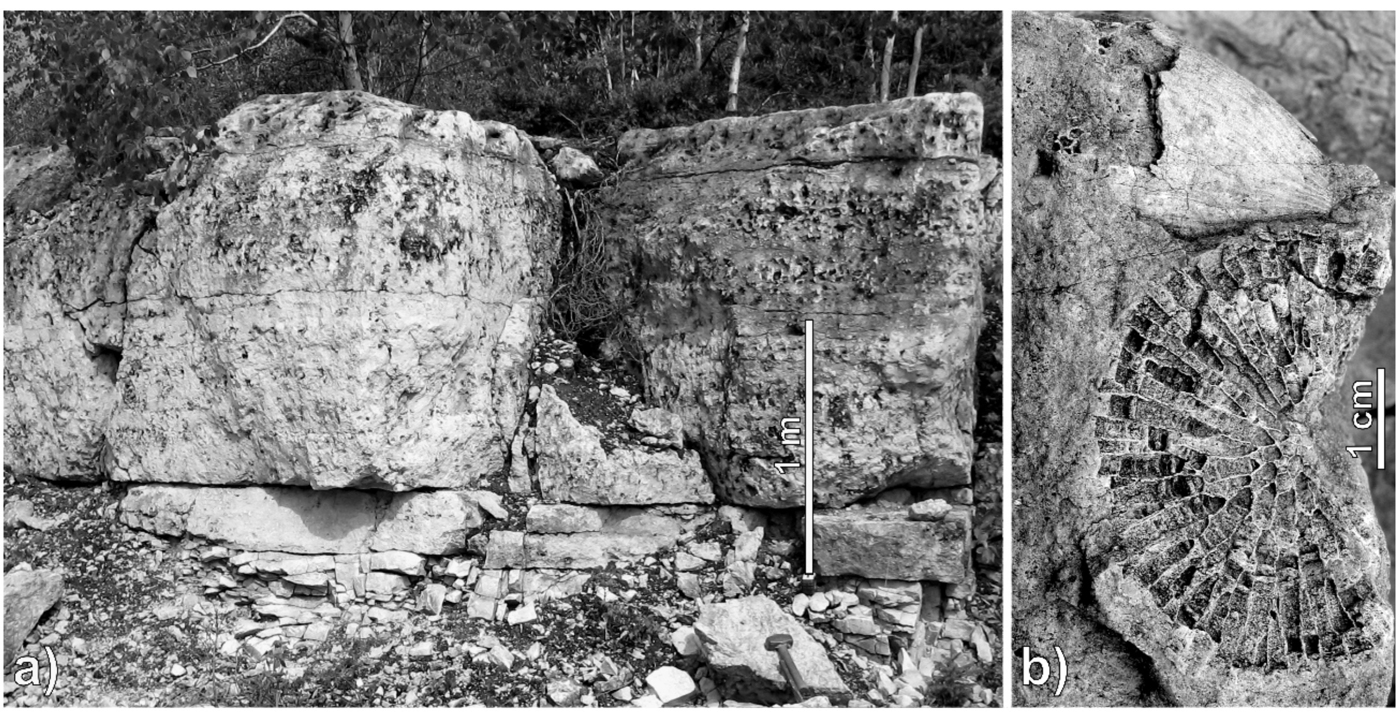

Figure 47: *Strata and fossils at Stop 11.* ***a)*** *Quarry exposure (photographed in 2010; see Figure 41); contact between the Stonewall Formation and the overlying Fisher Branch Formation is at the bottom of the 1-m scale bar.* ***b)*** *Corals in the Fisher Branch Formation: streptelasmatid solitary rugosan (upper), exterior lateral view; favositid tabulate (lower), interior longitudinal view of broken corallum.*

- Turn right (N) onto Wall St., travel 2.7 km to its end at Notre Dame Ave.
- Turn left (W) onto Notre Dame Ave., travel 1.5 km and bend right (N) onto Keewatin St.
- Travel 3.3 km on Keewatin St. to Inkster Blvd.
- Turn left (W) onto Inkster Blvd., travel 2.5 km to Brookside Blvd./Rte. 90.
- Turn right (N) onto Brookside Blvd./Rte. 90 which eventually becomes Hwy. 7, travel 14.8 km to Rd. 73N on right side (just past left-turn sign to Rd. 321).
- Turn right (E) onto Rd. 73 N, travel 0.25 km to Old Hwy. 7 (just past left-turn sign to Stony Mountain).
- Turn left (N) onto Old Hwy. 7, travel 1.0 km to Memorial Blvd. in Stony Mountain (see Figure 8a).
- Turn right (E) onto Memorial Blvd., travel 1.5 km to its end at Dufferin Dr.
- Turn left (NW) onto Dufferin Dr., travel 0.25 km and bend right (N) onto Sellars Hill Rd.
- Travel 0.6 km on Sellars Hill Rd., park vehicle on shoulder.
  - **arrive 8:40 a.m.**, **31.35 km** from Day 1 departure.
- **STOP 1**: carefully walk across road and continue W 500 m to exposures in NW area of quarry; be careful near quarry walls.
- SNACK/DRINK: provided.
  - **depart 10:10 a.m.** (90 min at Stop 1).
- Continue (N) 0.25 km on Sellars Hill Rd. to its end at Vincent Rd.
- Turn left (W) onto Vincent Rd., travel 0.8 km, follow bend left (S), continue 0.4 km to Quarry Rd.
- Turn right (W) onto Quarry Rd., travel 1.0 km to new Hwy. 7.
- Turn right (N) onto Hwy. 7, travel 5.2 km to Hwy. 67.
- Turn left (W) onto Hwy. 67, travel 5.0 km to junction with Rd. 236 in Stonewall (see Figure 8b).
- Continue straight (W) from Hwy. 67 onto 2 Ave. N for 0.35 km to Main St.
- Turn right (N) onto Main St., travel 0.25 km to Stonewall Quarry Park driveway on right side.
- Turn right (NE) onto driveway and travel 0.1 km to parking lot by foot bridge, park vehicle.
  - **arrive 10:20 a.m.**, **44.7 km** from Day 1 departure.
- **STOP 2**: walk N 100 m to Heritage Arts / Interpretive Centre and E 100 m to exposures in quarry; be careful near quarry walls.
- LUNCH: bag lunch/drink provided.
  - **depart 11:50 a.m.** (90 min at Stop 2 including Lunch).
- Return 5.7 km to Hwy. 7.
- Turn left (N) onto Hwy. 7, travel 27.9 km to junction with Hwy. 17 in Teulon.
- Turn left (W) onto Hwy. 17, travel 23.8 km to junction with Rd. 416 in Inwood (just past sign to Fisher Branch).
- Turn right (N) to continue on Hwy. 17, travel 68.7 km to XTR (fuel and convenience store) on left side just before junction with Rd. 233 in Fisher Branch, enter and park vehicle.
  - **arrive 1:10 p.m.**, **170.8 km** from Day 1 departure.
- REST STOP: snack/drink available for purchase.
  - **depart 1:25 p.m.** (15 min at Rest Stop).
- Turn left (W) onto Rd. 233, travel 4.9 km to N-S gravel road (Mile 9W).
- Turn right (N) onto gravel road (Mile 9W), travel 4.9 km to E-W gravel road (Mile 144N) (see Figure 8c).
- Turn right (E) onto gravel road (Mile 144N), travel 0.35 km to farm-yard driveway on left (N) side, park vehicle.
  - **arrive 1:35 p.m.**, **180.95 km** from Day 1 departure.
- **STOP 3**: drive or walk 1.2 km along farm trail to outcrops; be careful near rock faces.
  - **depart 2:45 p.m.** (70 min at Stop 3).
- Return 0.35 km to N-S gravel road (Mile 9W).
- Turn right (N) onto gravel road (Mile 9W), travel 6.7 km to junction with major E-W gravel road (Rd. 325).
- Turn left (W) onto Rd. 325, travel 47.2 km to junction with Hwy. 6 in Ashern.
- Turn left (S) onto Hwy. 6, travel 0.2 km to Esso (fuel and convenience store) on right side, enter and park vehicle.
  - **arrive 3:25 p.m.**, **235.4 km** from Day 1 departure.
- REST STOP: snack/drink available for purchase.
  - **depart 3:40 p.m.** (15 min at Rest Stop).
- Turn left (N) onto Hwy. 6, travel 245.3 km to Shell (fuel and convenience store) on right side in Grand Rapids, enter and park vehicle.
  - **arrive 6:10 p.m.**, **480.7 km** from Day 1 departure.
- DINNER: available for purchase at Pelican Nest Restaurant; evening snack/drink available for purchase at Shell.
  - **depart 7:25 p.m.** (75 min for Dinner).
- Turn right (N) onto Hwy. 6, travel 3.9 km to Grand Rapids Dr. in Grand Rapids.
- Turn left onto Grand Rapids Dr., travel 0.1 km to Northbrook Inn office (toll-free 1-888-868-9060, phone 204-639-2380), park vehicle.
- LODGING CHECK-IN: double-occupancy room provided.
- Travel 0.3 km to Lodge on opposite side of Hwy. 6, park vehicle.
  - **arrive 7:40 p.m.**, **485.0 km** from Day 1 departure.
- END of Day 1.
  - **11 h 55 min, 485.0 km.**

Day 2: Sunday, May 26, 2013

- DEPARTURE from Lodge for breakfast (prior to check-out from Northbrook Inn).
  - **depart 7:40 a.m.**

- Travel 0.2 km from Lodge to Hwy. 6.
- Turn left (SE) onto Hwy. 6, travel 3.9 km to Shell (fuel and convenience store) on left side, enter and park vehicle.
  - **arrive 7:45 a.m.**, **4.1 km** from Day 2 departure.
- BREAKFAST: available for purchase at Pelican Nest Restaurant; daytime snacks/drinks available for purchase at Shell.
  - **depart 8:45 a.m.** (60 min for Breakfast).
- Return 4.1 km to Lodge, park vehicle.
  - **arrive 8:50 a.m.**, **8.2 km** from Day 2 departure.
- REST STOP, CHECK-OUT AND DEPARTURE from Northbrook Inn.
  - **depart 9:10 a.m.** (20 min at Rest Stop).
- Travel 0.2 km from Lodge to Hwy. 6.
- Turn right (NW) onto Hwy. 6, travel 101.0 km to paved roundabout on left side (see Figure 24a).
- Turn left (W) onto roundabout, park vehicle.
  - **arrive 10:15 a.m.**, **109.4 km** from Day 2 departure.
- **STOP 4**: carefully walk across Hwy. 6 and continue E 100 m to exposure surface.
  - **depart 10:55 a.m.** (40 min at Stop 4).
- Turn right (S) from roundabout onto Hwy. 6, travel 2.6 km, park vehicle on shoulder.
  - **arrive 11:00 a.m.**, **112.0 km** from Day 2 departure.
- **STOP 5**: carefully walk across Hwy. 6 and continue E 150 m to exposure surface.
  - **depart 11:40 a.m.** (40 min at Stop 5).
- Continue (S) on Hwy. 6 for 0.8 km to beginning of roadcut on left side, park vehicle on shoulder.
  - **arrive 11:45 a.m.**, **112.8 km** from Day 2 departure.
- **STOP 6**: carefully walk across Hwy. 6 and continue E 100 m to exposure surface.
  - **depart 12:25 p.m.** (40 min at Stop 6).
  - return to vehicle.
- LUNCH: bag lunch/drink provided.
- **STOP 7**: carefully walk across Hwy. 6 to beginning of roadcut on E side, which continues uphill (S) for 600 m; beware of traffic and be careful near rock face.
  - return to bottom of roadcut and carefully cross Hwy. 6 to vehicle.
  - **depart 1:55 p.m.** (90 min at Stop 7 including Lunch).
- Continue (S) on Hwy. 6 for 5.7 km to beginning of roadcut on right side, park vehicle on shoulder.
  - **arrive 2:00 p.m.**, **118.5 km** from Day 2 departure.
- **STOP 8**: carefully walk uphill (S) along 350-m-long roadcut on W side of Hwy. 6; beware of traffic and be careful near rock face.
  - return to vehicle.
  - **depart 3:00 p.m.** (60 min at Stop 8).
- Carefully turn vehicle around on Hwy. 6.
- Travel (N) on Hwy. 6 for 82.6 km to junction with Hwy. 39.
- Turn right (E) to continue on Hwy. 6, travel 0.1 km to Petro-Canada (fuel and convenience store) on left side, enter and park vehicle.
  - **arrive 3:50 p.m.**, **201.2 km** from Day 2 departure.
- REST STOP: snack/drink available for purchase.
  - **depart 4:05 p.m.** (15 min at Rest Stop).
- Turn right (W) onto Hwy. 6, travel 0.1 km to junction with Hwy. 39.
- Continue straight (W) on Hwy. 39, travel 163.0 km to its end at Hwy. 10.
- Turn left (S) onto Hwy. 10, travel 73.3 km to Kikiwak Rd. in The Pas.
- Turn right onto Kikiwak Rd., travel 0.2 km to Kikiwak Inn (toll-free 1-888-545-4925, phone 204-623-1800), park vehicle.
  - **arrive 6:25 p.m.**, **437.8 km** from Day 2 departure.
- LODGING CHECK-IN: double-occupancy room provided.
- DINNER: available for purchase in Niska Dining Room at Kikiwak Inn or nearby Tim Hortons (fast-food restaurant); evening snack/drink available for purchase at nearby Tim Hortons and Shell (fuel and convenience store).
- END of Day 2:
  - **10 h 45 min**, **437.8 km**.

Day 3: Monday, May 27, 2013

- BREAKFAST: available for purchase at Niska Dining Room in Kikiwak Inn or nearby Tim Hortons (fast-food restaurant); daytime snacks/drinks available for purchase at nearby Tim Hortons and Shell (fuel and convenience store).
- CHECK-OUT AND DEPARTURE from Kikiwak Inn.
  - **depart 8:30 a.m.**
- Travel 0.2 km to Hwy. 10.
- Turn left (N) onto Hwy. 10, travel 18.0 km to junction with Rd. 287.
- Turn right (E) onto Rd. 287, travel 19.4 km to junction and turn right (E) to stay on Rd. 287 (sign to Cormorant).
- Continue on Rd. 287 for 30.8 km to driveway on right side (just past diamond-shaped road-sign on left side) (see Figure 24b).
- Turn right (E) onto driveway, travel 0.3 km to quarry entrance, park vehicle.
  - **arrive 9:20 a.m.**, **68.7 km** from Day 3 departure.
- **STOP 9**: carefully walk 100 m down ramp to exposures in quarry; be careful near quarry walls.
  - **depart 10:10 a.m.** (50 min at Stop 9).
- Return 0.3 km to Rd. 287.
- Turn right (N) onto Rd. 287, travel 3.7 km to just past lowest exposure of roadcut.
- Carefully turn vehicle around on Rd. 287, park on shoulder just before exposure.

- **arrive 10:15 a.m.**, **72.7 km** from Day 3 departure.

- **STOP 10**: carefully walk uphill (SW) along 250-m-long roadcut on NW side of Rd. 287; beware of traffic and be careful near rock face.
  - return to vehicle.
  - **depart 11:15 a.m.** (60 min at Stop 10).
- Continue (SW) on Rd. 287 for 0.9 km, park vehicle on shoulder.
  - **arrive 11:20 a.m.**, **73.6 km** from Day 3 departure.
- **STOP 11**: carefully walk 50 m N into small quarry; be careful near quarry walls.
  - **depart 11:40 a.m.** (20 min at Stop 11).
- Return 71.0 km to intersection of Hwy. 10 and Kikiwak Rd. in The Pas.
- Continue on Hwy. 10 for 3.5 km to A&W (fast-food restaurant) on right side, enter and park vehicle.
  - **arrive 12:35 p.m.**, **148.1 km** from Day 3 departure.
- LUNCH: available for purchase at A&W and nearby KFC (fast-food restaurant).
  - **depart 1:15 p.m.** (40 min for Lunch).
- Turn right (S) onto Hwy. 10, travel 71.9 km to junction with Hwy. 60.
- Turn left (E) onto Hwy. 60, travel 151.0 km to its end at Hwy. 6.
- Turn right (S) onto Hwy. 6, travel 1.0 km to Shell (fuel and convenience store) on right side, enter and park vehicle.
  - **arrive 3:35 p.m.**, **372.0 km** from Day 3 departure.
- REST STOP: snack/drink available for purchase at Shell and Tim Hortons (fast-food restaurant).
  - **depart 3:50 p.m.** (15 min at Rest Stop).
- Turn right (S) onto Hwy. 6, travel 216.0 km to Esso (fuel and convenience store) on right side in Ashern, enter and park vehicle.
  - **arrive 6:00 p.m.**, **588.0 km** from Day 3 departure.
- REST STOP: snack/drink available for purchase.
  - **depart 6:15 p.m.** (15 min at Rest Stop).
- Turn right (S) onto Hwy. 6, travel 163.0 km to its end at Perimeter Hwy. 101.
- Turn left (E) onto Perimeter Hwy. 101, travel 5.2 km to exit for Rte. 90 S/Brookside Blvd.
- Turn right (S) onto Rte. 90, travel 9.3 km to Notre Dame Ave.
- Turn left (E) onto Notre Dame Ave., travel 5.8 km to downtown Winnipeg as follows:
  - at 4.0 km Notre Dame Ave./Rte. 57 bends onto Cumberland Ave./Rte. 57;
  - at 5.3 km Cumberland Ave. merges with Donald St.;
  - at 5.8 km Donald St. intersects St. Mary Ave.
- Turn right (W) onto one-way St. Mary Ave., travel 0.2 km to Carlton St.
- Turn left (S) onto one-way Carlton St., travel 0.15 km to just before York Ave.
- Turn right (W) onto driveway in front of Winnipeg Convention Centre, travel 0.05 km to main entrance, park vehicle.
  - **arrive 8:20 p.m.**, **771.7 km** from Day 3 departure.
- END of Day 3 (and Field Trip):
  - **11 h 50 min**, **771.7 km (total 1695 km)**.

Acknowledgments

Much of the research presented in this guidebook was funded by grants from the Natural Sciences and Engineering Research Council (NSERC) to R.J. Elias and G.A. Young, donations from R.J. McAuley to the University of Manitoba (UM) in support of R.J. Elias's research program, and grants from The Manitoba Museum Foundation to G.A. Young. The Manitoba Career Start and Career Focus programs provided financial assistance for summer student researchers and assistants at UM. L.A. Stewart received support from an NSERC Postgraduate Scholarship, the UM Faculty of Graduate Studies Top-up Program, a William J. Hill Memorial Award, and a Rita Wadien Memorial Scholarship. M.W. Demski received NSERC Undergraduate Student Research Awards, an Alexander Graham Bell Canada Graduate Scholarship, support from the Clayton H. Riddell Faculty of Environment, Earth, and Resources (UM), and a Paleontological Society Student Research Grant (Kenneth E. & Annie Caster Award).

We are grateful to many individuals for their roles in various aspects of this research. Students in the UM Department of Geological Sciences (DGS) who assisted with field and/or laboratory work include B. Chapman, B.J. Duncan, R.S. St. Pierre, A. Sheng, T.N. Tuba, and B.J. Wheadon. D.P. Thompson (The Manitoba Museum) helped in the field. G. Benger, D. Berk, and V. Varga (Manitoba Geological Survey) drilled a core hole in the Grand Rapids Uplands, and provided access to drill cores, and cut samples from cores, at the Midland Laboratory and Rock Storage Facility in Winnipeg. Stable-isotope analyses (carbon and oxygen) of dolomite samples, drilled from dolomudstone or the micritic matrix of other types of dolostone, were conducted by W. Abdi, P. Middlestead, and P. Wickham at the G.G. Hatch Stable Isotope Laboratory (University of Ottawa) in 2009, and by M. Yun at the Stable Isotopes for Innovative Research Laboratory (UM DGS) in 2010 and 2011, following the standard analytical procedures of those laboratories (analytical precision [2 sigma] was ±0.1‰). N. Ball provided technical assistance in the X-Ray Diffraction Laboratory (UM DGS). Access to property during field work and on this field trip was kindly provided by G. Thorsteinson (Rural Municipality of Rockwood; Stop 1), C. Precourt (Stonewall Quarry Park; Stop 2), and J. Wagner (deceased), E. Wagner, and W. Wagner (Stop 3). We thank M.P.B. Nicolas (Manitoba Geological Survey) for reviewing the manuscript.

References

Achab, A., Asselin, E., Desrochers, A., Riva, J.F. and Farley, C. 2011: Chitinozoan biostratigraphy of a new Upper Ordovician stratigraphic framework for Anticosti Island, Canada; Geological Society of America, Bulletin, v. 123, p. 186–205.

Achab, A. and Paris, F. 2007: The Ordovician chitinozoan biodiversification and its leading factors; Palaeogeography, Palaeoclimatology, Palaeoecology, v. 245, p. 58–19.

Andrichuk, J.M. 1959: Ordovician and Silurian stratigraphy and sedimentation in southern Manitoba, Canada; American Association of Petroleum Geologists, Bulletin, v. 43, p. 2333–2398.

Baillie, A.D. 1951: Silurian geology of the Interlake area, Manitoba; Manitoba Department of Mines and Natural Resources, Mines Branch, Publication 50-1, 82 p.

Baillie, A.D. 1952: Ordovician geology of Lake Winnipeg and adjacent areas, Manitoba; Manitoba Department of Mines and Natural Resources, Mines Branch, Publication 51-6, 64 p. [Note: there are two editions of this publication, one with the author's name incorrectly printed as "Andrew W. Baillie".]

Bergström, S.M., Chen, X., Gutiérrez-Marco, J.C. and Dronov, A. 2009: The new chronostratigraphic classification of the Ordovician System and its relations to major regional series and stages and to $\delta^{13}C$ chemostratigraphy; Lethaia, v. 42, p. 97–107.

Bergström, S.M., Kleffner, M. and Schmitz, B. 2012: Late Ordovician–Early Silurian $\delta^{13}C$ chemostratigraphy in the Upper Mississippi Valley: implications for chronostratigraphy and depositional interpretations; Royal Society of Edinburgh, Earth and Environmental Science Transactions, v. 102, p. 159–178.

Bergström, S.M., Kleffner, M., Schmitz, B. and Cramer, B.D. 2011: Revision of the position of the Ordovician-Silurian boundary in southern Ontario: regional chronostratigraphic implication of $\delta^{13}C$ chemostratigraphy of the Manitoulin Formation and associated strata; Canadian Journal of Earth Sciences, v. 48, p. 1447–1470.

Bezys, R.K. 1991: Stratigraphic mapping (NTS 63F, 63K) and core hole program 1991; *in* Manitoba Energy and Mines, Minerals Division, Report of Activities, 1991, p. 61–73.

Bezys, R.K. and McCabe, H.R. 1996: Lower to Middle Paleozoic stratigraphy of southwestern Manitoba; Geological Association of Canada and Mineralogical Association of Canada Annual Meeting 1996, Winnipeg, Manitoba, Field Trip Guidebook B4, 92 p.

Brenchley, P.J., Marshall, J.D. and Underwood, C.J. 2001: Do all mass extinctions represent an ecological crisis? Evidence from the Late Ordovician; Geological Journal, v. 36, p. 329–340.

Brindle, J.E. 1960: The faunas of the Lower Palaeozoic carbonate rocks in the subsurface of Saskatchewan; Saskatchewan Department of Mineral Resources, Petroleum and Natural Gas Branch, Geology Division, Report 52, 45 p.

Cocks, L.R.M., Fortey, R.A. and Rushton, A.W.A. 2010: Correlation for the Lower Palaeozoic; Geological Magazine, v. 147, p. 171–180.

Cocks, L.R.M. and Torsvik, T.H. 2002: Earth geography from 500 to 400 million years ago: a faunal and palaeomagnetic review; Geological Society, London, Journal, v. 159, p. 631–644.

Corkery, M.T., Lauhn-Jensen, D.M., Franceschet, T. and Hopper, D.J. 1994: Manitoba geological highway map (2nd ed.); Manitoba Energy and Mines, Minerals Division, and Geological Survey of Canada, Geoscientific Map, 1994, scale 1:1 000 000.

Cowan, J.R. 1971: Ordovician and Silurian stratigraphy of the Interlake area, Manitoba; *in* Geoscience Studies in Manitoba, A.C. Turnock, (ed.), Geological Association of Canada, Special Paper 9, p. 235–241.

Cowan, J.R. 1977: Ordovician and Silurian stratigraphy in the Interlake area, Manitoba; MSc thesis, University of Manitoba, Winnipeg, 73 p. [Note: although bibliographic and literature citations give the year as 1977, the date on the title page is "January 1978".]

Cramer, B.D., Brett, C.E., Melchin, M.J., Männik, P., Kleffner, M.A., McLaughlin, P.I., Loydell, D.K., Munnecke, A., Jeppsson, L., Corradini, C., Brunton, F.R. and Saltzman, M.R. 2011: Revised correlation of Silurian provincial series of North America with global and regional chronostratigraphic units and $\delta^{13}C_{carb}$ chemostratigraphy; Lethaia, v. 44, p. 185–202.

Demski, M.W. 2010: The Ordovician-Silurian boundary in the Williston Basin outcrop belt of central Manitoba: new data and reinterpretations; BSc thesis, Department of Geological Sciences, University of Manitoba, Winnipeg, 113 p.

Demski, M.W., Stewart, L.A., Elias, R.J., Young, G.A., Nowlan, G.S. and Dobrzanski, E.P. 2010: Hirnantian (latest Ordovician) strata in the heart of the continent? Intriguing results from Williston Basin, Manitoba; GeoCanada 2010 — Working with the Earth, Calgary, Alberta, Conference Abstracts, URL <http://www.cseg.ca/conventions/abstracts/2010/2010abstracts/0208_GC2010_Hirnantian_Strata_in_Heart_of_the_Continent.pdf>.

Demski, M.W., Wheadon, B.J., Stewart, L.A., Elias, R.J., Young, G.A., Nowlan, G.S. and Dobrzanski, E.P. 2011a: Ordovician-Silurian boundary interval in the Williston and Hudson Bay basins, Manitoba: isotopic carbon excursion and conodont turnover; GAC-MAC-SEG-SGA Joint Annual Meeting 2011, Ottawa, Ontario, Abstracts Volume 34, p. 50–51.

Demski, M.W., Wheadon, B.J., Stewart, L.A., Elias, R.J., Young, G.A., Nowlan, G.S. and Dobrzanski, E.P. 2011b: Latest Ordovician glacio-eustatic fluctuation in the Williston and Hudson Bay basins of Manitoba, Canada: conodont turnover, isotopic carbon excursion, and subaerial exposure; Geological Society of America Annual Meeting 2011, Minneapolis, Minnesota, Abstracts with Programs, v. 43, p. 611.

Dowling, D.B. 1900: Report on the geology of the west shore and islands of Lake Winnipeg; Geological Survey of Canada, Annual Report (New Series), v. 11, pt. F, 100 p.

Elias, R.J. 1981: Solitary rugose corals of the Selkirk Member, Red River Formation (late Middle or Upper Ordovician), southern Manitoba; Geological Survey of Canada, Bulletin 344, 53 p.

Elias, R.J. 1982: Paleoecology and biostratinomy of solitary rugose corals in the Stony Mountain Formation (Upper Ordovician), Stony Mountain, Manitoba; Canadian Journal of Earth Sciences, v. 19, p. 1582–1598.

Elias, R.J. 1983: Late Ordovician solitary rugose corals of the Stony Mountain Formation, southern Manitoba, and its equivalents; Journal of Paleontology, v. 57, p. 924–956.

Elias, R.J. 1989: Extinctions and origins of solitary rugose corals, latest Ordovician to earliest Silurian in North America; *in* Fossil Cnidaria 5, P.A. Jell and J.W. Pickett, (ed.), Association of Australasian Palaeontologists, Memoir 8, p. 319–326.

Elias, R.J. 1991: Environmental cycles and bioevents in the Upper Ordovician Red River–Stony Mountain solitary rugose coral province of North America; *in* Advances in Ordovician Geology, C.R. Barnes and S.H. Williams, (ed.), Geological Survey of Canada, Paper 90-9, p. 205–211.

Elias, R.J., Nowlan, G.S. and Bolton, T.E. 1988: Paleontology of the type section, Fort Garry Member, Red River Formation (Upper Ordovician), southern Manitoba; *in* Contributions to Paleozoic Paleontology and Stratigraphy in Honor of Rousseau H. Flower, D.L. Wolberg, (compiler), New Mexico Bureau of Mines and Mineral Resources, Memoir 44, p. 341–359.

Elias, R.J. and Young, G.A. 1998: Coral diversity, ecology, and provincial structure during a time of crisis: the latest Ordovician to earliest Silurian Edgewood Province in Laurentia; Palaios, v. 13, p. 98–112.

Elias, R.J. and Young, G.A. 2004: Laurentian corals; *in* The Great Ordovician Biodiversification Event, B.D. Webby, F. Paris, M.L. Droser and I.G. Percival, (ed.), Columbia University Press, New York, p. 133–138.

Elias, R.J., Young, G.A., Lee, D.-J. and Bae, B.-Y. In press: Coral biogeography in the Late Ordovician (Cincinnatian) of Laurentia; *in* Early Palaeozoic Biogeography and Geography, D.A.T. Harper and T. Servais, (ed.), Geological Society (London), Memoir.

Finnegan, S., Bergmann, K., Eiler, J.M., Jones, D.S., Fike, D.A., Eisenman, I., Hughes, N.C., Tripati, A.K. and Woodward, W.F. 2011: The magnitude and duration of Late Ordovician–Early Silurian glaciation; Science, v. 331, p. 903–906.

Finnegan, S., Heim, N.A., Peters, S.E. and Fisher, W.W. 2012: Climate change and the selective signature of the Late Ordovician mass extinction; National Academy of Sciences (U.S.A.), Proceedings, v. 109, p. 6829–6834.

Finney, S.C., Berry, W.B.N., Cooper, J.D., Ripperdan, R.L., Sweet, W.C., Jacobson, S.R., Soufiane, A., Achab, A. and Noble, P.J. 1999: Late Ordovician mass extinction: a new perspective from stratigraphic sections in central Nevada; Geology, v. 27, p. 215–218.

Fuller, J.G.C.M. 1961: Ordovician and contiguous formations in North Dakota, South Dakota, Montana, and adjoining areas of Canada and United States; American Association of Petroleum Geologists, Bulletin, v. 45, p. 1334–1363.

Google Maps. URL <http://www.google.ca/maps> [August 22–24, 2012].

Goudge, M.F. 1945: Limestones of Canada, their occurrence and characteristics, part V, western Canada; Canada Department of Mines and Resources, Mines and Geology Branch, Bureau of Mines, No. 811, 233 p.

Haidl, F.M. 1992: Correlation of outcrop and subsurface data from Lower Paleozoic strata, Cumberland Lake–Namew Lake area, east-central Saskatchewan; *in* Summary of Investigations 1992, Saskatchewan Geological Survey, Saskatchewan Energy and Mines, Miscellaneous Report 92-4, p. 213–219.

Hammarlund, E.U., Dahl, T.W., Harper, D.A.T., Bond, D.P.G., Nielsen, A.T., Bjerrum, C.J., Schovsbo, N.H., Schönlaub, H.P., Zalasiewicz, J.A. and Canfield, D.E. 2012: A sulfidic driver for the end-Ordovician mass extinction; Earth and Planetary Science Letters, v. 331–332, p. 128–139.

Harper, D.A.T. 2006: The Ordovician biodiversification: setting an agenda for marine life; Palaeogeography, Palaeoclimatology, Palaeoecology, v. 232, p. 148–166.

Holland, S.M. and Patzkowsky, M.E. 2009: The stratigraphic distribution of fossils in a tropical carbonate succession: Ordovician Bighorn Dolomite, Wyoming, USA; Palaios, v. 24, p. 303–317.

Holland, S.M. and Patzkowsky, M.E. 2012: Sequence architecture of the Bighorn Dolomite, Wyoming, USA: transition to the Late Ordovician icehouse; Journal of Sedimentary Research, v. 82, p. 599–615.

International Commission on Stratigraphy. 2012: International chronostratigraphic chart; URL <http://www.stratigraphy.org/ics%20chart/ChronostratChart2012.pdf>.

Jin, J., Haidl, F.M., Bezys, R.K. and Gerla, G. 1999: The Early Silurian *Virgiana* brachiopod beds in the northeastern Williston Basin, Manitoba and Saskatchewan; *in* Summary of Investigations 1999, Volume 1, Saskatchewan Geological Survey, Saskatchewan Energy and Mines, Miscellaneous Report 99-4.1, p. 3–11.

Jin, J., Harper, D.A.T., Rasmussen, J.A. and Sheehan, P.M. 2012: Late Ordovician massive-bedded *Thalassinoides* ichnofacies along the palaeoequator of Laurentia; Palaeogeography, Palaeoclimatology, Palaeoecology, v. 367–368, p. 73–88.

Jin, J. and Zhan, R. 2001: Late Ordovician articulate brachiopods from the Red River and Stony Mountain formations, southern Manitoba; NRC Research Press, Ottawa, 117 p.

Johnson, M.E. and Lescinsky, H.L. 1986: Depositional dynamics of cyclic carbonates from the Interlake Group (Lower Silurian) of the Williston Basin; Palaios, v. 1, p. 111–121.

Jones, D.S., Fike, D.A., Finnegan, S., Fischer, W.W., Schrag, D.P. and McCay, D. 2011: Terminal Ordovician carbon isotope stratigraphy and glacioeustatic sea-level change across Anticosti Island (Québec, Canada); Geological Society of America, Bulletin, v. 123, p. 1645–1664.

Kendall, A.C. 1976: The Ordovician carbonate succession (Bighorn Group) of southeastern Saskatchewan; Saskatchewan Department of Mineral Resources, Saskatchewan Geological Survey, Sedimentary Geology Division, Report 180, 185 p.

Kindle, E.M. 1914: The Silurian and Devonian section of western Manitoba; Geological Survey of Canada, Department of Mines, Summary Report 1912, p. 247–261.

Krug, A.Z. and Patzkowsky, M.E. 2007: Geographic variation in turnover and recovery from the Late Ordovician mass extinction; Paleobiology, v. 33, p. 435–454.

Kupsch, W.O. 1952. Ordovician and Silurian stratigraphy of east central Saskatchewan; Saskatchewan Department of Mineral Resources, Geological Sciences Branch, Sedimentary Geology Division, Report 10, 62 p.

Lenton, T.M., Crouch, M., Johnson, M., Pires, N. and Dolan, L. 2012: First plants cooled the Ordovician; Nature Geoscience, v. 5, p. 86–89.

Lobdell, F.K. 1992: Arthrostylidae (Bryozoa: Cryptostomata) from the Gunn Member, Stony Mountain Formation (Upper Ordovician), North Dakota and Manitoba; *in* Proceedings of the F.D. Holland, Jr., Geological Symposium, J.M. Erickson and J.W. Hoganson, (ed.), North Dakota Geological Survey, Miscellaneous Series 76, p. 99–115.

Lukie, T.D. 1996: Genesis and bioturbation of limestone beds of the Gunn Member, Stony Mountain Formation (Upper Ordovician), Stony Mountain, Manitoba; BSc thesis, Department of Geological Sciences, University of Manitoba, Winnipeg, 128 p.

McCabe, H.R. 1971: Stratigraphy of Manitoba, an introduction and review; *in* Geoscience Studies in Manitoba, A.C. Turnock, (ed.), Geological Association of Canada, Special Paper 9, p. 167–187.

McCabe, H.R. 1979: GS-16 Stratigraphic and industrial minerals core hole program; *in* Report of Field Activities 1979, Manitoba Mines, Natural Resources and Environment, Mineral Resources Division, p. 76–78.

McCabe, H.R. 1980: GS-12 Stratigraphic mapping and core hole program southwest Manitoba; *in* Report of Field Activities 1980, Manitoba Energy and Mines, Mineral Resources Division, p. 70–73.

McCabe, H.R. 1986: GS-40 Stratigraphic mapping and stratigraphic and industrial minerals core hole program; *in* Report of Field Activities 1986, Manitoba Energy and Mines, Mineral Division, p. 191–198.

McCabe, H.R. 1988: Preliminary report on Ordovician-Silurian boundary rocks in the Interlake area, Manitoba, Canada; *in* A Global Analysis of the Ordovician-Silurian Boundary, L.R.M. Cocks and R.B. Rickards, (ed.), British Museum of Natural History (Geology), Bulletin, v. 43, p. 255–257.

McCabe, H.R. and Bannatyne, B.B. 1970: Lake St. Martin crypto-explosion crater and geology of the surrounding area; Manitoba Mines Branch, Department of Mines and Natural Resources, Geological Paper 3/70, 79 p.

McCabe, H.R. and Bezys, R.K. 1998: Subcrop-outcrop and structure contour map, Paleozoic erosion surface; Manitoba Energy and Mines, Geological Services, Stratigraphic Map Series, P-1, scale 1:1 000 000.

McGhee, G.R., Jr., Sheehan, P.M., Bottjer, D.J. and Droser, M.L. 2004: Ecological ranking of Phanerozoic biodiversity crises: ecological and taxonomic severities are decoupled; Palaeogeography, Palaeoclimatology, Palaeoecology, v. 211, p. 289–297.

Melchin, M.J. and Holmden, C. 2006: Carbon isotope chemostratigraphy in Arctic Canada: sea-level forcing of carbonate platform weathering and implications for Hirnantian global correlation; Palaeogeography, Palaeoclimatology, Palaeoecology, v. 234, p. 186–200.

Munnecke, A., Calner, M., Harper, D.A.T. and Servais, T. 2010: Ordovician and Silurian sea-water chemistry, sea level, and climate: a synopsis; Palaeogeography, Palaeoclimatology, Palaeoecology, v. 296, p. 389–413.

Nelson, S.J. 1959a: Arctic Ordovician fauna: an equatorial assemblage?; Alberta Society of Petroleum Geologists, Journal, v. 7, p. 45–47, 53.

Nelson, S.J. 1959b: Guide fossils of the Red River and Stony Mountain equivalents (Ordovician); Alberta Society of Petroleum Geologists, Journal, v. 7, p. 51–61.

Nicolas, M.P.B. and Barchyn, D. 2008: Williston Basin Project (Targeted Geoscience Initiative II): summary report on Paleozoic stratigraphy, mapping and hydrocarbon assessment, southwestern Manitoba; Manitoba Science, Technology, Energy and Mines, Manitoba Geological Survey, Geoscientific Paper GP2008-2, 21 p.

Norford, B.S., Haidl, F.M., Bezys, R.K., Cecile, M.P., McCabe, H.R. and Paterson, D.F. 1994: Middle Ordovician to Lower Devonian strata of the Western Canada Sedimentary Basin; *in* Geological Atlas of the Western Canada Sedimentary Basin, G.D. Mossop and I. Shetsen, (compilers), Canadian Society of Petroleum Geologists and Alberta Research Council, Special Report 4, p. 109–127.

Norford, B.S., Nowlan, G.S., Haidl, F.M. and Bezys, R.K. 1998: The Ordovician-Silurian boundary interval in Saskatchewan and Manitoba; *in* Eighth International Williston Basin Symposium, J.E. Christopher, C.F. Gilboy, D.F. Paterson and S.L. Bend, (ed.), Saskatchewan Geological Society, Special Publication 13, p. 27–45.

Nowlan, G.S. 1989: Report on sixty samples from Ordovician and Silurian strata of Manitoba; Geological Survey of Canada, unpublished Report 002-GSN-1989, 23 p.

Nowlan, G.S. 2008: Report on five samples from Upper Ordovician–Lower Silurian strata from the Stonewall Formation, north of Grand River, Manitoba; Geological Survey of Canada, unpublished Paleontological Report 004-GSN-2008, 4 p.

Nowlan, G.S. 2009a: Report on twenty-two samples from Upper Ordovician Stonewall Formation exposed in a roadcut on east side of Highway 6 north of Grand Rapids, Manitoba; Geological Survey of Canada, unpublished Paleontological Report 002-GSN-2009, 13 p.

Nowlan, G.S. 2009b: Report on forty-five samples from Upper Ordovician–Lower Silurian strata exposed in road-cuts on Highway 6, north of Grand Rapids, Manitoba; unpublished Paleontological Report 003-GSN-2009; Geological Survey of Canada (Calgary), 25 p.

Nowlan, G.S. 2013: Report on one sample from Lower Silurian strata of the Stonewall Formation exposed in a road-cut on Highway 6 north of Grand Rapids, Manitoba; unpublished Paleontological Report 002-GSN-2013; Geological Survey of Canada (Calgary), 2 p.

Nowlan, G.S. and Haidl, F.M. 2001: Biostratigraphy and paleoecology of Late Ordovician conodonts from a composite section in the subsurface of Saskatchewan; *in* Summary of Investigations 2001, Volume 1, Saskatchewan Geological Survey, Saskatchewan Energy and Mines, Miscellaneous Report 2001-4.1, p. 14–31.

Okulitch, V.J. 1943: The Stony Mountain Formation of Manitoba; Royal Society of Canada, Transactions, v. 37, p. 59–74.

Porter, J.W. and Fuller, J.G.C.M. 1959: Lower Paleozoic rocks of northern Williston Basin and adjacent areas; American Association of Petroleum Geologists, Bulletin, v. 43, p. 124–189.

Porter, M.J. 2011: Stratigraphy and depositional history of the upper Stony Mountain and lower Stonewall formations in the Stonewall area, southern Manitoba; BSc thesis, Department of Geological Sciences, University of Manitoba, Winnipeg, 81 p.

Pratt, B.R. and Haidl, F.M. 2008: Microbial patch reefs in Upper Ordovician Red River strata, Williston Basin, Saskatchewan: signal of heating in a deteriorating epeiric sea; *in* Dynamics of Epeiric Seas, B.R. Pratt and C. Holmden, (ed.), Geological Association of Canada, Special Paper 48, p. 303–340.

Railsback, L.B., Holland, S.M., Hunter, D.M., Jordan, E.M., Díaz, J.R. and Crowe, D.E. 2003: Controls on geochemical expression of subaerial exposure in Ordovician limestones from the Nashville Dome, Tennessee, U.S.A.; Journal of Sedimentary Research, v. 73, p. 790–805.

Rasmussen, C.M.Ø. and Harper, D.A.T. 2011: Did the amalgamation of continents drive the end Ordovician mass extinctions?; Palaeogeography, Palaeoclimatology, Palaeoecology, v. 311, p. 48–62.

Rudkin, D.M., Young, G.A. and Nowlan, G.S. 2008: The oldest horseshoe crab: a new xiphosurid from Late Ordovician Konservat-Lagerstätten deposits, Manitoba, Canada; Palaeontology, v. 51, p. 1–9.

Schmitz, B., Harper, D.A.T., Peucker-Ehrenbrink, B., Stouge, S., Alwmark, C., Cronholm, A., Bergström, S.M., Tassinari, M. and Xiaofeng, W. 2008: Asteroid breakup linked to the Great Ordovician Biodiversification Event; Nature Geoscience, v. 1, p. 49–53.

Sepkoski, J.J., Jr. 1984: A kinetic model of Phanerozoic taxonomic diversity, III, post-Paleozoic families and mass extinctions; Paleobiology, v. 10, p. 246–267.

Sepkoski, J.J., Jr. 1995: The Ordovician radiations: diversification and extinction shown by global genus-level taxonomic data; *in* Ordovician Odyssey: Short Papers for the Seventh International Symposium on the Ordovician System, J.D. Cooper, M.L. Droser and S.C. Finney, (ed.), Pacific Section, Society for Sedimentary Geology (SEPM), Book 77, p. 393–396.

Servais, T., Harper, D.A.T., Li, J., Munnecke, A., Owen, A.W. and Sheehan, P.M. 2009: Understanding the Great Ordovician Biodiversification Event (GOBE): influences of paleogeography, paleoclimate, or paleoecology?; GSA Today, v. 19, no. 4/5, p. 4–10.

Servais, T., Owen, A.W., Harper, D.A.T., Kröger, B. and Munnecke, A. 2010: The Great Ordovician Biodiversification Event (GOBE): the palaeoecological dimension; Palaeogeography, Palaeoclimatology, Palaeoecology, v. 294, p. 99–119.

Sharma, S. and Dix, G.R. 2004: Magnesian calcite and chamositic ooids forming shoals peripheral to Late Ordovician (Ashgill) muddy siliciclastic shores: southern Ontario; Palaeogeography, Palaeoclimatology, Palaeoecology, v. 210, p. 347–366.

Sheehan, P.M. 2001: The Late Ordovician mass extinction; Annual Review of Earth and Planetary Sciences, v. 29, p. 331–364.

Sinclair, G.W. and Leith, E.I. 1958: New name for an Ordovician shale in Manitoba; Journal of Paleontology, v. 32, p. 243–244.

Smith, D.L. 1963: A lithologic study of the Stony Mountain and Stonewall formations in southern Manitoba; MSc thesis, University of Manitoba, Winnipeg, 219 p.

Smith, M.E., Singer, B.S. and Simo, T. 2011: A time like our own? Radioisotopic calibration of the Ordovician greenhouse to icehouse transition; Earth and Planetary Science Letters, v. 311, p. 364–374.

Stearn, C.W. 1953: Ordovician-Silurian boundary in Manitoba; Abstracts of Papers Submitted for the November Meeting in Toronto, Canada, November 9–11, 1953, Geological Society of America, Bulletin, v. 64, p. 1477–1478.

Stearn, C.W. 1956: Stratigraphy and palaeontology of the Interlake Group and Stonewall Formation of southern Manitoba; Geological Survey of Canada, Memoir 281, 162 p.

Stewart, L.A. 2012: Paleoenvironment, paleoecology, and stratigraphy of the uppermost Ordovician section, north of Grand Rapids, Manitoba; MSc thesis, University of Manitoba, Winnipeg, 254 p.

Sweet, W.C. 1979: Late Ordovician conodonts and biostratigraphy of the Western Midcontinent Province; *in* Conodont Biostratigraphy of the Great Basin and Rocky Mountains, C.A. Sandberg and D.L. Clark, (ed.), Brigham Young University, Geology Studies, v. 26, pt. 3, p. 45–85.

Sweet, W.C. 1982: Conodonts from the Winnipeg Formation (Middle Ordovician) of the northern Black Hills, South Dakota; Journal of Paleontology, v. 56, p. 1029–1049.

Theiling, B.P., Railsback, L.B., Holland, S.M. and Crowe, D.E. 2007: Heterogeneity in geochemical expression of subaerial exposure in limestones, and its implications for sampling to detect exposure surfaces; Journal of Sedimentary Research, v. 77, p. 159–169.

Webby, B.D., Cooper, R.A., Bergström, S.M. and Paris, F. 2004: Stratigraphic framework and time slices; *in* The Great Ordovician Biodiversification Event, B.D. Webby, F. Paris, M.L. Droser and I.G. Percival, (ed.), Columbia University Press, New York, p. 41–47.

Westrop, S.R. and Ludvigsen, R. 1983: Systematics and paleoecology of Upper Ordovician trilobites from the Selkirk Member of the Red River Formation, southern Manitoba; Manitoba Department of Energy and Mines, Mineral Resources Division, Geological Report, GR 82-2, 51 p.

Witzke, B.J. 1980: Middle and Upper Ordovician paleogeography of the region bordering the Transcontinental Arch; *in* Paleozoic Paleogeography of the West-Central United States, T.D. Fouch and E.R. Magathan, (ed.), Rocky Mountain Section, Society of Economic Paleontologists and Mineralogists, p. 1–18.

Young, G.A. and Elias, R.J. 1999: Coral distribution and associations in the Upper Ordovician Stony Mountain Formation of Manitoba; *in Quo vadis* Ordovician?, P. Kraft and O. Fatka, (ed.), Acta Universitatis Carolinae, Geologica, v. 43, no. 1/2, p. 429–432.

Young, G.A., Elias, R.J., Wong, S. and Dobrzanski, E.P. 2008: Upper Ordovician rocks and fossils in southern Manitoba; Canadian Paleontology Conference 2008, Winnipeg, Manitoba, Field Trip Guidebook No. 13, 97 p.

Young, G.A., Rudkin, D.M., Dobrzanski, E.P., Robson, S.P., Cuggy, M.B., Demski, M.W. and Thompson, D.P. 2012: Great Canadian Lagerstätten 3. Late Ordovician Konservat-Lagerstätten in Manitoba; Geoscience Canada, v. 39, p. 201–213.

Young, G.A., Rudkin, D.M., Dobrzanski, E.P., Robson, S.P. and Nowlan, G.S. 2007: Exceptionally preserved Late Ordovician biotas from Manitoba, Canada; Geology, v. 35, p. 883–886.

Zhang, S. 2011: Timing and extent of maximum transgression across Laurentia during Late Ordovician: new evidence from Slave Craton, Canadian Shield; Palaeogeography, Palaeoclimatology, Palaeoecology, v. 306, p. 196–204.